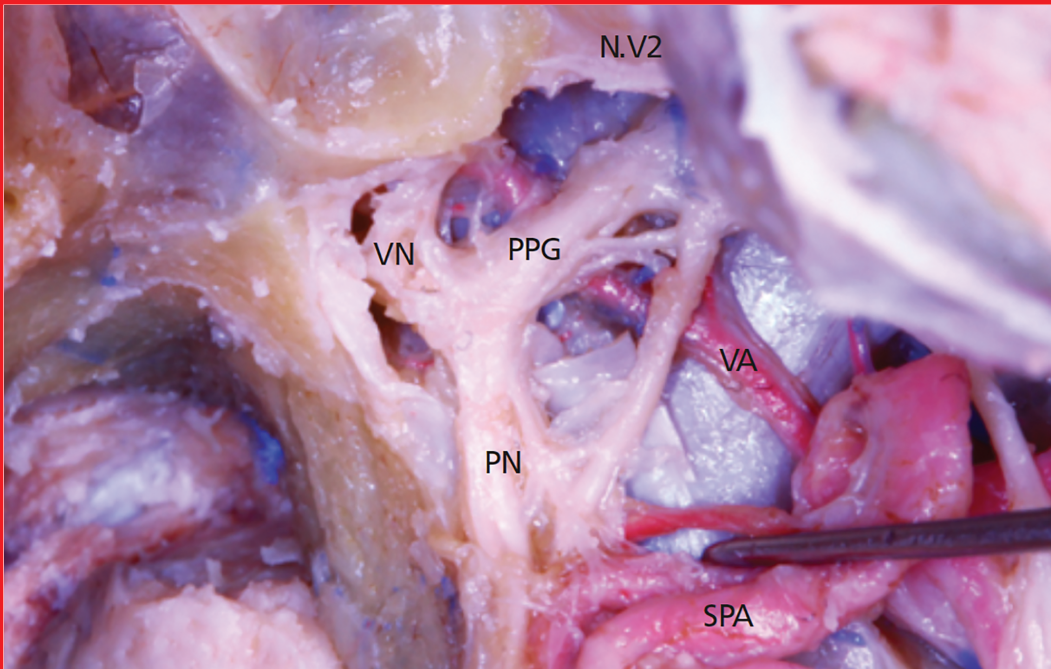


# anatomy

An International Journal of Experimental and Clinical Anatomy

Volume 16 / Issue 3 / December 2022

Published three times a year



# anatomy

An International Journal of Experimental and Clinical Anatomy

## Official Publication of the Turkish Society of Anatomy and Clinical Anatomy

### Aim and Scope

**Anatomy**, an international journal of experimental and clinical anatomy, is a peer-reviewed journal published three times a year with an objective to publish manuscripts with high scientific quality from all areas of anatomy. The journal offers a forum for anatomical investigations involving gross, histologic, developmental, neurological, radiological and clinical anatomy, and anatomy teaching methods and techniques. The journal is open to original papers covering a link between gross anatomy and areas related with clinical anatomy such as experimental and functional anatomy, neuroanatomy, comparative anatomy, modern imaging techniques, molecular biology, cell biology, embryology, morphological studies of veterinary discipline, and teaching anatomy. The journal is currently indexing and abstracting in TUBITAK ULAKBIM Turkish Medical Index, Proquest, EBSCO Host, Index Copernicus and Google Scholar.

### Publication Ethics

**Anatomy** is committed to upholding the highest standards of publication ethics and observes the principles of Journal's Publication Ethics and Malpractice Statement which is based on the recommendations and guidelines for journal editors developed by the Committee on Publication Ethics (COPE), Council of Science Editors (CSE), World Association of Medical Editors (WAME) and International Committee of Medical Journal Editors (ICMJE). For detailed information please visit the online version of the journal which is available at <https://dergipark.org.tr/pub/anatomy>

### Authorship

All persons designated as authors should have participated sufficiently in the work to take public responsibility for the content of the manuscript. Authorship credit should be based on substantial contributions to (1) conception and design or analysis and interpretation of data, (2) drafting of the manuscript or revising it for important intellectual content and, (3) final approval of the version to be published. The Editor may require the authors to justify assignment of authorship. In the case of collective authorship, the key persons responsible for the article should be identified and others contributing to the work should be recognized with proper acknowledgment.

### Copyright

Copyright © 2022, by the Turkish Society of Anatomy and Clinical Anatomy, TSACA. All rights reserved. No part of this publication may be reproduced, stored or transmitted in any form without permission in writing from the copyright holder beforehand, exceptionally for research purpose, criticism or review. The publisher and the Turkish Society of Anatomy and Clinical Anatomy assume no liability for any material published in the journal. All statements are the responsibility of the authors. Although all advertising material is expected to conform ethical standards, inclusion in this publication does not constitute a guarantee or endorsement of the quality or value of such product or of the claims made of it by its manufacturer. Permission requests should be addressed to the publisher.

### Publisher

Deomed Publishing  
Gür Sok. No:7/B Kadıköy, İstanbul, Türkiye  
Phone: +90 216 414 83 43 (Pbx) / Fax: +90 216 414 83 42  
[www.deomed.com](http://www.deomed.com) / e-mail: [medya@deomed.com](mailto:medya@deomed.com)

### Publication Information

**Anatomy** (e-ISSN 1308-8459) as an open access electronic journal is published by Deomed Publishing, İstanbul, for the Turkish Society of Anatomy and Clinical Anatomy, TSACA. Due the Press Law of Turkish Republic dated as June 26, 2004 and numbered as 5187, this publication is classified as a periodical in English language.

#### Ownership

On behalf of the Turkish Society of Anatomy and Clinical Anatomy,  
Ahmet Kağan Karabulut, MD, PhD; Konya, Türkiye

#### Editor-in-Chief

Nihal Apaydin, MD  
Department of Anatomy,  
Faculty of Medicine, Ankara University,  
06100, Sıhhiye, Ankara, Türkiye  
Phone: 0090 312 595 82 48  
e-mail: [napaydin@gmail.com](mailto:napaydin@gmail.com); [napaydin@medicine.ankara.edu.tr](mailto:napaydin@medicine.ankara.edu.tr)

#### Administrative Office

Güven Mah. Güvenlik Cad. Onlar Ap. 129/2 Aşağı Ayrancı, Ankara, Türkiye  
Phone: +90 312 447 55 52-53

### Submission of Manuscripts

Manuscripts should be submitted at our manuscript submission and information portal <https://dergipark.org.tr/en/pub/anatomy>

### Categories of Articles

- **Original Articles** describe substantial original research that falls within the scope of the Journal.
- **Teaching Anatomy** section contains regular or all formats of papers which are relevant to comparing teaching models or to introducing novel techniques, including especially the own experiences of the authors.
- **Reviews** section highlights current development in relevant areas of anatomy. The reviews are generally invited; other prospective authors should consult with the Editor-in-Chief.
- **Case Reports** include new, noteworthy or unusual cases which could be of help for basic notions and clinical practice.
- **Technical Note** articles cover technical innovations and developments with a specific technique or procedure or a modification of an existing technique. They should be sectioned like an original research article but not exceed 2000 words.
- **Viewpoint** articles give opinions on controversial topics or future projections, some of these are invited.
- **Historical View** category presents overview articles about historical sections from all areas of anatomy.
- **Terminology Zone** category is a platform for the articles which discuss some terminological controversies or opinions.

The categories above are peer-reviewed. They should include abstract and keywords. There are also categories including Letters to the Editor, Book Reviews, Abstracts, Obituary, News and Announcements which do not require a peer review process.

For detailed instructions concerning the submission of manuscripts, please refer to the Instructions to Authors.

### Advertising and Reprint Requests

Please direct to publisher. e-mail: [medya@deomed.com](mailto:medya@deomed.com)

### Honorary Editor

**Doğan Aksit**, Ankara, Türkiye

### Founding Editors

**Salih Murat Akkın**, Gaziantep, Türkiye

**Hakan Hamdi Çelik**, Ankara, Türkiye

### Former Editors-in-Chief and Advising Editors

**Salih Murat Akkın** (2007–2013)  
Gaziantep, Türkiye

**Gülgün Şengül** (2014–2019)  
Izmir, Türkiye

### Editor-in-Chief

**Nihal Apaydın**, Ankara, Türkiye

### Editors

**Ceren Günenç Beşer**, Ankara, Türkiye

**Zeliha Kurtoğlu Olgunus**, Mersin, Türkiye

**Luis Puelles**, Murcia, Spain

**Gülgün Şengül**, Izmir, Türkiye

**Shane Tubbs**, Birmingham, AL, USA

**Emel Ulupınar**, Eskişehir, Türkiye

### Associate Editors

**Vaclav Baca**, Prague, Czech Republic

**Çağatay Barut**, Istanbul, Türkiye

**Jon Cornwall**, Dunedin, New Zealand

**Ayhan Cömert**, Ankara, Türkiye

**Mirela Eric**, Novi Sad, Serbia

**Georg Feigl**, Graz, Austria

**Quentin Fogg**, Melbourne, Australia

**David Kachlik**, Prague, Czech Republic

**Marko Korschake**, Innsbruck, Austria

**Scott Lozanoff**, Honolulu, HI, USA

**Levent Sarıkçıoğlu**, Antalya, Türkiye

**Cristian Stefan**, Boston, MA, USA

**İlkan Tatar**, Ankara, Türkiye

**Trifon Totlis**, Thessaloniki, Greece

### Executive Board of Turkish Society of Anatomy and Clinical Anatomy

**Piraye Kervancıoğlu** (President)

**Çağatay Barut** (Vice President)

**Nadire Ünver Doğan** (Vice President)

**İlke Ali Gürses** (Secretary General)

**Ceren Günenç Beşer** (Treasurer)

**Esat Adıgüzel** (Member)

**Selçuk Tunalı** (Member)

### Scientific Advisory Board

**Peter H. Abrahams**  
Cambridge, UK

**Halil İbrahim Açar**  
Ankara, Türkiye

**Marian Adamkov**  
Martin, Slovakia

**Esat Adıgüzel**  
Denizli, Türkiye

**Mustafa Aktekin**  
Istanbul, Türkiye

**Abduelmenem Alashkham**  
Edinburgh, UK

**Mahindra Kumar Anand**  
Gujarat, India

**Serap Arbak**  
Istanbul, Türkiye

**Alp Bayramoğlu**  
Istanbul, Türkiye

**Brion Benninger**  
Lebanon, OR, USA

**Susana Biasutto**  
Cordoba, Argentina

**Dragica Bobinac**  
Rijeka, Croatia

**David Bolender**  
Milwaukee, WI, USA

**Eric Brenner**  
Innsbruck, Austria

**Mustafa Büyükmumcu**  
Istanbul, Türkiye

**Richard Halti Cabral**  
Sao Paulo, Brazil

**Safiye Çavdar**  
Istanbul, Türkiye

**Katharina D'Herde**  
Ghent, Belgium

**Fabrice Duparc**  
Rouen, France

**Behice Durgun**  
Adana, Türkiye

**İzzet Duyar**  
Istanbul, Türkiye

**Mete Ertürk**  
Izmir, Türkiye

**Reha Erzurumlu**  
Baltimore, MD, USA

**Ali Fırat Esmir**  
Ankara, Türkiye

**António José Gonçalves Ferreira**  
Lisboa, Portugal

**Christian Fontaine**  
Lille, France

**Figen Gövsay Gökmen**  
Izmir, Türkiye

**Rod Green**  
Bendigo, Australia

**Bruno Grignon**  
Nancy Cedex, France

**Nadir Gülekon**  
Ankara, Türkiye

**Mürvet Hayran**  
Izmir, Türkiye

**David Heylings**  
Norwich, UK

**Lazar JeleV**  
Sofia, Bulgaria

**Samet Kapakin**  
Erzurum, Türkiye

**Ahmet Kağan Karabulut**  
Konya, Türkiye

**S. Tuna Karahan**  
Ankara, Türkiye

**Simel Kendir**  
Ankara, Türkiye

**Piraye Kervancıoğlu**  
Gaziantep, Türkiye

**Hee-Jin Kim**  
Seoul, Korea

**Necdet Kocabıyık**  
Ankara, Türkiye

**Cem Kopuz**  
Samsun, Türkiye

**Mustafa Ayberk Kurt**  
Istanbul, Türkiye

**Marios Loukas**  
Grenada, West Indies

**Veronica Macchi**  
Padua, Italy

**Ali Mirjalili**  
Auckland, New Zealand

**Bernard Moxham**  
Cardiff, Wales, UK

**Konstantinos Natsis**  
Thessaloniki, Greece

**Lia Lucas Neto**  
Lisboa, Portugal

**Helen Nicholson**  
Dunedin, New Zealand

**Davut Özbağ**  
Malatya, Türkiye

**P. Hande Özdinler**  
Chicago, IL, USA

**Adnan Öztürk**  
Istanbul, Türkiye

**Ahmet Hakan Öztürk**  
Mersin, Türkiye

**Friedrich Paulsen**  
Erlangen, Germany

**Wojciech Pawlina**  
Rochester, MN, USA

**Tuncay Veysel Peker**  
Ankara, Türkiye

**Vid Persaud**  
Winnipeg, MB, Canada

**David Porta**  
Louisville, KY, USA

**Jose Ramon Sanudo**  
Madrid, Spain

**Tatsuo Sato**  
Tokyo, Japan

**Mohammadali M. Shoja**  
Birmingham, AL, USA

**Ahmet Sinav**  
Istanbul, Türkiye

**Takis Skandalakis**  
Athens, Greece

**Isabel Stabile**  
Msida, Malta

**Vildan Sümbüloğlu**  
Gaziantep, Türkiye

**(Biostatistics)**

**Muzaffer Seker**  
Konya, Türkiye

**Erdoğan Şendemir**  
Bursa, Türkiye

**İbrahim Tekdemir**  
Ankara, Türkiye

**Hironubu Tokuno**  
Tokyo, Japan

**Mehmet İbrahim Tuğlu**  
Manisa, Türkiye

**Selçuk Tunalı**  
Ankara, Türkiye

**Uğur Türe**  
Istanbul, Türkiye

**Aysun Uz**  
Ankara, Türkiye

**Mehmet Üzel**  
Istanbul, Türkiye

**Ivan Varga**  
Bratislava, Slovakia

**Tuncay Varol**  
Manisa, Türkiye

**Stephanie Woodley**  
Otago, New Zealand

**Bülent Yalçın**  
Ankara, Türkiye

**Gazi Yaşargil**  
Istanbul, Türkiye

**Hiroshi Yorifuji**  
Gunma, Japan

**Anatomy**, an international journal of experimental and clinical anatomy, is the official publication of the Turkish Society of Anatomy and Clinical Anatomy, TSACA. It is a peer-reviewed e-journal that publishes scientific articles in English. For a manuscript to be published in the journal, it should not be published previously in another journal or as full text in congress books and should be found relevant by the editorial board. Also, manuscripts submitted to *Anatomy* must not be under consideration by any other journal. Relevant manuscripts undergo conventional peer review procedure (at least three reviewers). For the publication of accepted manuscripts, author(s) should reveal to the Editor-in-Chief any conflict of interest and transfer the copyright to the Turkish Society of Anatomy and Clinical Anatomy, TSACA.

In the Materials and Methods section of the manuscripts where experimental studies on humans are presented, a statement that informed consent was obtained from each volunteer or patient after explanation of the procedures should be included. This section also should contain a statement that the investigation conforms with the principles outlined in the appropriate version of 1964 Declaration of Helsinki. For studies involving animals, all work must have been conducted according to applicable national and international guidelines. Prior approval must have been obtained for all protocols from the relevant author's institutional or other appropriate ethics committee, and the institution name and permit numbers must be provided at submission.

Anatomical terms used should comply with Terminologia Anatomica by FCAT (1998).

No publication cost is charged for the manuscripts but reprints and color printings are at authors' cost.

#### Preparation of manuscripts

During the preparation of the manuscripts, uniform requirements of the International Committee of Medical Journal Editors, a part of which is stated below, are valid (see ICMJE). Uniform requirements for manuscripts submitted to biomedical journals. Updated content is available at [www.icmje.org](http://www.icmje.org). The manuscript should be typed double-spaced on one side of a 21x29.7 cm (A4) blank sheet of paper. At the top, bottom and right and left sides of the pages a space of 2.5 cm should be left and all the pages should be numbered except for the title page.

Manuscripts should not exceed 15 pages (except for the title page). They must be accompanied by a cover letter signed by corresponding author and the Conflicts of Interest Disclosure Statement and Copyright Transfer Form signed by all authors. The contents of the manuscript (original articles and articles for Teaching Anatomy category) should include: 1- Title Page, 2- Abstract and Keywords, 3- Introduction, 4- Materials and Methods, 5- Results, 6- Discussion (Conclusion and/or Acknowledgement if necessary), 7- References

#### Title page

In all manuscripts the title of the manuscript should be written at the top and the full names and surnames and titles of the authors beneath. These should be followed with the affiliation of the author. Manuscripts with long titles are better accompanied underneath by a short version (maximum 80 characters) to be published as running head. In the title page the correspondence address and telephone, fax and e-mail should be written. At the bottom of this page, if present, funding sources supporting the work should be written with full names of all funding organizations and grant numbers. It should also be indicated in a separate line if the study has already been presented in a congress or likewise scientific meeting. Other information such as name and affiliation are not to be indicated in pages other than the title page.

#### Abstract

Abstract should be written after the title in 100–250 words. In original articles and articles prepared in IMRAD format for Teaching Anatomy category the abstract should be structured under sections Objectives, Methods, Results and Conclusion. Following the abstract at least 3 keywords should be added in alphabetical order separated by semicolons.

#### References

Authors should provide direct references to original research sources. References should be numbered consecutively in square brackets, according to the order in which they are first mentioned in the manuscript. They should follow the standards detailed in the NLM's Citing Medicine, 2nd edition (Citing medicine: the NLM style guide for authors, editors, and publishers [Internet]. 2nd edition. Updated content is available at [www.ncbi.nlm.nih.gov/books/NBK7256](http://www.ncbi.nlm.nih.gov/books/NBK7256)). The names of all contributing authors should be listed, and should be in the order they appear in the original reference. The author is responsible for the accuracy and completeness of references. When necessary, a copy of a referred article can be requested from the author. Journal names should be abbreviated as in *Index Medicus*. Examples of main reference types are shown below:

- **Journal articles:** Author's name(s), article title, journal title (abbreviated), year of publication, volume number, inclusive pages
  - *Standard journal article:* Sargon MF, Celik HH, Aksit MD, Karaagaoglu E. Quantitative analysis of myelinated axons of corpus callosum in the human brain. *Int J Neurosci* 2007;117:749–55.

- *Journal article with indication article published electronically before print:* Sengul G, Fu Y, Yu Y, Paxinos G. Spinal cord projections to the cerebellum in the mouse. *Brain Struct Funct Epub* 2014 Jul 10. DOI 10.1007/s00429-014-0840-7.
- **Books:** Author's name(s), book title, place of publication, publisher, year of publication, total pages (entire book) or inclusive pages (contribution to a book or chapter in a book)
  - *Entire book:*
    - *Standard entire book:* Sengul G, Watson C, Tanaka I, Paxinos G. Atlas of the spinal cord of the rat, mouse, marmoset, rhesus and human. San Diego (CA): Academic Press Elsevier; 2013. 360 p.
    - *Book with organization as author:* Federative Committee of Anatomical Terminology (FCAT). Terminologia anatomica. Stuttgart: Thieme; 1998. 292 p.
    - *Citation to a book on the Internet:* Bergman RA, Afifi AK, Miyauchi R. Illustrated encyclopedia of human anatomic variation. Opus I: muscular system [Internet]. [Revised on March 24, 2015] Available from: <http://www.anatomyatlases.org/AnatomicVariants/AnatomyHPshhtml>
  - *Contribution to a book:*
    - *Standard reference to a contributed chapter:* Potten CS, Wilson JW. Development of epithelial stem cell concepts. In: Lanza R, Gearhart J, Blau H, Melton D, Moore M, Pedersen R, Thomson J, West M, editors. Handbook of stem cell. Vol. 2, Adult and fetal. Amsterdam: Elsevier; 2004. p. 1–11.
    - *Contributed section with editors:* Johnson D, Ellis H, Collins P, editors. Pectoral girdle and upper limb. In: Standring S, editor. Gray's anatomy: the anatomical basis of clinical practice. 29th ed. Edinburgh (Scotland): Elsevier Churchill Livingstone; 2005. p. 799–942.
  - *Chapter in a book:*
    - *Standard chapter in a book:* Doyle JR, Botte MJ. Surgical anatomy of the hand and upper extremity. Philadelphia (PA): Lippincott Williams and Wilkins; 2003. Chapter 10, Hand, Part 1, Palmar hand; p. 532–641.

#### Illustrations and tables

Illustrations and tables should be numbered in different categories in the manuscript and Roman numbers should not be used in numbering. Legends of the illustrations and tables should be added to the end of the manuscript as a separate page. Attention should be paid to the dimensions of the photographs to be proportional with 10x15 cm. Some abbreviations out of standards can be used in related illustrations and tables. In this case, abbreviation used should be explained in the legend. Figures and tables published previously can only be used when necessary for a comparison and only by giving reference after obtaining permission from the author(s) or the publisher (copyright holder).

#### Author Contribution

Each manuscript should contain a statement about the authors' contribution to the Manuscript. Please note that authorship changes are no longer possible after the final acceptance of an article.

List each author by the initials of names and surnames and describe each of their contributions to the manuscript using the following terms:

- Protocol/project development
- Data collection or management
- Data analysis
- Manuscript writing/editing
- Other (please specify briefly using 1 to 5 words)

**For example:** NBA: Project development, data collection; AS: Data collection, manuscript writing; STR: Manuscript writing

**Funding:** information that explains whether and by whom the research was supported.

**Conflicts of interest/Competing interests:** include appropriate disclosures.

**Ethics approval:** include appropriate approvals or waivers. Submitting the official ethics approval by whom the research was approved, including the approval date, number or code is necessary.

If the submission uses cadaveric tissue, please acknowledge the donors in an acknowledgement at the end of the paper.

#### Control list

- Length of the manuscript (max. 15 pages)
- Manuscript format (double space; one space before punctuation marks except for apostrophes)
- Title page (author names and affiliations; running head; correspondence)
- Abstract (100–250 words)
- Keywords (at least three)
- References (relevant to *Index Medicus*)
- Illustrations and tables (numbering; legends)
- Conflicts of Interest Disclosure Statement and Copyright Transfer Form
- Cover letter

All manuscripts must contain the following declaration sections. These should be placed before the reference list at the end of the manuscript.

# Clinical implications of the anatomical relationships of the pterygopalatine fossa and Vidian canal: an endonasal endoscopic cadaveric study

Hakan Kına<sup>1</sup> , Koral Çağlar Kuş<sup>2</sup> , İsmet Demirtaş<sup>2</sup> 

<sup>1</sup>Department of Neurosurgery, School of Medicine, İstinye University, İstanbul, Türkiye

<sup>2</sup>Department of Anatomy, School of Medicine, İstinye University, İstanbul, Türkiye

## Abstract

**Objectives:** The aim of our study was to describe a surgical access to pterygopalatine fossa and Vidian canal using an endonasal endoscopic approach. We also intend to reveal the anatomical relations of the neurovascular structures in the surgical corridors and to determine the relationships between previously defined reference points in order to prevent surgical complications during surgical access to these regions.

**Methods:** Our study was carried out between October-December 2016 in Cerrahpaşa Faculty of Medicine Microneurosurgery and Neuroanatomy Laboratory. A total of 7 silicon dye-injected cadavers (4 males and 3 females) were studied. 3D images were obtained by photographing the approaches applied to the pterygopalatine fossa and Vidian canal and related anatomical structures.

**Results:** We succeeded in exposing and examining the pterygopalatine fossa and Vidian canal endoscopically in all samples. First, the posterior wall of the maxillary sinus was opened to reach the pterygopalatine fossa. The pterygopalatine fossa was divided into 3 anatomical compartments. The first layer encountered was the periosteum covering the pterygopalatine fossa. After removing the periosteum, the fat layer was revealed. Under the fat layer, the vascular compartment and finally the neural compartment were encountered.

**Conclusion:** Our study revealed three-dimensional anatomical data related to the surgical margins involved in approaches to the pterygopalatine fossa and Vidian canal; and specifically defined various neurovascular structures encountered in these approaches. Our study provides information to decrease potential complications that may develop during endonasal endoscopic surgery. We conclude that as the anatomy of the pterygopalatine fossa and Vidian canal is known in details, the endonasal endoscopic approach is likely to become the standard method to access lesions in these regions.

**Keywords:** endonasal endoscopic surgery; pterygopalatine fossa; Vidian canal

Anatomy 2022;16(3):139–145 ©2022 Turkish Society of Anatomy and Clinical Anatomy (TSACA)

## Introduction

Endoscopic endonasal approaches were initially used to treat only sellar lesions, particularly pituitary gland tumors.<sup>[1–6]</sup> Surgical approaches to midline pathologies, which are the most common among skull base lesions, can be applied by neurosurgeons frequently with endonasal methods. The development of endoscopic endonasal skull base approaches has increased markedly over the past 20 years compared to the traditional open approaches. However, approaching lesions of the anterior and anterolateral skull base seems to be more challenging due to the region's complex anatomy and the

close relationship of its neurovascular structures.<sup>[7–10]</sup> Over time, the anatomical relationships became more understandable, so did endoscopic equipment and technological developments. The addition of neurophysiological monitoring and neuronavigation systems have brought new approaches to various lesions involving the central cranial base extending from the crista galli to the foramen magnum.<sup>[11–13]</sup>

With the expansion of endoscopic endonasal approaches (EEA), methods of access to midline pathologies and then to lateral region pathologies were developed.<sup>[14]</sup> Endoscopic approaches to the cavernous sinus,

clivus, odontoid process, pterygopalatine fossa (PPF), petrous apex, and middle cranial fossa were described previously.<sup>[15-17]</sup> With these approaches, there is no need for brain retraction or neurovascular manipulation, there is early revascularization of the lesion, and there is easy access to the deeply located supradiaphragmatic, retrosellar and clival sections of the brain, which are usually particularly difficult to access.<sup>[11,13,16]</sup> Recent studies have observed that low morbidity has been achieved with endoscopic approaches in skull base surgeries and with minimally invasive methods in pterygopalatine fossa and Vidian (pterygoid) canal (VC) access.<sup>[4,17]</sup>

The PPF is a difficult area to access surgically because it is located in the deep part of the middle cranial fossa and has complex neurovascular relationships. The PPF contains the maxillary artery and its branches, maxillary nerve and its branches, pterygopalatine ganglion (PPG) and the Vidian nerve.<sup>[18-26]</sup> It connects laterally with the infratemporal fossa (ITF) via the pterygomaxillary fissure, medially with the nasal cavity via the sphenopalatine foramen, and anteriorly with the orbita via the inferior orbital fissure.<sup>[27]</sup> The location and neighborhood of the PPF and its close connections with the orbit and nasal cavity increase its clinical importance. The spread of tumors and inflammatory diseases occurring in the skull base to the middle cranial fossa is of great importance due to the structures and anatomical localization of the PPF.<sup>[8]</sup>

VC is a bony tunnel located in the skull base, anterior to the foramen lacerum, above the pterygoid processes of the sphenoid bone. This canal links the Vidian artery, vein, and nerve to the PPF.<sup>[2]</sup> The aim of our study was to describe the anatomy of the PPF and VC in details and to define surgical access to these areas using the endonasal endoscopic approach. At the same time, we aimed to reveal the anatomical relations of the neurovascular structures in the surgical corridors and to determine the relationships between previously defined reference points in order to prevent iatrogenic complications during endonasal endoscopic access to these regions.

## Materials and Methods

This study was carried out between October and December 2016 in Cerrahpaşa Faculty of Medicine Microneurosurgery and Neuroanatomy Laboratory, Istanbul. A total of 7 cadaveric heads (4 males and 3 females) were dissected. Before starting the study, red and blue colored silicone was prepared and injected into the common carotid artery and internal jugular vein respectively. The injection was given with a 50-cc syringe into one side of the main vessels, with the contralateral vessels left open. Injection continued until a free flow of mixture escaped from the open vessel. The cadavers have not

undergone any previous craniofacial or endonasal surgery, the integrity of the skull base was preserved, had no impaired mucosa and bony tissue and were older than 18 years old.

The cadaveric heads were first fixed on the table by giving the head 15 degrees of flexion. After the Medtronic high speed drill and aspirator were placed, the procedure was initiated. Dissections were performed under a microscope (Zeiss OPMI Pico) at 4× and 40× magnification using a microsurgery kit. A surgical drill (Medtronic Midas Rex Legend, Minneapolis, MN, USA) and an angled drill bit were used for the drilling process. When choosing AT10 and ATT12 attachments, 2-5 mm torque tip was preferred.

PPF and VC were exposed by endoscopic endonasal method using transmaxillary approach. The superior concha, the inferior border of the maxillary sinus, and the skin and subcutaneous tissue up to the malar eminence were passed superiorly, inferiorly and laterally. The nostrils were retracted preserving the nasal septum (**Figure 1**). Then, the anterior wall of the maxillary sinus was drilled superiorly from the level of the maxillary nerve. The maxillary sinus mucosa was removed. The medial wall of the maxillary sinus was elevated, preserving the inferior concha. The nasal septum was removed. The parts of the conchae other than the bone attachment sites were excised to increase surgical exploration (**Figure 2**). The posterior wall of the maxillary sinus was removed with the help of a drill and the PPF and VC were finally reached.

The skull base images of the cadavers were photographed using a macro lens camera (Canon EOS 650 D, Tokyo, Japan) and 3D shooting technique with 55-100 mm lenses. Tripod and sled were used for 3D shooting. The photos were converted into optimized anaglyph 3D photos in the computer program.



**Figure 1.** Dissection procedure on a cadaveric head. The external nose was removed, the bony septum was preserved. IC: inferior concha; IO.N: infraorbital nerve; MC: middle concha; NS: nasal septum.

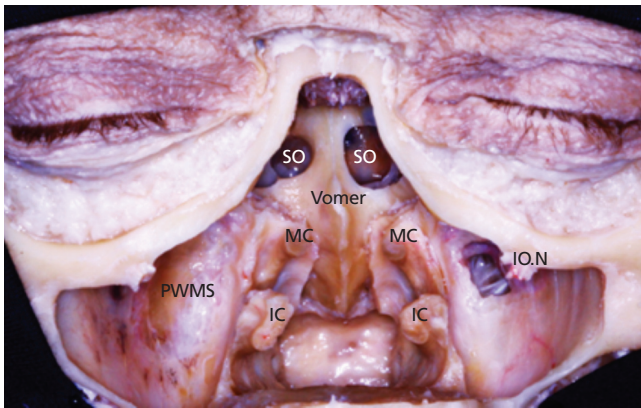


**Figure 2.** Further steps of dissection procedure. Anterior wall of the maxillary sinus was drilled superiorly from the level of the maxillary nerve. The maxillary sinus mucosa was removed. The medial wall of the maxillary sinus was lifted, preserving the inferior concha. The nasal septum was removed. IC: inferior concha; IO.N: infraorbital nerve; MC: middle concha; PWMS: posterior wall of the maxillary sinus; SO: sphenoid ostium.

## Results

We succeeded in exposing and examining the PPF and VC endoscopically in all samples. First, the posterior wall of the maxillary sinus was opened to reach the PPF. The PPF contained 3 anatomical compartments. The first layer encountered was the periosteum covering the PPF. After removing the periosteum, the fat layer was revealed. Under the fat layer, the vascular compartment and finally the neural compartment were encountered. In the vascular compartment layer, fat dissection exposed the arteries, including the sphenopalatine artery and descending palatine artery, which are the distal branches of the maxillary artery reaching from the ITF to the PPF through the pterygomaxillary fissure. This main branch and two terminal branches were different in each cadaver. The neural layer was encountered in the posterior part of the vascular layer and the PPG was found first in this layer. The PPG is associated with many neural structures and its relationship with the Vidian nerve entering the VC medially was noted (**Figure 3**). When the VC was followed posteriorly from the PPG, the lacerum segment of the internal carotid artery (ICA) was reached; proceeding backward from this point, it was noted as the union of greater and lesser petrosal nerves. When the greater petrosal nerve followed backwards, it was seen to merge with the geniculate ganglion. Continuing inferiorly from the PG, the greater petrosal nerve was entering the greater palatine foramen. PPG was defined as the anterolateral part of the VC, superior to the greater palatine foramen, and posterior to the sphenopalatine artery and its branches. The PPF occupied the oral cavity inferiorly, the lateral sphenoid sinus

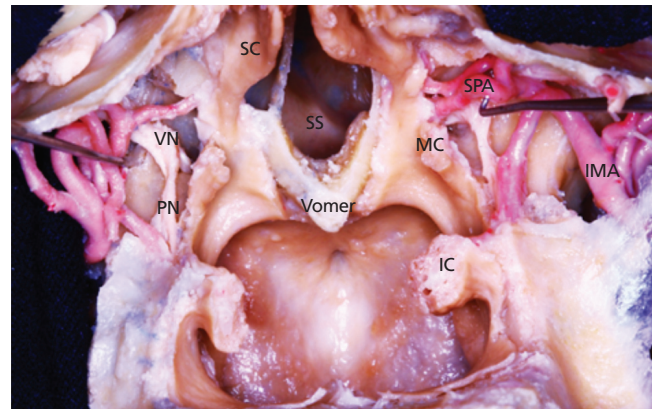


**Figure 3.** After removing the posterior wall of the maxillary sinus completely, the pterygopalatine ganglion and palatine nerve was exposed. IC: inferior concha; IMA: (internal) maxillary artery MC: middle concha; PN: palatine nerve; SC: superior concha; SPA: sphenopalatine artery; SS: sphenoid sinus; VN: Vidian nerve.

supero-medially, the nasal cavity medially, the orbital apex supero-laterally, the ITF laterally, the maxillary sinus anteriorly, and the pterygoid process posteriorly.

The most important landmark in the transpterygoid approach to the lateral skull base was the petrous segment of ICA. During drilling of the pterygoid process, the structure that would guide the surgery up to the ICA petrous segment was the Vidian nerve and the Vidian artery passing through the VC (**Figure 4**). Thus, the most important step after opening the PPF was to find the Vidian nerve. The VC was found with the “H-shape”

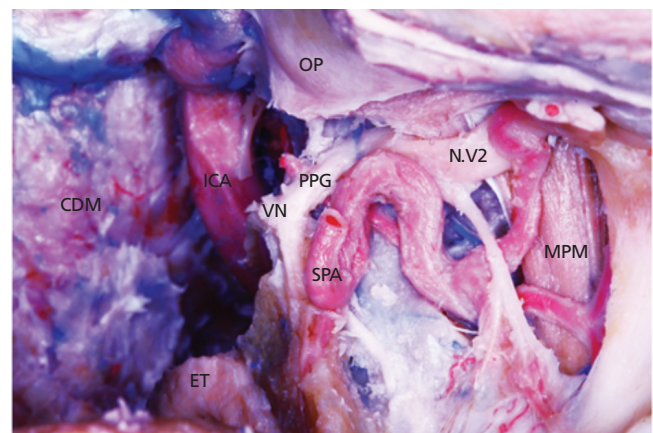


**Figure 4.** During drilling of the pterygoid process, the structure that guided the surgery up to the petrous segment of the internal carotid artery is the Vidian nerve and the Vidian artery passing through the Vidian canal. CDM: clival dura mater; ET: Eustachian tube; ICA: internal carotid artery; MPM: medial pterygoid muscle; N.V2: maxillary nerve; OP: orbital periosteum; PPG: pterygopalatine ganglion; SPA: sphenopalatine artery; VN: Vidian nerve.

technique used by Kassam et al.<sup>[21]</sup> by defining the pterygoid triangle to locate the canal. At the intersection of the “H-shape”, a bony triangle was exposed at the root of the pterygoid process, with its apex facing the base of the sphenoid sinus. Medially to the pterygoid triangle, the Vidian nerve was found in all cadavers and the Vidian artery in one cadaver (Figure 5). The areas medial and inferior to the VC were drilled posteriorly. It was observed that the VC terminated at the junction of the petrous and paraclival ICA at the level of the foramen lacerum in all cadavers. While the medial pterygoid process was drilled along the Vidian nerve trace, the lateral pterygoid process was drilled along the maxillary nerve trace. The petrous ICA was reached by drilling the medial pterygoid process, and the middle cranial fossa was reached by drilling the maxillary nerve.

## Discussion

Technological developments have defined new approaches to surgeries using endonasal skull base endoscopy. Today the endonasal techniques are used for reaching all midline lesions from the frontal sinus to the odontoid process.<sup>[15,20,21]</sup> In addition, close and high-resolution images were obtained from different angles despite narrow anatomical corridors.<sup>[13]</sup> From the patient's perspective, an important advantage to endoscopic surgery is the reduced manipulation of the brain parenchyma and neurovascular structures, which may reduce the causes of morbidity such as contusion due to tissue damage, brain edema and bleeding. Thus, faster recovery can be achieved, and hospital stay, and health care costs can be reduced.<sup>[5,9]</sup> Given these factors, the field of endoscope-based anatomy becomes an important area for research.<sup>[28-32]</sup>

The PPF is an important junction between narrow anatomical corridors containing complex neurovascular structures. Depending on the localization of the lesion, the transpterygoid approach can be applied with a combination of transmaxillary, transsphenoidal, transethmoidal and transnasal methods.<sup>[20]</sup> In approaches to this region, after reaching the maxillary sinus, if the posterior wall of the maxillary nerve medial to the infraorbital nerve is opened, the PPF is reached, and if the lateral wall of the maxillary sinus lateral to the infraorbital nerve is opened, the ITF is reached. Though few in number, endoscopic endonasal approaches to PPF have also been reported.<sup>[1,15]</sup> This region can be accessed by the central or transpalatine route with an endonasal approach.<sup>[8]</sup> Although this approach is minimally invasive and has a clear field of view, the narrow surgical corridor, the difficulty of orientation with 30 and 45 degree telescopes, and the presence of complex neurovascular structures

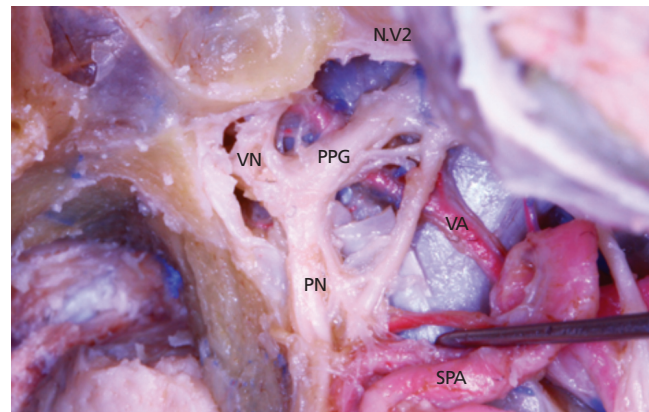


**Figure 5.** Medially to the pterygoid triangle, the Vidian nerve was found in all cadavers and the Vidian artery in one cadaver. NV2: maxillary nerve; PN: palatine nerve; PPG: pterygopalatine ganglion; SPA: sphenopalatine artery; VA: vidian artery; VN: vidian nerve.

under the adipose tissue are disadvantages of this approach. In our study, the fat layer covering the neurovascular structures was carefully dissected; at this point, knowing the anatomy and the anomalies and variations of the region will greatly benefit the surgery.

Alfieri et al.<sup>[1]</sup> described three approaches for transpterygoid surgery; (1) the medial transpalatine approach for reaching the medial PPF; (2) the middle meatal transantral approach for reaching the lateral PPF; and (3) the transantral approach with inferior turbinectomy for reaching the PPF and ITF. With the transpalatine approach, only the medial part of the PPF can be partially reached without opening the posterior wall of the maxillary sinus, and this approach is not applicable in skull base lesions. With the middle meatal transantral approach, a wider field of view is provided and it is possible to reach as far as the lateral infraorbital nerve. Among the described methods, the middle meatal approach is the most suitable method because it has sufficient field of view in skull base lesions and does not require resection of the inferior concha.

The PPF is a quadrangular pyramidal space extending from the ITF posteriorly to the nasal cavity anteriorly by the sphenopalatine foramen. Its surgical importance stems from its being an important junction point between different skull base regions containing complex neurovascular structures. The sphenoid bone body on the superior surface, the perpendicular lamina of the palatine bone on the medial surface, the posterior wall of the maxillary sinus on the anterior surface, the pterygoid process root on the posterior surface, and the ITF on the lateral surface of the inverted quadrangular pyramid-shaped structure. The apex of the pterygoid fossa is asso-

ciated with the oral cavity. The central approach to PPF with facial incision was described in 1858 and is still applied microscopically.<sup>[18]</sup> However, in this approach, the risk of damage to the arteries and nerves of the teeth in the oral plexus is high, since the anterior and posterior maxillary walls are opened.

Since inferior turbinectomy is not performed with the middle meatal trans-central approach, phonation disorder does not develop.<sup>[22]</sup> In this method, after excision of the uncinat process and enlargement of the maxillary ostium, the ethmoid bulla and suprabullar cells are removed, the basal lamella is passed, and posterior ethmoidectomy is performed. The fovea ethmoidalis should be identified and preserved and the sphenopalatine artery should be controlled. The sphenoid sinus should then be exposed. After the maxillary sinus ostium has been enlarged, the sinus mucosa must be stripped from the posterior wall of the maxillary sinus. The posterior wall of the maxillary sinus is removed and the PPF is exposed.<sup>[30]</sup> At this point, care should be taken not to injure the greater palatine nerve in the infero-medial part of the PPF. After reaching the lateral recess of the sphenoid sinus, interventions can be applied to structures such as the cavernous sinus, Meckel cave, middle cranial fossa, petrous apex or infrapetrous according to the localization of the lesion (**Figure 1**).<sup>[12,18]</sup> A study by Prevedello et al.,<sup>[29]</sup> reported that the pterygoid process can be drilled by preserving the Vidian nerve. However, Pinherio-Neto et al.<sup>[28]</sup> reported that the Vidian nerve transposition was not sufficient for removal of the pterygoid process, and the greater descending palatine artery and greater palatine nerve had to be sacrificed. Although ipsilateral hard palate anesthesia occurs in the damage of these structures, patients can tolerate this situation. In addition, the Vidian nerve, located at the junction of the medial pterygoid process and the inferior wall of the sphenoid sinus, is an important landmark for locating the petrous ICA but can be sacrificed if necessary.<sup>[18]</sup> Furthermore, there is no proof that resection of a malignant tumor in the PPF/ITF is more efficient by an external approach than an EEA, because en-bloc resection is rarely feasible in this area and piecemeal tumor removal is not less efficient if resection is complete at the end of surgery.<sup>[19]</sup>

The VC has a close relationship with the anterior genu of the petrous ICA. Vertical part of the cavernous segment of the ICA can be reached by drilling the sphenoid corpus along the Vidian nerve.<sup>[31,32]</sup> The Vidian nerve joins the deep petrosal nerve from the ICA sympathetic trunk and enters the VC and courses together towards the PPG. This nerve, which had not previously

attracted the attention of neurosurgeons, became one of the cornerstones of endoscopic surgery after Kassam.<sup>[20]</sup> Kassam et al.<sup>[21]</sup> reported the Vidian nerve to be the key anatomical point in the transpterygoid approach. In the same study, the authors suggested transpterygoid approach to be performed by drilling the VC and the canal can be found using the “H” shape method. In the light of this information, it has been determined that the Vidian nerve is an important anatomical structure in detecting the lacerum segment of the ICA. The most effective method for the preservation of the Vidian nerve has been reported as the “clock concept”.<sup>[19,21]</sup> This method was applied by drilling the inferior of the VC from medial to lateral. Vidian nerve stimulates lacrimation through its parasympathetic fibers, but it is not the only nerve responsible for lacrimation. Dry eye rarely develops as a result of damage to the Vidian nerve, but when it does develop, dry eye causes complications such as keratitis. Overall the Vidian nerve should be protected if possible. In addition, especially during EEA to Meckel’s cave, petrous apex, or middle cranial fossa, the Vidian nerve can be sacrificed to avoid damage to important neurovascular structures and difficulties in imaging deep structures.<sup>[31]</sup>

At this point, it should be kept in mind that corneal ulcer and ocular complications are inevitable if loss of corneal sensation due to ophthalmic nerve damage and dry eye due to Vidian nerve damage are seen together.<sup>[15]</sup> The petrous and paraclinoid segments of the ICA are an important landmarks for determining the junction of the vidian nerve and the ICA. This junction is lateral to the region where the petrous ICA passes through the foramen lacerum. For this reason, the safe surgical site is inferior to the VC.

## Conclusion

Our study elucidates and explains anatomical and surgical access to the PPF and VC with the EEA. We suggest that the three-dimensional anatomical data revealed in our study may help understanding of the surgical margins of the approaches to the PPF and VC and identification of the different neurovascular structures. Detailed knowledge of these regions has utmost importance to prevent iatrogenic complications during endonasal endoscopic access to these regions.

## Acknowledgments

The authors sincerely thank those who donated their bodies to science so that anatomical research could be performed.

### Conflict of Interest

No potential conflict of interest relevant to this article was reported.

### Author Contributions

HK: conceptualization, data acquisition, data analysis or interpretation, drafting the manuscript, approval of the final version of the manuscript; KÇK: drafting the manuscript, critical revision of the manuscript, approval of the final version of the manuscript; ID: conceptualization, critical revision of the manuscript, approval of the final version of the manuscript.

### Ethics Approval

This cadaveric study involving human participants complies with the ethical standards of the institutional and national research committee and the 1964 Declaration of Helsinki and subsequent amendments or comparable ethical standards. This study was approved by Ethics Committee of Bakırköy Mazhar Osman Mental and Neurological Diseases Training and Research Hospital (protocol 571, 06 September 2016).

### Funding

The authors did not receive support from any organization for the submitted work.

### References

- Alfieri A, Jho HD, Schettino R, Tschabitscher M. Endoscopic endonasal approach to the pterygopalatine fossa: anatomic study. *Neurosurgery* 2003;52:374–80.
- Bahşi İ, Orhan M, Kervancıoğlu P, Yalçın ED. The anatomical and radiological evaluation of the Vidian canal on cone-beam computed tomography images. *Eur Arch Otorhinolaryngol* 2019;276:1373–83.
- Baldauf J, Hosemann W, Schroeder HW. Endoscopic endonasal approach for craniopharyngiomas. *Neurosurg Clin N Am* 2015;26:363;75.
- Bolger WE. Endoscopic transpterygoid approach to the lateral sphenoid recess: surgical approach and clinical experience. *Otolaryngol Head Neck Surg* 2005;133:20–6.
- Buchmann L, Larsen C, Pollack A, Tawfik O, Sykes K, Hoover LA. Endoscopic techniques in resection of anterior skull base/paranasal sinus malignancies. *Laryngoscope* 2006;116:1749–54.
- Cappabianca P, Alfieri A, De Divitiis E. Endoscopic endonasal transsphenoidal approach to the sella: towards functional endoscopic pituitary surgery (FEPS). *Minim Invasive Neurosurg* 1998;41:66–73.
- Cappabianca P, Cavallo LM, de Divitiis O, de Angelis M, Chiaramonte C, Solari D. Endoscopic endonasal extended approaches for the management of large pituitary adenomas. *Neurosurg Clin N Am* 2015;26:323–31.
- Choi J, Park HS. The clinical anatomy of the maxillary artery in the pterygopalatine fossa. *J Oral Maxillofac Surg* 2003;61:72–8.
- Dave SP, Bared A, Casiano RR. Surgical outcomes and safety of transnasal endoscopic resection for anterior skull tumors. *J Otolaryngol Head Neck Surg* 2007;136:920–7.
- De Divitiis E, Cappabianca P, Cavallo LM. Endoscopic transsphenoidal approach: adaptability of the procedure to different sellar lesions. *Neurosurgery* 2002;51:699–707.
- De Divitiis E, Cavallo LM, Cappabianca P, Esposito F. Extended endoscopic endonasal transsphenoidal approach for the removal of suprasellar tumors: part 2. *Neurosurgery* 2007;60:46–59.
- De Lara D, Ditzel Filho LF, Prevedello DM, Carrau RL, Kasemsiri P, Otto BA, Kassam AB. Endonasal endoscopic approaches to the paramedian skull base. *World Neurosurg* 2014;82:S121–9.
- Dehdashti AR, Ganna A, Witterick I, Gentili F. Expanded endoscopic endonasal approach for anterior cranial base and suprasellar lesions: indications and limitations. *Neurosurgery* 2009;64:677–89.
- Ditzel Filho LF, Prevedello DM, Dolci RL, Jamshidi AO, Kerr EE, Campbell R, Otto BA, Carrau RL. The endoscopic endonasal approach for removal of petroclival chondrosarcomas. *Neurosurg Clin N Am* 2015;26:453–62.
- Fortes FS, Sennes LU, Carrau RL, Brito R, Ribas GC, Yasuda A, Rodrigues Jr AJ, Synderman CH, Kassam AB. Endoscopic anatomy of the pterygopalatine fossa and the transpterygoid approach: development of a surgical instruction model. *Laryngoscope* 2008;118:44–9.
- Frank G, Pasquini E, Doglietto F, Mazzatenta D, Sciarretta V, Farneti G, Calbucci F. The endoscopic extended transsphenoidal approach for craniopharyngiomas. *Neurosurgery* 2006;ONS75–83.
- Har-El G. Combined endoscopic transmaxillary-transnasal approach to the pterygoid region, lateral sphenoid sinus, and retrobulbar orbit. *Ann Otol Rhinol Laryngol* 2005;114:439–42.
- Hofstetter CP, Singh A, Anand VK, Kacker A, Schwartz TH. The endoscopic, endonasal, transmaxillary transpterygoid approach to the pterygopalatine fossa, infratemporal fossa, petrous apex, and the Meckel cave. *J Neurosurg* 2010;113:967–74.
- Karkas A, Zimmer LA, Theodosopoulos PV, Keller JT, Prades JM. Endonasal endoscopic approach to the pterygopalatine and infratemporal fossae. *Eur Ann Otorhinolaryngol Head Neck Dis* 2021;138:391–5.
- Kassam AB, Gardner P, Snyderman C, Mintz A, Carrau R. Expanded endonasal approach: fully endoscopic, completely transnasal approach to the middle third of the clivus, petrous bone, middle cranial fossa, and infratemporal fossa. *Neurosurg Focus* 2005;19:E6.
- Kassam A B, Vescan AD, Carrau RL, Prevedello DM, Gardner P, Mintz AH, Synderman CH, Rhoton AL. Expanded endonasal approach: vidian canal as a landmark to the petrous internal carotid artery. *J Neurosurg* 2008;108:177–83.
- Klossek JM, Ferrie JC, Goujon JM, Fontanel JP. Endoscopic approach of the pterygopalatine fossa: report of one case. *Rhinology* 1994;32:208–10.
- Kutlay M, Durmaz A, Özer İ, Kural C, Temiz Ç, Kaya S, Solmaz İ, Daneyemez M, İzci Y. Extended endoscopic endonasal approach to the ventral skull base lesions. *Clin Neurol Neurosurg* 2018;167:129–40.
- Laufer I, Anand VK, Schwartz TH. Endoscopic, endonasal extended transsphenoidal, transplanum transtuberculum approach for resection of suprasellar lesions. *J Neurosurg* 2007;106:400–6.

25. Lobo B, Zhang X, Barkhoudarian G, Griffiths CF, Kelly DF. Endonasal endoscopic management of parasellar and cavernous sinus meningiomas. *Neurosurg Clin N Am* 2015;26:389–401.
26. Loukas M. Book review: clinically oriented anatomy, 5th ed. by Keith L. Moore and Arthur F. Dalley II. *Clin Anat* 2006;16:367
27. Morton AL, Khan A. Internal maxillary artery variability in the pterygopalatine fossa. *Otolaryngol Head Neck Surg* 1991;104:204–9.
28. Pinheiro-Neto CD, Fernandez-Miranda JC, Prevedello DM, Carrau RL, Gardner PA, Snyderman CH. Transposition of the pterygopalatine fossa during endoscopic endonasal transpterygoid approaches. *J Neurol Surg B Skull Base* 2013;74:266–70.
29. Prevedello DM, Pinheiro-Neto CD, Fernandez-Miranda JC, Carrau RL, Snyderman CH, Gardner PA, Kassam AB. Vidian nerve transposition for endoscopic endonasal middle fossa approaches. *Neurosurgery* 2010;67:478–84.
30. Schwartz TH, Fraser JF, Brown S, Tabaei A, Kacker A, Anand VK. Endoscopic cranial base surgery: classification of operative approaches. *Neurosurgery* 2008;62:991–1005.
31. Snyderman C, Gardner P. Master techniques in otolaryngology-head and neck surgery: skull base surgery. Philadelphia (PA): Wolters Kluwer; 2015. p. 469.
32. Vescan AD, Snyderman CH, Carrau RL, Mintz A, Gardner P, Branstetter 4th B, Kassam AB. Vidian canal: analysis and relationship to the internal carotid artery. *Laryngoscope* 2007;117:1338–42.

**ORCID ID:**

H. Kına 0000-0002-9741-7720;  
K. C. Kuş 0000-0003-3286-7218;  
İ. Demirtaş 0000-0001-5789-6985

**Correspondence to:** İsmet Demirtaş, PhD

Department of Anatomy, School of Medicine,  
İstinye University, Topkapı Kampüsü, İstanbul, Türkiye  
Phone: +90 212 481 36 88  
e-mail: ismetdemirtas21@gmail.com

*Conflict of interest statement:* No conflicts declared.

This is an open access article distributed under the terms of the Creative Commons Attribution-NonCommercial-NoDerivs 4.0 Unported (CC BY-NC-ND4.0) Licence (<http://creativecommons.org/licenses/by-nc-nd/4.0/>) which permits unrestricted noncommercial use, distribution, and reproduction in any medium, provided the original work is properly cited. *How to cite this article:* Kına H, Kuş KÇ, Demirtaş İ. Clinical implications of the anatomical relationships of the pterygopalatine fossa and Vidian canal: an endonasal endoscopic cadaveric study. *Anatomy* 2022;16(3):139–145.

# The influence of brightness, age and refractive errors on pupil size

Tolga Yılmaz , Ferah Özçelik 

Department of Ophthalmology, Beyoğlu Eye Training and Research Hospital, İstanbul, Türkiye

## Abstract

**Objectives:** In this study, we aimed to investigate the influence of age, gender and refractive status on pupil size under different illuminance conditions in presbyopic healthy people.

**Methods:** A total of 75 volunteers (49 females and 26 males) were included in the study. The medical records of each participant was reviewed. Patients were divided into three groups according to their age and refractive errors. Pupil responses were evaluated with the automated pupillometry function of the Sirius Topographer. Relationship between pupil size and age, sex, laterality, dominant eye, refractive errors were analyzed by statistical analyses.

**Results:** In the early aged presbyopia group of patients the mean value of the hyperopic group was higher than the other two groups in photopic measurements. In scotopic condition, the mean value of the myopic group was found to be higher than the emmetropic and hyperopic groups. No difference was observed in the comparison of mesopic measurements in all three groups. In the patients with established presbyopia, myopic pupil diameter was higher compared to emmetropic and hyperopic pupils in all illuminances. There was a difference only in the scotopic condition when comparing the emmetropic and hyperopic groups. Pupil size did not change with age in all three conditions in emmetropic eyes. Pupil diameter decreased in all three conditions with age in hyperopics. Photopic and mesopic pupil size increased with age in myopics.

**Conclusion:** The results of this study support that the effects of patient age and refractive status on pupil diameter are important in optimal lens design.

**Keywords:** hyperopics; myopics; presbyopics; pupil size; sirius cornea topography

Anatomy 2022;16(3):146–151 ©2022 Turkish Society of Anatomy and Clinical Anatomy (TSACA)

## Introduction

The pupil regulates the light entering the eye to reduce glare, to control retinal illumination, and to achieve adequate depth of field.<sup>[1]</sup> Scotopic vision is used at light brightness below 0.05 Lux, and pure photopic vision is used above 40 Lux. The vision between these two ranges is defined as mesopic vision.<sup>[2]</sup> Pupil diameter is an important element in the optical quality of the eye. Increase in pupil size increases high-order monochromatic aberrations, and this results in reduced image quality. In smaller pupil diameters, diffraction occurs; however, the depth of focus increases with a decrease in pupil size.<sup>[3]</sup>

Pupil diameter is a valuable parameter with important clinical implications. Its measurement can help detecting anomalies and knowledge of its normal range is essential for the optical industry.<sup>[4]</sup> It is considered the

key factor for optimal optical quality in refractive surgery.<sup>[5]</sup> Several studies have evaluated the relationship between ablation site and pupil diameter with a focus on night vision problems after refractive surgery.<sup>[6,7]</sup> Scotopic and mesopic visions are the most important factors causing visual complaints after refractive laser surgery.<sup>[8]</sup> Pupil diameter also plays an important role in the design of bifocal or multifocal contact lenses, which are designed to get through optimal visual performance under various lighting conditions and at all viewing distances.<sup>[4,9]</sup> Pupil size is also an important consideration for intraocular multifocal or bifocal lenses. Because after successful intraocular placement of these lenses, optimal visual performance should be achieved at all viewing distances under varying brightness conditions.

Therefore, pupil diameter measurement has an important place for all ages and type of refractive errors.

This study aimed to determine the influence of age, gender and refractive status on pupil size under different illuminance conditions in presbyopic healthy people using the pupillometry software of Sirius Topographer.

## Materials and Methods

This retrospective study was conducted at the ophthalmology department of a tertiary hospital in accordance with the ethical standards of the Declaration of Helsinki. The records of 75 patients who were admitted to the contact lens department of Beyoğlu Eye Training and Research Hospital, Istanbul were retrospectively analyzed through the hospital's electronic database.

The medical records of each participant were reviewed. A comprehensive ophthalmologic examination including fundoscopic examination, slit lamp biomicroscopy and best corrected distance visual acuity (D-BCVA) testing were also performed. Pupil responses were evaluated with the automated pupillometry function of the Sirius Topographer (Costruzione Strumenti Oftalmici, Firenze, Italy) using Phoenix v2.1 software (Costruzione Strumenti Oftalmici, CSO, Firenze, Italy). All measurements were performed on the both eye of the subjects and performed by the same experienced clinician who was blinded to medical conditions of the patients.

Sirius Topographer is a placido-based videokeratoscope with two Scheimpflug cameras, one central and one rotating. The device allows both static and dynamic pupillometry, and uses different illumination levels to measure pupil size in scotopic (0.04 Lux) mesopic (4 Lux), and photopic (40 Lux) conditions. LED lighting was the only light source in the room, and the illumination conditions were tested and adjusted using a photometer. During the measurements, the subjects were advised to look straight ahead, not at the light source.

Emmetropia was defined as a mean spherical equivalent equal to and between +0.75 and -0.75 diopter (D). Moreover, myopia was defined as a spherical equivalent of -0.75 D or worse and hypermetropia was defined as a spherical equivalent of +0.75 D or worse. Patients were divided into groups according to age and refractive errors. Those aged between 43–52 were grouped as early presbiopia, and those aged between 52–62 were grouped as established presbiopia. Patients with any history of previous ocular or refractive surgery, ocular or systemic disease, or any history of ocular or systemic drugs which might affect the pupil size, were excluded from the study. Also, smokers and heavy alcohol drinkers (drinking five or more drinks on the same occasion on each of five or more days in the past 30 days) were excluded. Relationship between

pupil size and age, sex, laterality, dominant eye, refractive errors were analyzed by statistical analysis.

The results for each parameter was displayed as mean±standard deviation (SD). For statistical analysis, the chi-square test was employed to compare the frequencies and percentages of the groups. The Kolmogorov–Smirnov test was applied to assess the normal distribution of data. To compare pupillometric measurements in each group, a paired sample t-test was performed. The Wilcoxon signed-rank test was used for variables that did not show normal distribution. The Statistical Package for the Social Sciences (SPSS) version 20 (IBM Inc., Chicago, IL, USA) was used for data analysis, for which values of  $p < 0.05$  were considered to be statistically significant.

## Results

A total of 75 volunteers (49 females and 26 males) were included to the study. The mean age of the patients was  $51.4 \pm 0.88$  (range: 40–62 years). No statistically significant difference was observed in the comparison of the mean age of both genders ( $p > 0.05$ ).

The mean photopic, mesopic and scotopic pupil diameter values in the whole population was  $4.20 \pm 0.88$  mm (range: 2.14–6.67 mm). The mean photopic pupil diameter was  $3.22 \pm 0.24$  mm in males and  $3.32 \pm 0.31$  mm in females; the mesopic pupil diameter was  $4.20 \pm 0.14$  mm in males,  $4.21 \pm 0.21$  mm in females, and the scotopic pupil diameter was  $5.13 \pm 0.24$  mm in males and  $5.12 \pm 0.22$  mm in females. There was no statistically significant difference between the two genders for all three measurements ( $p = 0.482$ ,  $p = 0.751$  and  $p = 0.971$  respectively) (Table 1).

The mean photopic pupil diameter of the right eye was  $3.29 \pm 0.19$  mm, the mean mesopic pupil diameter was  $4.18 \pm 0.21$  mm, and the mean scotopic pupil diameter was  $5.14 \pm 0.16$  mm. In the left eye, mean photopic pupil diameter was  $3.29 \pm 0.21$  mm, mean mesopic pupil diameter was  $4.23 \pm 0.18$  mm, and mean scotopic pupil diameter was  $5.10 \pm 0.14$  mm. There was no statistically significant differences between the right and left eyes for all three measurements ( $p = 0.922$ ,  $0.861$  and  $p = 0.669$ , respectively) (Table 2).

In the dominant and non-dominant eye measurements of our study population, the mean photopic pupil diameter of the dominant eye was  $3.19 \pm 0.26$  mm, the mean mesopic pupil diameter was  $4.03 \pm 0.19$  mm, and the mean scotopic pupil diameter was  $5.01 \pm 0.24$  mm. The mean photopic pupil diameter of the non-dominant eye was  $3.22 \pm 0.16$  mm, the mean mesopic pupil diameter was  $4.09 \pm 0.21$  mm, and the mean scotopic pupil diameter was  $4.96 \pm 0.14$  mm. There was no statistically

**Table 1**

The mean±SD photopic, mesopic and scotopic pupil diameter values in males and females.

Gender	Photopic	Mesopic	Scotopic
Male	3.22±0.24	4.20±0.14	5.13±0.24
Female	3.32±0.31	4.21±0.21	5.12±0.22

**Table 2**

The mean±SD photopic, mesopic and scotopic pupil diameter values on different sides.

Side	Photopic	Mesopic	Scotopic
Right	3.29±0.19	4.18±0.21	5.14±0.16
Left	3.29±0.21	4.23±0.18	5.10±0.14

**Table 3**

The mean±SD photopic, mesopic and scotopic pupil diameter values in the dominant and non-dominant eye.

Dominance	Photopic	Mesopic	Scotopic
Dominant	3.19±0.26	4.03±0.19	5.01±0.24
Non-dominant	3.22±0.16	4.09±0.21	4.96±0.14

significant differences between the right and left eyes for all three measurements ( $p=0.941$ ,  $p=0.763$  and  $p=0.682$  respectively) (**Table 3**).

There were statistically significant differences in the photopic, mesopic and scotopic measurement comparisons of the patients within all groups (female, male, right, left, dominant, non-dominant) ( $p\leq 0.05$  in all).

In the group of patients aged 43–52 years (early presbyopia) the mean photopic pupil diameter was  $3.15\pm 0.22$  mm, the mean mesopic pupil diameter was  $4.16\pm 0.18$  mm, and the mean scotopic pupil diameter was  $5.14\pm 0.14$  mm; and in the myopic patient group the mean photopic pupil diameter was  $3.15\pm 0.16$  mm, the mean mesopic pupil diameter was  $4.33\pm 0.29$  mm, and the mean scotopic pupil diameter was  $5.49\pm 0.18$  mm; in

the hyperopic patient group, the mean photopic pupil diameter was  $3.40\pm 0.20$  mm, the mean mesopic pupil diameter was  $4.31\pm 0.09$  mm, and the mean scotopic pupil diameter was  $5.01\pm 0.14$  mm (**Table 4**). In photopic measurements, the mean value of the hyperopic group was statistically higher than the other two groups ( $p\leq 0.05$ ). In scotopic measurements, the mean value of the myopic group was significantly higher than that of the emmetropic and hyperopic groups ( $p\leq 0.05$ ). No statistically significant difference was observed in the comparison of mesopic measurements in all three groups ( $p> 0.05$ ).

In the patients with established presbyopia between the ages of 52 and 62, the mean photopic pupil diameter was  $3.22\pm 0.16$  mm, the mean mesopic pupil diameter was  $4.05\pm 0.09$  mm, and the mean scotopic pupil diameter was

**Table 4**

The mean±SD photopic, mesopic and scotopic pupil diameter values in early presbyopia group.

Early presbyopia (age: 43–52years)	Photopic	Mesopic	Scotopic
Emmetropia	3.15±0.22	4.16±0.18	5.14±0.14
Myopia mean:-3.00	3.15±0.16	4.33±0.29	5.49±0.18
Hypermetropia mean:+2.50	3.40±0.20	4.31±0.09	5.01±0.14

**Table 5**

The mean±SD photopic, mesopic and scotopic pupil diameter values in established presbyopia group.

Established presbyopia (age: 52–62 years)	Photopic	Mesopic	Scotopic
Emmetropia	3.22±0.16	4.05±0.09	5.09±0.22
Myopia mean:-3.25	3.92±0.26	4.56±0.19	5.42±0.14
Hypermetropia mean:+2.25	3.20±0.28	3.95±0.17	4.79±0.14

5.09±0.22 mm. In the myopic patient group, the mean photopic pupil diameter was 3.92±0.26 mm, the mean mesopic pupil diameter was 4.56±0.19 mm, and the mean scotopic pupil diameter was 5.42±0.14 mm; and in the hypermetropic patient group, the mean photopic pupil diameter was 3.20±0.28 mm, the mean mesopic pupil diameter was 3.95±0.17 mm, and the mean scotopic pupil diameter was 4.79±0.14 mm (**Table 5**). In all conditions, myopic pupil diameter was statistically significantly higher compared to emmetropic and hyperopic pupils (p<0.05). There was a statistically significant difference only in the scotopic condition when comparing the emmetropic and hyperopic groups (p<0.05).

Pupil size did not change with age in all three conditions in emmetropic eyes. Pupil diameter decreased in all three conditions with age in hyperopics. Photopic and mesopic pupil diameters increased with age in myopia (**Figure 1**).

### Discussion

Pupil size has a great influence on visual function, and it is mainly dependent on adaptive luminance, which is modulated by other external factors.<sup>[3]</sup> Pupil diameter measurement has been the subject of many studies.<sup>[2,6]</sup> It is well known that pupil size decreases with increasing luminance. Factors investigated for possible relationships with pupil size are gender, iris color, age, refractive error etc.<sup>[4,10,11]</sup> In the literature, it was emphasized that there was no significant difference in pupil size between males and females; and there was no correlation with iris color.<sup>[10]</sup> In our study, we did not find any difference in mean pupil diameters between males and females, in agreement with the literature. Also, we did not find any statistical difference in the comparison of the right and left eyes of the patients. In addition, no difference was observed in the comparison of the dominant eye and the non-dominant eye. It is shown that, the mean pupil

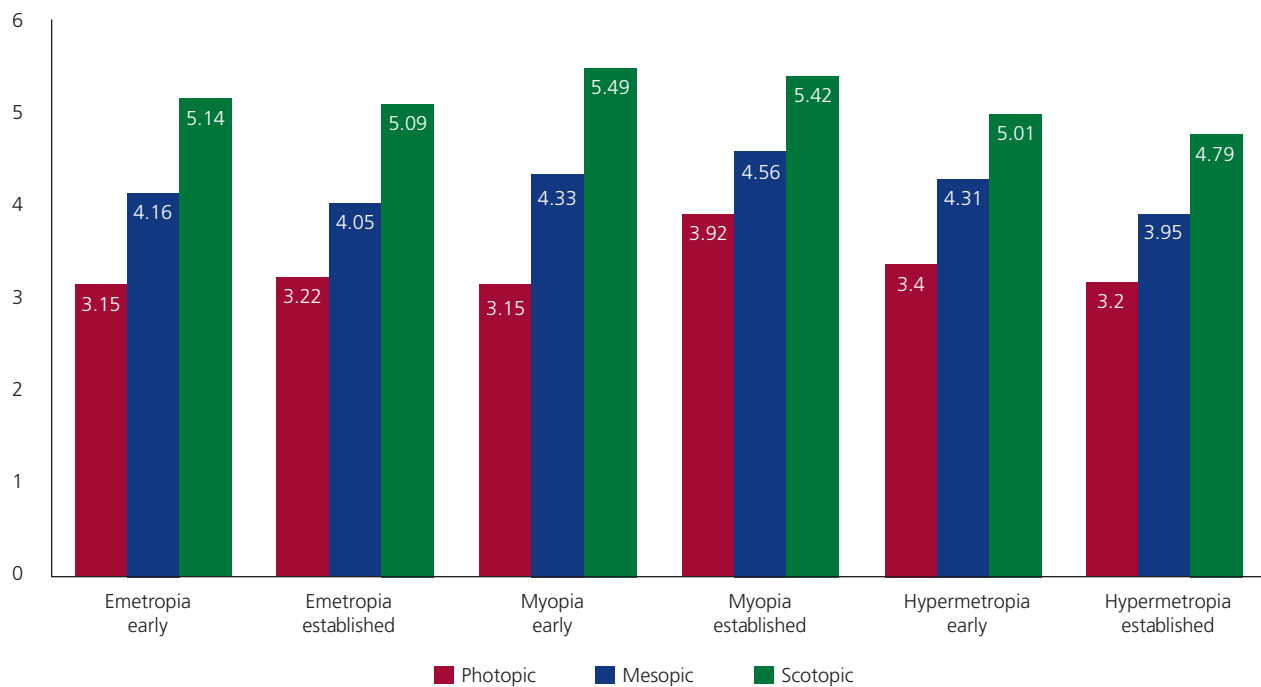


**Figure 1.** Change in pupil size with age in all three conditions.

diameter measurement data obtained were not related to gender, laterality or dominance.

In the human eye, the pupil diameter ranges from about 2 to 8 mm.<sup>[3]</sup> Pupil diameter has a great influence on the optical transfer function of the eye. It has a direct effect on retinal illumination, which affects the depth of field and contrast sensitivity.<sup>[1]</sup> In the first studies on pupil size, it was shown that the strongest determinant factor for the patient was age. Birren et al.<sup>[11]</sup> reported a nonlinear decrease in pupil size with age; however, the effect of changes in illumination level was not investigated in their study. Winn et al.<sup>[12]</sup> measured pupil size under different light levels in their study of 91 patients aged 17 to 83 years and found that for each brightness level, pupil width decreased linearly with age. And, they were the first team to take age into account when formulating it. Subsequent large population studies confirmed the inverse relationship between age and pupil size under various illumination levels.<sup>[10,13]</sup> However, in our study, pupil diameter did not change with age in all three conditions in emmetropic eyes. Pupil diameter decreased with age in hyperopia in all three conditions. While the photopic and mesopic pupil diameters increased with age in myopics, the scotopic diameter remained the same. We suspect that the different results were due to the comparison of subgroups formed according to the refractive errors of the patients in our study. It is also possible that the results were different because the age group was a presbyopic population. Guillon et al.<sup>[14]</sup> noted age progression as an important factor in decreasing pupil diameter. But overall, the difference was only significant between early presbyopia and established presbyopia patients. They noticed that the pupil size decreased significantly with increasing age, and the effect of age was more pronounced at low brightness.

Different results have been obtained in studies on the effect of refractive error on pupil diameter. Hirsch and Weymouth<sup>[15]</sup> conducted the first study investigating the relationship between refractive error and pupillary width, and reported that hyperopics had a smaller pupil diameter than myopics. Winn et al.<sup>[12]</sup> reported in their study that there was no significant relationship between refractive error and pupil size in the population consisting of myopia, emmetropia and hyperopia; however, the groups were not age matched in this study, with hyperopics being an average of 10 years older than myopics and emmetropics, so the age difference may therefore have been a confounding factor. Two studies which are involving a large number of refractive surgery candidates reported that preoperative refractive status is a determining factor in pupil size when measured under mesopic conditions, with smaller pupil sizes in hyperopics.<sup>[6,16]</sup> Yazdani et al.<sup>[17]</sup>

reported that the pupil size was larger in myopics than in emmetropes in all light conditions. Truong et al.<sup>[18]</sup> emphasized that pupil sizes are affected only in high refractive errors. Cakmak et al.<sup>[5]</sup> found higher values in the myopic and astigmatic groups and lower values in the hypermetropic group in patients who had a mesopic pupil diameter before refractive surgery. In our study, the mean value of the hypermetropic group was higher in photopic measurements in early presbyopia patients compared to the other two groups. In scotopic measurements, the mean value of the myopic group was found to be significantly higher than the emmetropic and hyperopic groups. No difference was observed in the comparison of mesopic measurements in all three groups. In the established presbyopic group, myopic pupil diameter was found to be higher in all lighting conditions compared to emmetropic and hypermetropic pupils. There was a statistically significant difference only in the scotopic condition when comparing the emmetropic and hypermetropic groups. Guillon et al.<sup>[14]</sup> also noted in their study that when both age and refractive error were taken separately, the largest differences in pupil diameter between age groups and between refractive conditions were recorded at low luminance, and the differences diminished as luminosity increased. The smallest pupil diameter was measured in hyperopia and the largest in myopia. Although refractive error was not a significant factor only, the largest differences in pupil diameter occurred between low-brightness myopes and emmetropes.

There are some limitations in the study. Our study was conducted in the population over 40 years of age; different results may occur for younger individuals and children. There was no advanced myopia or hyperopia in our patient groups; results may vary in high myopia and hyperopia. The individuals we investigated were completely healthy; different results may be encountered in patients with systemic diseases such as diabetes and hypertension, in neuropsychiatric patient groups, or in those who use systemic medication. In addition, studies on pupil diameter can be performed in patients with various eye diseases such as dry eye, keratoconus, different types of glaucoma, strabismus, nystagmus and amblyopia, or in subjects with a history of eye surgery.

## Conclusion

As the luminance is the most influential factor in determining pupil diameter, it is not surprising that the smallest pupil size was measured at high luminance levels. Larger values were obtained for myopia and younger individuals, and these differences were pronounced the most at low brightness levels. Multifocal contact lenses

and intraocular multifocal lenses are routinely used in myopia, presbyopia, and hyperopia and they must provide good visual performance in various brightness conditions. Because pupil size plays a crucial role in visual performance, the results of this study support that the effects of patient age and refractive status on pupil diameter are important in optimal lens design.

### Conflict of Interest

Authors have no conflict of interest to declare.

### Author Contributions

TY: project development, data analyses, manuscript writing; FÖ: project development, data collection, manuscript editing.

### Ethics Approval

Approval for this study was obtained from a local ethics committee.

### Funding

This research did not receive any specific grant from funding agencies in the public, commercial, or not-for-profit sectors.

### References

- Sulutvedt U, Zavagno D, Lubell J, Leknes S, de Rodez Benavent SA, Laeng B. Brightness perception changes related to pupil size. *Vision Res* 2021;178:41–7.
- Whang AJ, Chen YY, Tseng WC, Tsai CH, Chao YP, Yen CH, Liu CH, Zhang X. Pupil size prediction techniques based on convolution neural network. *Sensors (Basel)* 2021;21:4965.
- Zeile AJ, Gamlin PD. Editorial: the pupil: behavior, anatomy, physiology and clinical biomarkers. *Front Neurol* 2020;11:211.
- Oster J, Huang J, White BJ, Radach R, Itti L, Munoz DP, Wang CA. Pupillary responses to differences in luminance, color and set size. *Exp Brain Res* 2022;240:1873–85.
- Cakmak HB, Cagil N, Simavli H, Duzen B, Simsek S. Refractive error may influence mesopic pupil size. *Curr Eye Res* 2010;35:130–6.
- Robl C, Sliesoraityte I, Hillenkamp J, Prahns P, Lohmann CP, Helbig H, Herrmann WA. Repeated pupil size measurements in refractive surgery candidates. *J Cataract Refract Surg* 2009;35:2099–102.
- Salz JJ, Trattler W. Pupil size and corneal laser surgery. *Curr Opin Ophthalmol* 2006;17:373–9.
- Alarcón A, Rubiño M, Pééérez-Ocón F, Jiménez JR. Theoretical analysis of the effect of pupil size, initial myopic level, and optical zone on quality of vision after corneal refractive surgery. *J Refract Surg* 2012;28:901–6.
- Monsálvez-Romín D, González-Méijome JM, Esteve-Taboada JJ, García-Lázaro S, Cerviño A. Light distortion of soft multifocal contact lenses with different pupil size and shape. *Cont Lens Anterior Eye* 2020; 43:130–6.
- Kiel M, Grabitz SD, Hopf S, Koeck T, Wild PS, Schmidtman I, Lackner KJ, Münzel T, E Beutel ME, Pfeiffer N, Schuster AK. Distribution of pupil size and associated factors: results from the population-based Gutenberg health study. *J Ophthalmol* 2022;9520512: 1–8.
- Birren J, Casperson RC, Botwinick J. Age changes in pupil size. *J Gerontol* 1950;5:216–21.
- Winn B, Whitaker D, Elliott DB, Phillips NJ. Factors affecting light-adapted pupil size in normal human subjects. *Invest Ophthalmol Vis Sci* 1994;35:1132–7.
- Lee YS, Kim HJ, Lim DK, Kim MH, Lee KJ. Age-specific influences of refractive error and illuminance on pupil diameter. *Medicine (Baltimore)* 2022;101:e29859.
- Guillon M, Dumbleton K, Theodoratos P, Gobbe D, Wooley CB, Moody K. The effects of age, refractive status, and luminance on pupil size. *Optom Vis Sci* 2016;93:1093–100.
- Hirsch MJ, Weymouth FW. Pupil size in ametropia. *J Appl Physiol* 1949;1:646–8.
- Salz JJ, Trattler W. Pupil size and corneal laser surgery. *Curr Opin Ophthalmol* 2006;17:373–9.
- Yazdani N, Sharif M, Karimpour N, Asieh ME. Assessment of the pupil size in emmetropic and myopic eyes. *Reviews in Clinical Medicine* 2020;7:110–3.
- Truong JQ, Joshi NR, Ciuffreda KJ. Influence of refractive error on pupillary dynamics in the normal and mild traumatic brain injury (mTBI) populations. *J Optom* 2018;11:93–102.

#### ORCID ID:

T. Yılmaz 0000-0002-4502-4423;  
F. Özçelik 0000-0001-7153-2950



#### Correspondence to:

Tolga Yılmaz, MD  
Department of Ophthalmology, Beyoğlu Eye Training and  
Research Hospital, İstanbul, Türkiye  
Phone: +90 505 258 19 54  
e-mail: dr.tolgayilmaz@hotmail.com

*Conflict of interest statement:* No conflicts declared.

This is an open access article distributed under the terms of the Creative Commons Attribution-NonCommercial-NoDerivs 4.0 Unported (CC BY-NC-ND4.0) Licence (<http://creativecommons.org/licenses/by-nc-nd/4.0/>) which permits unrestricted noncommercial use, distribution, and reproduction in any medium, provided the original work is properly cited. *How to cite this article:* Yılmaz T, Özçelik F. The influence of brightness, age and refractive errors on pupil size. *Anatomy* 2022;16(3):146–151.

# Investigation of the relationship between inflammatory markers and grade of disease in patients with acute ischemic stroke with partial anterior circulation infarct

Sadettin Ersoy<sup>1</sup> , Canan Akünel Türel<sup>1</sup> , Ömer Çetin<sup>2</sup> 

<sup>1</sup>Department of Neurology, Faculty of Medicine, Bolu Abant İzzet Baysal University, Bolu, Türkiye

<sup>2</sup>Department of Emergency Medicine, Faculty of Medicine, Bolu Abant İzzet Baysal University, Bolu, Türkiye

## Abstract

**Objectives:** The aim of this study was to investigate the relationship between National Institutes of Health Stroke Scale scores and Glasgow coma scores of patients with partial anterior ischemic stroke and laboratory results, particularly serum CRP, albumin, platelet and other complete blood count data, and prognosis.

**Methods:** In this retrospective study 226 of patients with partial anterior circulation infarction who were admitted to the Bolu Abant İzzet Baysal University Neurology Clinic between January 2021 and 2022 with the diagnosis of acute ischemic stroke and hospitalized within the first 24 hours were investigated. The demographic data, stroke etiology and risk factors, National Institutes of Health Stroke Scale, Glasgow coma scores, complete blood count, certain inflammatory markers and biochemical parameters, length of hospital stay and mortality rates were examined. And the relationship between inflammatory markers and grade of disease was evaluated statistically.

**Results:** The patients with moderate Glasgow coma score had a lower lymphocyte level, severe patients had higher PCT level and moderate patients had higher CRP level among others. Patients with moderate GCS had higher CRP/ALB values than those with mild. Patients with moderate and moderate-severe National Institutes of Health Stroke Scale had higher RBC and HGB levels than the patients with mild. Moderate-severe patients had lower albumin levels.

**Conclusion:** CRP-albumin ratio, serum platelet and serum albumin levels may have prognostic value in acute partial anterior ischemic stroke patients.

**Keywords:** albumin; CRP-albumin ratio; HDL-uric acid ratio; stroke

Anatomy 2022;16(3):152–158 ©2022 Turkish Society of Anatomy and Clinical Anatomy (TSACA)

## Introduction

Acute ischemic stroke (AIS) ranks first among the emergent neurological diseases and stroke is the second most common cause of death after acute cardiac diseases worldwide.<sup>[1]</sup> With the aging of the human population, the importance of stroke continues to increase day by day since it is a significant cause of mortality, morbidity and economic burden in advanced age.<sup>[2]</sup>

Low HDL cholesterol levels are associated with impaired metabolic status and cerebrovascular risk.<sup>[3]</sup> Uric acid is a product of purine metabolism, and high serum levels are associated with impaired metabolic states and increased cerebrovascular risk.<sup>[4]</sup> C-reactive protein (CRP)

is an acute phase protein produced by the activation of cytokines secondary to ischemia, infection, trauma and other inflammatory conditions.<sup>[5]</sup> Again, low serum albumin levels were found to be associated with poor prognosis and mortality.<sup>[6,7]</sup> The combination of these two metabolic parameters was thought to be a good predictor of stroke risk.<sup>[8]</sup> The use of simple parameters measured in serum is important in terms of prognosis and evaluation of recurrent stroke risk factors of patients, since they are both cost-effective and easy to use.<sup>[2,9,10]</sup> For these reasons, we aimed to investigate the relationship between degree of the disease and inflammatory markers in stroke patients with acute partial anterior circulation infarction.

## Materials and Methods

Medical files of 226 of patients (105 females, 121 males) aged between 41–97 (median: 75, IQR: 65–83) with partial anterior circulation infarction who were admitted to the Bolu Abant İzzet Baysal University Neurology Clinic between January 2021 and 2022 with the diagnosis of acute ischemic stroke and hospitalized within the first 24 hours were investigated retrospectively. The demographic data, stroke etiology and risk factors, National Institute of Health Stroke Scale (NIHSS), Glasgow coma score (GCS), modified ranking scale (mRS) at the time of admission to the hospital, complete blood count parameters, CRP, albumin (alb), uric acid, HDL, AST, CRP/albumin, HDL/uric acid values, length of hospital stay and mortality rates were examined. Patients were grouped under 3 categories according to their GCS as severe (3–8), moderate (9–12) and mild (13–15). According to the GCS; 131 were mild, 81 were moderate, and 14 were severe. The patients were further grouped under 5 according to their NIHSS as asymptomatic (0), mild (1–4), moderate (5–15), moderate-severe (16–20) and severe (21–42). According to the NIHSS, 60 were mild, 141 were moderate, 22 were moderate-severe, and 3 were severe. There were no asymptomatic patients. Those who had previously been diagnosed with cancer and those with other neurological diseases were not included in the study.

Continuous data were compared using Student's t-test, Mann-Whitney U test or Kruskal-Wallis test and categorical data were compared using Pearson's chi-squared test or Fisher's exact test. In order to determine the factors affecting mortality and length of stay, multiple logistic regression (forward Wald method) and multiple linear regression analyses were applied. Parameters with a simple analysis result of  $p < 0.20$  were included in the multiple model. Log-transform was applied on length of stay to the normality of the residual's assumption. SPSS (Version 23.0, IBM Corp., Armonk, NY, USA) was used for the analyses. Significance level was determined as  $p < 0.05$ .

## Results

Among the other diseases accompanying the stroke, the most common comorbid factor was hypertension (51.77%) (Table 1).

The patients with moderate and severe GCS had a higher mRS of 3 and above than those with mild ( $p < 0.001$ ). The patients with moderate GCS a lower lymphocyte (LYM) level, severe patients had higher PCT level and moderate patients had higher CRP level among others ( $p = 0.049$ ,  $p = 0.029$  and  $p = 0.001$ , respectively). Patients with moderate GCS had higher CRP/ALB values than those with mild ( $p = 0.001$ ). Patients with GCS

severe stayed in hospital for a shorter time than other GCS groups ( $p < 0.001$ ) (Table 2).

Patients with moderate, moderate-severe and severe NIHSS had a higher mRS of 3 and above than mild ones ( $p < 0.001$ ). Patients with moderate and moderate-severe NIHSS had higher RBC and HGB levels than the patients with mild NIHSS ( $p < 0.001$  and  $p = 0.008$ , respectively). Moderate-severe patients had lower albumin levels ( $p = 0.010$ ). It was observed that the AST level was higher in patients with moderate than those with mild ( $p = 0.022$ ). As the NIHSS scores increased, the patients stayed in the hospital longer ( $p < 0.001$ ) (Table 3).

Mortality rate was lower in patients with mild GCS and higher in patients with severe ( $p < 0.001$ ). Mortality rate was higher in patients with mRS of 3 and above ( $p = 0.016$ ). PLT, MONO, PCT, albumin levels were found to be higher and MCV levels were lower in patients who died ( $p = 0.003$ ,  $p = 0.007$ ,  $p = 0.006$ ,  $p = 0.010$  and  $p = 0.047$ , respectively) (Table 4).

The mortality risk was found to be 21.05 (95% CI: 5.4–82.04) times higher in patients with GCS severe ( $p < 0.001$ ). It was concluded that a one-unit increase in MONO caused a 3.72 (95% CI: 1.1–12.6) fold increase in mortality risk ( $p = 0.035$ ). In the mortality estimation model, the overall accuracy rate was 91.2%, sensitivity 20%, specificity 98.1%. The factors affecting the length of stay in the hospital were determined as GCS (mild group), NIHSS (Moderate and Moderate-Severe), LYM, NEU and RDW. The coefficients shared in Table 5 was determined for log-transformed hospitalization time. After applying the back transformation; it was determined that the hospitalization times increased

**Table 1**  
Characteristics of the patients.

	n	%
<b>Additional disease</b>		
Hypertension	117	51.77
Diabetes	69.0	30.53
Hyperlipidemia	18	7.96
Coronary disease	52	23.01
MI/stroke	45	19.91
Atrial fibrillation	71	31.42
Chronic kidney disease	6	2.65
Pulmonary hypertension	1	0.44
<b>Smoking history</b>	31	13.72
<b>Modified ranking scale score</b>		
<3	78	35
≥3	148	65

**Table 2**  
Comparison of data according to Glasgow coma score.

	Mild (n=131)	Moderate (n=81)	Severe (n=14)	p-value
Age (year)	76.5 (58.25–80.75)	73 (64–83.5)	75 (66–82)	0.929
Sex (female)	5 (35.71)	46 (56.79)	54 (41.22)	0.062
Hypertension	8 (57.14)	38 (46.91)	71 (54.2)	0.539
Diabetes	5 (35.71)	23 (28.4)	41 (31.3)	0.824
Hyperlipidemia	1 (7.14)	6 (7.41)	11 (8.4)	0.960
Coronary disease	3 (21.43)	22 (27.16)	27 (20.61)	0.540
MI/stroke	2 (14.29)	14 (17.28)	29 (22.14)	0.596
Atrial fibrillation	3 (21.43)	31 (38.27)	37 (28.24)	0.220
Chronic kidney disease	1 (7.14)	1 (1.23)	4 (3.05)	0.283 <sup>†</sup>
Pulmonary hypertension	1 (7.14)	0 (0)	0 (0)	-
Smoking	1 (7.14)	8 (9.88)	22 (16.79)	0.277
mRS				
<3	73 (55.73) <sup>a</sup>	5 (6.17) <sup>b</sup>	0 (0) <sup>b</sup>	<0.001
≥3	58 (44.27) <sup>b</sup>	76 (93.83) <sup>a</sup>	14 (100) <sup>a</sup>	
WBC	8.74 (6.81–10.9)	8.96 (7.19–11.7)	10.02 (8.83–11.87)	0.158
RBC*	4.7±0.63	4.47±0.74	4.69±0.69	0.053
HGB*	13.49±1.73	12.94±2.46	12.9±2.56	0.145
PLT	229 (192–276)	233 (195.5–284)	266.5 (211.25–398.75)	0.087
MCV	88.2 (84.8–91.9)	88.2 (84.4–91.3)	86.05 (81.83–90.33)	0.328
RDW	13.9 (12.9–15.8)	13.8 (12.9–15.7)	13.75 (12.68–17.05)	0.997
LYM	1.71 (1.25–2.21) <sup>a</sup>	1.5 (0.94–2.06) <sup>b</sup>	1.74 (1.1–2.68) <sup>a,b</sup>	0.049
MONO	0.59 (0.47–0.84)	0.63 (0.5–0.79)	0.77 (0.53–0.93)	0.313
NEU	5.81 (3.94–7.8)	6.65 (4.61–8.84)	6.71 (5.27–10.23)	0.109
BASO	0.05 (0.03–0.07)	0.05 (0.02–0.06)	0.05 (0.03–0.06)	0.532
EOS	0.11 (0.04–0.21)	0.08 (0.03–0.18)	0.07 (0.05–0.14)	0.244
PDW	13.7 (11.5–17.2)	12.9 (11.25–16.2)	11.4 (10.83–13.93)	0.134
MPV	10.2 (9.1–11.1)	10.4 (9.55–11.2)	10.05 (9.47–10.33)	0.487
PCT	0.22 (0.18–0.27) <sup>b</sup>	0.25 (0.19–0.3) <sup>a,b</sup>	0.26 (0.21–0.39) <sup>a</sup>	0.029
CRP	4.3 (0.7–11) <sup>b</sup>	10.3 (2.35–43.7) <sup>a</sup>	7.6 (0.58–14.5) <sup>a,b</sup>	0.001
Albumin	40 (37.2–42.8)	38.8 (34.5–42.6)	40 (32.08–43.63)	0.116
Uric acid	5.4 (4.5–6.4)	5.3 (4.5–6.75)	6.2 (5.2–7.05)	0.338
HDL	43 (37–51.4)	43.1 (36.95–49.1)	43.5 (37.68–53.88)	0.919
AST	21 (17–25)	22 (17–32)	20 (17.5–25.75)	0.341
CRP/albumin	1.17 (0.16–3) <sup>b</sup>	2.59 (0.57–11.45) <sup>a</sup>	2.13 (0.17–3.84) <sup>a,b</sup>	0.001
HDL/uric acid	7.95 (6.55–10.7)	8.13 (5.83–10.91)	7.45 (5.66–10.81)	0.824
Hospital stay	8 (4.5–15.5) <sup>a</sup>	6 (4–12) <sup>a</sup>	4 (2–7) <sup>b</sup>	<0.001

Continuous data were summarized as median (IQR, 25th–75th percentile) and analyzed with Kruskal-Wallis test (post-hoc Dunn test). Qualitative data were summarized by frequency and percentage and analyzed using Pearson's chi-squared test (post-hoc adj. Bonferroni method). \*Data were summarized as mean±sd (one-way ANOVA). <sup>†</sup>Fisher's exact test. <sup>a,b</sup>According to the results of the post-hoc tests, different letters indicate a significant difference between the groups, p<0.05.

approximately 24.85% and 97% in NIHSS moderate and moderate-severe group, and 25% decreased in GCS moderate group, respectively. A 1-unit increase in LYM and RDW values resulted in an approximately 25% and 4.6% decrease in the length of hospital stay, and a 1-unit increase in neu value resulted in 9.7% increase in the length of hospital stay (Table 5).

## Discussion

The main target of our study was to determine the relationship between inflammatory markers and grade of disease in patients with acute ischemic stroke with partial anterior circulation infarct. According to the results of our study, CRP-albumin ratios and HDL-uric acid ratios did not have a statistically significant relationship with

**Table 3**  
Comparison of data according to National Institute of Health Stroke Scale (NIHSS) stroke score.

	Mild (n=60)	Moderate (n=141)	Moderate-Severe (n=22)	Severe† (n=3)	p-value
Age (year)	74.5 (65.25–81.75)	74 (64.5–82)	81.5 (67–86.25)	59 (47–79)	0.573
Sex (female)	22 (36.67)	72 (51.06)	11 (50)	0 (0)	0.100
Hypertension	32 (53.33)	75 (53.19)	10 (45.45)	0 (0)	0.349
Diabetes	14 (23.33)	49 (34.75)	5 (22.73)	1 (33.33)	0.309
Hyperlipidemia	4 (6.67)	12 (8.51)	1 (4.55)	1 (33.33)	0.381
Coronary disease	16 (26.67)	31 (21.99)	5 (22.73)	0 (0)	0.791
MI/stroke	11 (18.33)	30 (21.28)	4 (18.18)	0 (0)	0.951
Atrial fibrillation	17 (28.33)	45 (31.91)	9 (40.91)	0 (0)	0.555
Chronic kidney disease	0 (0)	5 (3.55)	1 (4.55)	0 (0)	0.319
Pulmonary hypertension	0 (0)	0 (0)	1 (4.55)	0 (0)	-
Smoking	6 (10)	24 (17.02)	1 (4.55)	0 (0)	0.334
mRS					
<3	51 (85) <sup>a</sup>	24 (17.02) <sup>b</sup>	3 (13.64) <sup>b</sup>	0 (0) <sup>b</sup>	<0.001
≥3	9 (15) <sup>b</sup>	117 (82.98) <sup>a</sup>	19 (86.36) <sup>a</sup>	3 (100) <sup>a</sup>	
WBC	8.78 (6.76–10.6)	8.86 (6.93–10.99)	9.74 (7.31–12.07)	9.26 (9.14–14.25)	0.386
RBC*	4.83 (4.45–5.25) <sup>a</sup>	4.51 (4.07–5.02) <sup>b</sup>	4.41 (4.05–4.75) <sup>b</sup>	5.3±0.64	<0.001
HGB*	13.8 (12.8–15.08) <sup>a</sup>	12.8 (11.6–14.6) <sup>b</sup>	12.65 (11.88–14.2) <sup>b</sup>	15.27±2.1	0.008
PLT	238 (196–278.75)	231 (193–284)	234 (206.25–279)	319 (197–544)	0.929
MCV	88.35 (84.7–91.88)	88.1 (84.5–91.3)	89.4 (84.9–93.65)	86.1 (81.1–88.1)	0.620
RDW	13.85 (12.9–15.7)	14.1 (12.85–15.8)	14.05 (12.9–15.85)	12.7 (11.5–12.8)	0.850
LYM	1.86 (1.22–2.45)	1.67 (1.16–2.15)	1.58 (1.05–1.8)	1.43 (1.11–1.66)	0.172
MONO	0.6 (0.48–0.88)	0.62 (0.49–0.79)	0.58 (0.45–0.82)	0.67 (0.46–0.98)	0.793
NEU	5.54 (3.9–7.42)	6.05 (4.44–8.5)	7.1 (5.09–10.61)	6.68 (6.24–12.62)	0.153
BASO	0.05 (0.03–0.08)	0.05 (0.03–0.06)	0.04 (0.02–0.05)	0.05 (0.02–0.06)	0.074
EOS	0.11 (0.04–0.24)	0.1 (0.04–0.18)	0.06 (0.01–0.15)	0.15 (0.01–0.51)	0.164
PDW	13.55 (11.33–17.3)	13 (11.35–16.75)	13.65 (10.85–17.68)	11.2 (10.2–11.6)	0.606
MPV	10.15 (8.45–10.7)	10.3 (9.5–11.2)	10.15 (9.35–10.83)	10.2 (9.7–10.3)	0.216
PCT	0.22 (0.18–0.28)	0.24 (0.19–0.3)	0.25 (0.19–0.28)	0.33 (0.2–0.53)	0.450
CRP	4.25 (1–11.23)	5.8 (1.3–17.65)	9.2 (2.75–45.3)	20.8 (1.8–43.5)	0.095
Albumin	40.2 (38–43) <sup>a</sup>	39.1 (36–42.7) <sup>a</sup>	36 (31.5–40.45) <sup>b</sup>	39 (29–45)	0.010
Uric acid	5.6 (4.63–6.88)	5.3 (4.5–6.4)	5.7 (4.33–7.53)	6.4 (2.5–7.6)	0.162
HDL	43 (37.18–52.68)	43 (37–49.95)	42.6 (38.05–48.5)	38.3 (23.6–47.2)	0.966
AST	19.5 (16–24) <sup>b</sup>	22 (18–31) <sup>a</sup>	21.5 (18.5–25.75) <sup>a,b</sup>	23 (19–37)	0.022
CRP/albumin	1.07 (0.25–2.94)	1.4 (0.32–4.73)	2.49 (0.7–15.2)	5.33 (0.4–15)	0.072
HDL/uric acid	7.29 (6.11–10.52)	8.14 (6.43–10.85)	8.09 (5.58–10.95)	7.38 (5.04–9.44)	0.398
Hospital stay	3 (2–6) <sup>a</sup>	5 (3–9) <sup>b</sup>	10 (6–18.25) <sup>c</sup>	11 (2–0)	<0.001

Continuous data were summarized as median (IQR, 25th–75th percentile) and analyzed with Kruskal-Wallis test (post-hoc Dunn test). Qualitative data were summarized by frequency and percentage and analyzed using Fisher’s exact test (post-hoc adj. Bonferroni method). \*Data were summarized as mean±sd (one-way ANOVA). †Continuous data could not be compared due to insufficient number of observations. <sup>a,b,c</sup>According to the results of the post-hoc tests, different letters indicate a significant difference between the groups, p<0.05.

NIHSS and mortality. However, the CRP-albumin ratio had a significant relationship only between the mild and moderate GCS groups. It was previously shown that CAR ratio may be a predictor of mortality in ischemic stroke patients.<sup>[11]</sup> Although it was mentioned that CAR ratio would be a better predictor than only serum albumin

and serum CRP levels alone. Our study revealed that only albumin ratio was correlated with NIHSS and thus can be suggested as a better predictor than CAR ratio. PCT, which is one of the complete blood count parameters, draws attention because it is associated with both the NIHSS and the mortality rate. The limitation

**Table 4**  
Comparison of data with mortality.

	Survived (n=206)	Dead (n=20)	p-value
Age (year)	75 (65–83)	75.5 (64.75–82.75)	0.974
Sex (female)	94 (45.63)	11 (55)	0.423
Hypertension	109 (52.91)	8 (40)	0.270
Diabetes	60 (29.13)	9 (45)	0.141
Hyperlipidemia	18 (8.74)	0 (0)	0.380†
Coronary disease	47 (22.82)	5 (25)	0.785
MI/stroke	40 (19.42)	5 (25)	0.560
Atrial fibrillation	64 (31.07)	7 (35)	0.718
Chronic kidney disease	5 (2.43)	1 (5)	0.430†
Pulmonary hypertension	0 (0)	1 (5)	-
Smoking	30 (14.56)	1 (5)	0.324†
GCS			
Mild	125 (60.68) <sup>a</sup>	6 (30) <sup>b</sup>	<0.001
Moderate	74 (35.92) <sup>a</sup>	7 (35) <sup>a</sup>	
Severe	7 (3.4) <sup>b</sup>	7 (35) <sup>a</sup>	
NIHSS			
Mild	58 (28.16)	2 (10)	0.090**
Moderate	127 (61.65)	14 (70)	
Moderate-severe	19 (9.22)	3 (15)	
Severe	2 (0.97)	1 (5)	
mRS			
<3	76 (36.89)	2 (10)	0.016
≥3	130 (63.11)	18 (90)	
WBC	8.83 (6.97–10.95)	9.85 (8.47–18.04)	0.057
RBC*	4.62±0.69	4.61±0.58	0.942
HGB*	13.33±2.07	12.49±2.07	0.086
PLT	228 (192–278)	276.5 (242.25–580)	0.003
MCV	88.15 (84.78–91.83)	85.6 (79.5–93.6)	0.047
RDW	13.8 (12.88–15.63)	14.95 (12.83–22.4)	0.268
LYM	1.63 (1.15–2.15)	1.74 (1.26–3.93)	0.316
MONO	0.6 (0.47–0.8)	0.8 (0.62–1.58)	0.007
NEU	5.96 (4.44–8.36)	7.59 (4.59–12.96)	0.180
BASO	0.05 (0.03–0.06)	0.05 (0.02–0.14)	0.997
EOS	0.1 (0.04–0.18)	0.07 (0.04–0.59)	0.497
PDW	13.1 (11.3–17.1)	12.25 (10.93–18.2)	0.132
MPV	10.2 (9.35–11)	10.2 (9.5–11.9)	0.957
PCT	0.23 (0.18–0.28)	0.3 (0.21–0.45)	0.006
CRP	5.4 (1.38–15.63)	11.9 (4.3–110.1)	0.084
Albumin	40 (36.45–43)	36.25 (32.7–46)	0.010
Uric acid	5.4 (4.5–6.6)	5.15 (4.43–40)	0.707
HDL	43 (37–51.4)	41.15 (36.33–63)	0.329
AST	21.5 (17–26)	21.5 (16.5–124)	0.747
CRP/albumin	1.3 (0.33–4.27)	3.18 (1.13–32.38)	0.074
HDL/uric acid	8.03 (6.08–10.72)	7.57 (6.43–17.41)	0.759

Continuous data were summarized as median (IQR, 25th–75th percentile) and analyzed with Mann-Whitney U test. Qualitative data were summarized by frequency and percentage and analyzed using Pearson's chi-squared test (post-hoc adj. Bonferroni method). \*Data were summarized as mean±sd and analyzed by Student's t-test. †Fisher's exact test.

**Table 5**

Multiple regression analyzes for mortality, multiple linear regression analyzes for length of hospital stay (LOS).

		Mortality			Ln(LOS)		
		Odds	Odds 95% CI	p-value	β(se)	Std. β	p-value
GCS	Mild	(Ref.)			-0.29 (0.11)	-0.18	0.008
	Moderate	2.22	0.7–7.1	0.177	-	-	-
	Severe	21.05	5.4–82.04	<0.001	-	-	-
NIHSS	Mild	-	-	-	-	-	-
	Moderate	-	-	-	0.22 (0.11)	0.14	0.055
	Moderate-severe	-	-	-	0.68 (0.2)	0.25	0.001
	Severe	-	-	-	-	-	-
LYM					-0.1 (0.06)	-0.11	0.070
NEU					0.06 (0.01)	0.23	0.000
MONO		3.72	1.1–12.6	0.035			
RDW		-	-	-	-0.05 (0.02)	-0.14	0.016
Model summary		Nagelkerke R <sup>2</sup> = 0.22; ACC: 91.2%, SE: 20%, SP: 98.1%			Adjusted R <sup>2</sup> : 0.22; Model: F=11.85, p<0.001		

ACC: accuracy; β(se): model coefficient (standart error); Ln(LOS): logarithmic transformation of length of stay; SE: sensitivity; SP: specificity.

of our study was low number of severe cases included to our study. We suggest this condition should be evaluated in more details in studies with higher number of severe cases. The decrease in albumin level in some chronic diseases and the fact that it is affected by conditions such as malnutrition may limit its use in such patients. Due to insufficient data, we could not exclude patients with malnutrition in our study. Although, since the prognosis of patients with malnutrition would be worse after stroke, it may not have adversely affected our results.

The results of study showed that serum CRP-value did not correlate with NIHSS. It did only show statistically significant difference in patients with moderate and mild GCS scores, similar to previous studies. In a previous study, CRP-value at admission was not found to be associated with prognosis, while serum CRP-values during follow-up were found to be associated with prognosis.<sup>[12]</sup> In another study, it was shown that the serum platelet value of the patient may be related to the prognosis in ischemic stroke.<sup>[13]</sup> In our study, we found that mortality rates were correlated with high serum platelet levels. Serum MONO and MCV levels were also correlated with mortality. As a result of our findings, we thought that CAR, serum albumin, PCT, PLT, MONO and MCV levels could be predictors that can be evaluated while regulating the treatment of patients. We found that neutrophil-lymphocyte ratio, HDL-uric acid ratio, and lymphocyte-monocyte ratios, which are frequently

studied in other diseases recently, were not correlated with GCS and NIHSS.

In conclusion, since these parameters are easily accessible and cost-effective, it is important to guide the prognosis and it will be beneficial to studies conducted in larger case series.

### Conclusion

In conclusion, since these parameters are easily accessible and cost-effective, it is important to guide the prognosis and it will be beneficial to studies conducted in larger case series.

### Acknowledgments

The authors would like to express their sincere gratitude to the volunteers.

### Conflict of Interest

The authors declare no conflict of interest.

### Author Contributions

SE: project development, data analysis, drafting the article; CAT: data collection, data analysis, drafting the article, revising it critically for important intellectual content; ÖÇ: data collection, data analysis, drafting the article. All authors approved the final of the version to be published, agree to be accountable for all aspects of the work if questions arise related to its accuracy or integrity.

## Ethics Approval

The study was approved by Ethical Committee of Bolu Abant İzzet Baysal University (No:2022-300).

## Funding

The authors declare no financial support.

## References

1. Güven HH, Çilliler AE, Sarıkaya SA, Köker C, Çomoğlu SS. The etiologic and prognostic importance of high leukocyte and neutrophil counts in acute ischemic stroke. *Journal of Neurological Sciences (Turkish)* 2010;27:311–8.
2. Guven H, Çilliler AE, Koker C, Sarıkaya SA, Comoglu SS. Association of serum calcium levels with clinical severity of acute ischemic stroke. *Acta Neurol Belg* 2011;111:45–9.
3. Dehghan A, van Hoek M, Sijbrands EJ, Hofman A, Witteman JCM. High serum uric acid as a novel risk factor for type 2 diabetes. *Diabetes Care* 2008;31:361–2.
4. Guerreiro S, Ponceau A, Toulorge D, Martin E, Alvarez-Fischer D, Hirsch EC, Michel PP. Protection of midbrain dopaminergic neurons by the end-product of purine metabolism uric acid: potentiation by low-level depolarization. *J Neurochem* 2009;109:1118–28.
5. Thijs LG, Hack CE. Time course of cytokine levels in sepsis. *Intensiv Care Med* 1995;21 Suppl 2:S258–63.
6. Artero A, Zaragoza R, Camarena JJ, Sancho S, Gonzalez R, Nogueira JM. Prognostic factors of mortality in patients with community-acquired bloodstream infection with severe sepsis and septic shock. *J Crit Care* 2010;25:276–81.
7. Goldwasser P, Feldman J. Association of serum albumin and mortality risk. *J Clin Epidemiol* 1997;50:693–703.
8. Demirel ME. The correlation of c-reactive protein/albumin, Mii-1 and Mii-2 indexes with hospitalization and mortality in Stanford type A aortic dissection. *Medical Records* 2022;4:361–6.
9. Demirel ME. Acute coronary syndromes and diagnostic methods. *Medical Research and Innovations* 2019;3:1–8.
10. Mert I, Cetinkaya A, Gurler M, Turel CA, Celik H, Torun IE, Turel I. Anti-inflammatory potential of liraglutide, a glucagon-like peptide-1 receptor agonist, in rats with peripheral acute inflammation. *Inflammopharmacology* 2022;30:1–13.
11. Kocatürk M, Kocatürk Ö. Assessment of relationship between C-reactive protein to albumin ratio and 90-day mortality in patients with acute ischaemic stroke. *Neurol Neurochir Pol* 2019;53:205–11.
12. Rocco A, Ringleb PA, Grittner U, Nolte CH, Schneider A, Nagel S. Follow-up C-reactive protein level is more strongly associated with outcome in stroke patients than admission levels. *Neurol Sci* 2015; 36:2235–41.
13. Yang M, Pan Y, Li z, Yan H, Zhao X, Liu L, Meng X, Wang Y, Wang Y. Platelet count predicts adverse clinical outcomes after ischemic stroke or TIA: subgroup analysis of CNSR II. *Frontiers in Neurology* 2019;10:370.

### ORCID ID:

S. Ersoy 0000-0003-0837-8756;  
C. Akünel Türel 0000-0001-8791-235X;  
Ö. Çetin 0000-0003-3588-2077



### Correspondence to:

Sadettin Ersoy, MD  
Department of Neurology, Faculty of Medicine,  
Bolu Abant İzzet Baysal University, Bolu, Türkiye  
Phone: +90 505 931 67 54  
e-mail: ersoysadettin@gmail.com

*Conflict of interest statement:* No conflicts declared.

This is an open access article distributed under the terms of the Creative Commons Attribution-NonCommercial-NoDerivs 4.0 Unported (CC BY-NC-ND4.0) Licence (<http://creativecommons.org/licenses/by-nc-nd/4.0/>) which permits unrestricted noncommercial use, distribution, and reproduction in any medium, provided the original work is properly cited. *How to cite this article:* Ersoy S, Akünel Türel C, Çetin Ö. Investigation of the relationship between inflammatory markers and grade of disease in patients with acute ischemic stroke with partial anterior circulation infarct. *Anatomy* 2022;16(3):152–158.

# White to white cornea diameter and mesopic pupil size in patients with keratoconus

Ferah Özçelik , Tolga Yılmaz , Güneş Gümüş 

Department of Ophthalmology, Beyoğlu Eye Training and Research Hospital, İstanbul, Türkiye

## Abstract

**Objectives:** Keratoconus is characterized by the abnormal cornea structure and it is manifested by changes in anterior segment parameters responsible for ocular high order spherical aberrations. The aim of the study is to investigate cornea horizontal white to white diameter and mesopic pupil size in patients with keratoconus.

**Methods:** The medical records of each participant were reviewed. The horizontal white to white cornea diameter and the mesopic pupil size were measured with the Sirius Topography System in 215 eyes of 123 subjects. Two groups were formed, the first group included 113 eyes with keratoconus and the second group is composed of 102 healthy eyes. Differences in sex, age, cornea diameter and mesopic pupil size between two groups were analyzed statistically.

**Results:** There were no statistically significant differences in sex and age distribution between the two groups ( $p>0.05$ ). The average horizontal corneal diameter was  $11.98\pm 0.33$  mm in the 1st group and  $11.81\pm 0.24$  mm in group 2. It was significantly higher in patients with keratoconus than in healthy subjects. ( $p=0.04$ ) The mean mesopic pupil size was  $3.64\pm 0.12$  mm in group 1 and it was  $3.73\pm 0.14$  mm in group 2. The mesopic pupil size was significantly higher in healthy subjects than in patients with keratoconus ( $p=0.03$ ).

**Conclusion:** This study showed that while the horizontal white to white diameter of the cornea increases in keratoconus, the mesopic pupil size decreases. In clinical practice, these two parameters should be considered in treatment procedures of patients with keratoconus.

**Keywords:** cornea topography; horizontal cornea diameter; keratoconus; mesopic pupil size

Anatomy 2022;16(3):159–164 ©2022 Turkish Society of Anatomy and Clinical Anatomy (TSACA)

## Introduction

Horizontal white-to-white corneal diameter or horizontal visible iris diameter (HVID) can be measured with various devices. Different methods ranging from simple measurements with a ruler to complex measurements with imaging devices led to varying normal values in study reports.<sup>[1,2]</sup> HVID is abnormal in some corneal diseases and glaucoma. Previously, HVID value assisted in determining macrocornea, microcornea, and screening glaucoma risk factors.<sup>[3]</sup> However, HVID has become essential in ophthalmic clinical practice, as it is critical to plan cataract and refractive surgery and calculate the power and diameter of phakic intraocular and contact lenses.<sup>[4,5]</sup> Pupil diameter should be checked for each patient. Pupil size is crucial because refractive corneal surgery, multifocal or toric contact lens wear, and intraocular multifocal lens implantation are completely

personalized treatments.<sup>[6]</sup> Before refractive surgery, most surgeons plan the effective ablation zone considering the mesopic pupil size. The mesopic pupil size and effective optical zone on the cornea are incompatible. This incompatibility causes troublesome symptoms such as ghost images, blurred vision, and frequently, glare and haloes.<sup>[7]</sup> Previous studies have shown that mesopic pupil size is related to the dimensions of other ocular structures.<sup>[8]</sup> Mesopic pupil size may also have a relationship with corneal diameters.

Keratoconus is a progressive non-inflammatory problem diagnosed with corneal ectasia and thinning in the central zone.<sup>[9]</sup> The abnormal corneal structure that develops from keratectasia leads to irregular astigmatism and reduces the quality of vision.<sup>[10]</sup> Cornea topographic indices are critical for assessing the severity and development of keratoconus. There is an insidious progression in

keratoconus over time. The corneal topography system can easily detect this progression. However, further clinical information is required to validate this progression. For example, to the best of our knowledge there is no direct study in the literature on the measurement of mesopic pupil size in keratoconus patients. Nevertheless, varying pupil diameters may increase spherical aberrations in these patients.<sup>[11]</sup> HVID is critical in contact lens examination in keratoconus patients, yet there is no direct study on HVID.

To our knowledge, no study has researched the relationship between mesopic pupil size and HVID in some diseases. Therefore, the aim of the present study was to analyze the mesopic pupil size and HVID in patients with keratoconus.

## Materials and Methods

This retrospective study took place at the Ophthalmology Department of a third-stage hospital following the ethical standards of the Declaration of Helsinki. The records of 123 subjects admitted to the Ophthalmology Department of Beyoğlu Eye Training and Research Hospital were retrospectively analyzed through the hospital's electronic database.

The medical records of each participant were reviewed. A comprehensive ophthalmologic examination included fundoscopic examination, slit lamp biomicroscopy, and distant best corrected visual acuity (D-BCVA) testing were performed. Emmetropia was defined as the mean spherical equivalent between +0.75 and -0.75 diopter (D). For HVID and mesopic pupil size measurements, we used the Sirius system, a Placido-based videokeratoscope with two Scheimpflug cameras, one central and one rotating (Costruzione Strumenti Oftalmici, Scandicci, Italy).

The diagnosis of keratoconus was made clinically and considering the topography values. While there were newly diagnosed keratoconus patients in group 1 and no treatment was applied, there were healthy control subjects

in group 2 whose age and sex distribution was compatible with group 1. Patients with a history of previous ocular or refractive surgery, ocular or systemic disease, or a history of ocular or systemic drugs that might affect pupil size were excluded. In addition, smokers and heavy alcohol drinkers (drinking five or more drinks on the same occasion on each of five or more days in the past 30 days) were also excluded.

The parameters of the study were also compared between the groups. The Kolmogorov-Smirnov test evaluated the distribution of the data. Chi-square test or paired sample t-test compared the data. The results for each parameter were in mean±standard deviation (SD). The Statistical Package for the Social Sciences version 20 (SPSS, Chicago, IL, USA) was used for data analysis. A value of  $p < 0.05$  was considered to be statistically significant.

## Results

This study investigated the examination records of 215 eyes of 123 participants. There were 113 eyes in group 1 and 102 eyes in group 2. The ages were between 17 and 38, and the mean was  $24.33 \pm 3.87$ . No statistically significant difference were present between the groups in the comparison of sex and mean age ( $p > 0.05$ ) (Table 1). Group 1 mean HVID was  $11.98 \pm 0.33$  mm, whereas group 2 mean HVID was  $11.81 \pm 0.24$  mm (Figure 1). The mean HVID was significantly higher in patients with keratoconus than in healthy subjects ( $p = 0.04$ ). In group 1, the mean mesopic pupil size was  $3.64 \pm 0.12$  mm, on the other hand the mean mesopic pupil size was  $3.73 \pm 0.14$  mm in group 2 (Figure 2). The mean mesopic pupil size was significantly higher in healthy subjects than in patients with keratoconus ( $p = 0.03$ ).

## Discussion

HVID is the longest measurement from limbus to the opposite limbus in the horizontal plane. In normal pop-

**Table 1**  
Demographics and clinical features of the study population.

Characteristic	Group 1 (mean±SD)	Group 2 (mean±SD)
Age (years)	23.13±4.27 (17–37)	24.88±5.05 (17–39)
Sex (% female)	%59.2	%56.3
Manifest spherical equivalent (D)	-6.89±1.10 D	-0.29±0.51 D
Cylinder (D)	-4.65±0.37 D	-0.24±0.18 D
HVID (mm)	11.98±0.33 (11.54–12.87)	11.81±0.24 (11.26–12.17)
Mesopic pupil size (mm)	3.64±0.12 (2.54–5.67)	3.73±0.14 (2.68–5.74)

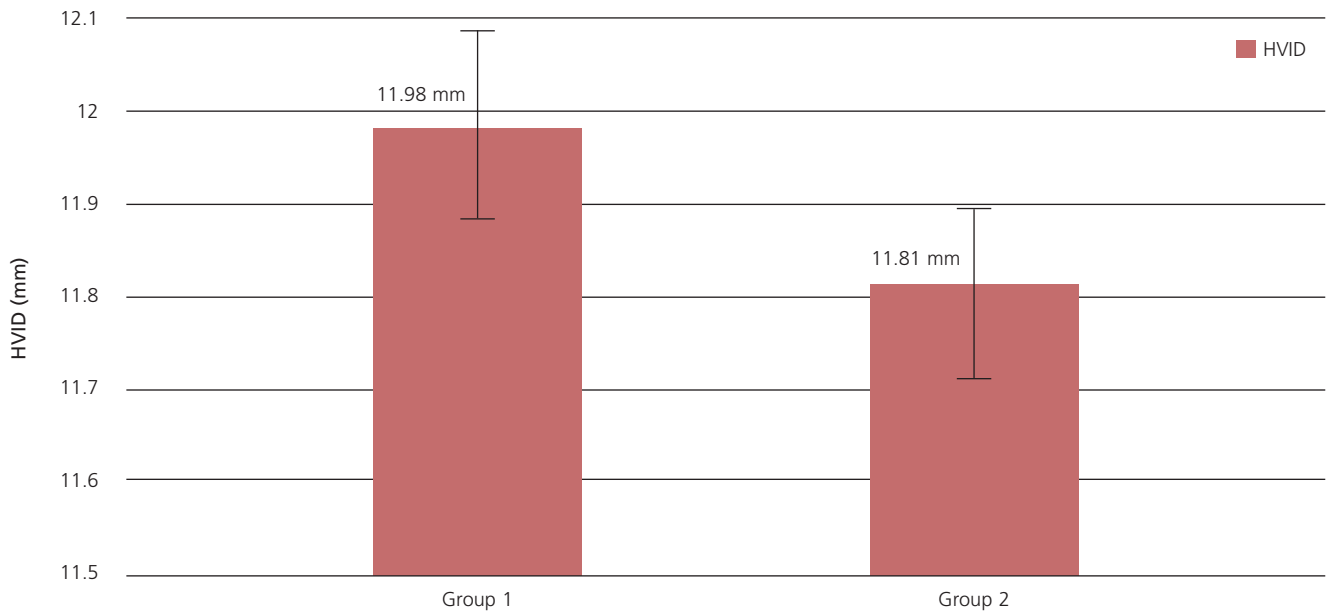


Figure 1. The mean HVID in the groups.

ulation studies, HVID was generally between 11.5 mm and 12.5 mm, and approximately 11.80 mm.<sup>[2,12]</sup> In our study, healthy control group subjects were close to these results, similar to the literature. Macrocornea is a corneal diameter greater than 12.5 mm, on the other hand, the definition of microcornea varies in horizontal diameters between less than 10.0 mm to 11.0 mm.<sup>[13,14]</sup> Seitz

reported that large corneal diameters were present in keratoconus, lattice, and granular dystrophies, whereas smaller diameters were present in Fuchs' and macular corneal dystrophies.<sup>[15]</sup> Furthermore, different studies showed that age, sex, and height might affect this value.<sup>[2,16,17]</sup> In our study, healthy control group subjects and keratoconus patients showed a similar distribution in

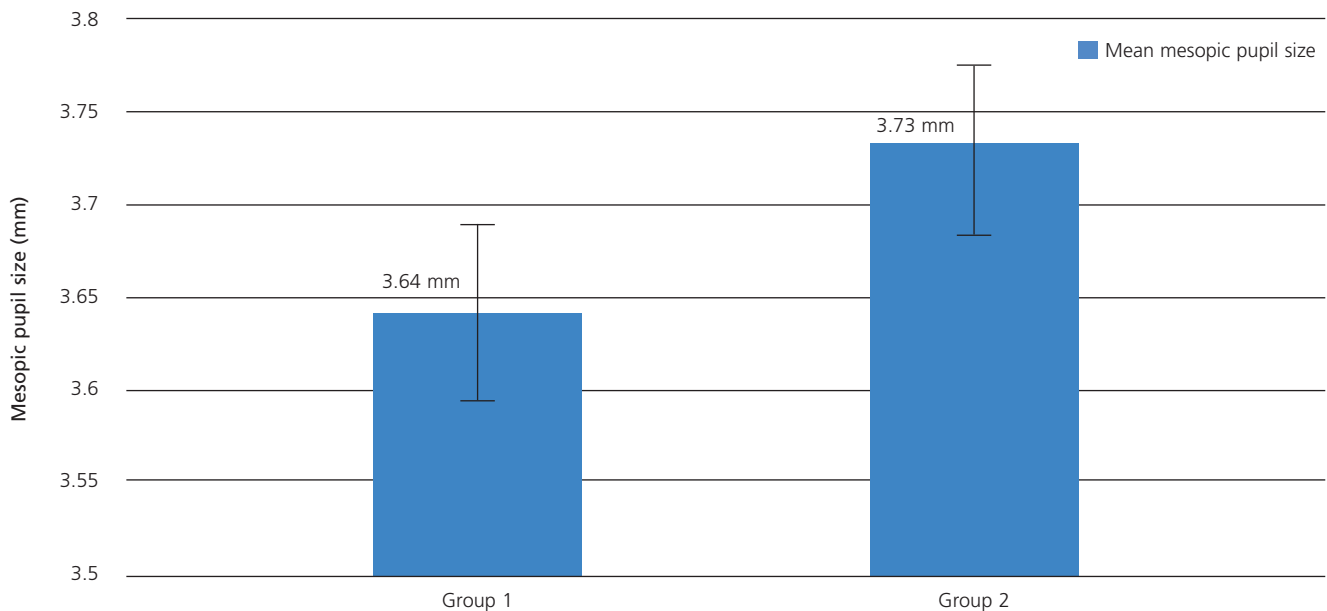


Figure 2. The mean mesopic pupil size in the groups.

age and sex. HVID was significantly higher in patients with keratoconus, and we were expecting such a result. However to the best of our knowledge no such study used HVID parameter of corneal topography in keratoconus patients before. There are increased in elasticity, keratometry values and anterior chamber depth in keratoconus compared to normal cornea. Perhaps, the increase in HVID may have occurred in parallel with the increase in corneal elasticity. HVID is a topographic measurement of clinical importance that must be considered when performing surgery with the indication of keratoplasty or when contact lens trials are performed on these patients and an appropriate lens prescription is created. Also increased HVID in these patients is a parameter that should be considered in the selection of suitable contact lenses and in the production of these lenses.

Pupil size is a valuable parameter with critical clinical implications.<sup>[18]</sup> Its measurement can help detect anomalies. Moreover, knowledge of its normal range is essential to the optical industry. Different normal values have been reported in various studies.<sup>[19,20]</sup> Because, mesopic pupil diameter is evaluated in a wide range from simple measurements with a ruler to complex measurements with devices using advanced imaging methods. Sanchis-Gimeno et al.<sup>[16]</sup> found the mesopic pupil diameter to be  $3.6 \pm 0.4$  mm ranged between 3 and 4.7 mm with radiological and anatomical measurements in their study on healthy large population individuals with a mean age of 29.2. Guillon et al.<sup>[21]</sup> found that the mesopic pupil diameter to be 3.82 mm on average in a healthy young population without refractive defects in their study using a dynamic pupillometer. In our study, the mean mesopic pupil diameter of the healthy control group was 3.74 mm. Mesopic pupil diameter values are generally affected by variables such as age, sex, refraction and device used for measurement.<sup>[22-24]</sup> Although the pupil diameter measurement results are contradictory in sex comparisons, values are generally close to each other.<sup>[25,26]</sup> Mesopic pupil diameter decreases with age.<sup>[27,28]</sup> We considered these two variables significant and selected the healthy control group as compatible with the keratoconus group in age and sex. To the best of our knowledge, there are no publications in the literature on mesopic pupil diameter measurements in keratoconus patients. The mesopic pupil diameter was significantly smaller in eyes with keratoconus compared to the healthy control group. High myopia and astigmatism values stand out in the eyes with keratoconus. In the literature, the mesopic pupil diameter tends to increase in myopic and astigmatic refraction defects.<sup>[22,29,30]</sup> It is curi-

ous to find that the mean mesopic pupil diameter decreases in the eyes with keratoconus while the pupil diameters increase in myopia and astigmatism. Spherical aberrations can become more complicated with increased pupil diameter and changes in anterior segment parameters. In their study, Hondur et al.<sup>[31]</sup> primarily revealed a greater pupillary offset in the eyes with keratoconus than the healthy controls, which was mostly in the superior direction (the positive y-offset). Mihaltz et al.<sup>[32]</sup> found that the pupillary offset due to mild to moderate keratoconus was evaluated with total ocular aberrometry, and a shift in the line of sight (LoS) was observed, which was interpreted as a compensating mechanism for increased corneal higher-order aberrations. Perhaps the reduction of the pupil diameter as a compensation mechanism may prevent spherical and chromatic aberrations in keratoconus patients.

Various comparative studies utilized different devices to measure anterior segment parameters.<sup>[33]</sup> In general, cornea topography devices have a very valuable place since they are easy to use and have good reproducibility in cornea and anterior segment measurements. The Sirius device we use has both two scheinplflug cameras and orb-scan topography. Thanks to the versatile operation of the device and the intelligent mapping system, the margin of error in the measurements have been minimized. Furthermore, the reliability of the measurements has been increased by successfully combining the anatomical and clinical parameters in the device. HVID was generally higher in keratoconus patients in our study, while mesopic pupil diameter tended to decrease. HVID is a significant parameter for selecting appropriate contact lenses in keratoconus patients.<sup>[34]</sup> In addition, it is a measurement that should be considered while preparing the donor cornea in patients who need keratoplasty.<sup>[35]</sup> Mesopic pupil diameter is also a parameter worthy of attention in using contact lenses and implantation of intraocular toric lens in these patients.<sup>[36]</sup>

One of the limitations of the study is its retrospective design. Since retrospective research may include several biases, such as information bias and selection bias, there may be some minor errors. Another limitation was the relatively small sample size. These results cannot be generalized to thousands of patients with keratoconus. Finally, because we conducted the study using patient records, we could not identify all predictive indices for keratoconus. Although this study employed two basic parameters, other parameters used in the keratoconus grading examination can be beneficial.

## Conclusion

The present study has revealed the quantitative anatomy of the HVID and mesopic pupil diameter of patients with keratoconus and healthy emmetropic subjects. The results of the study showed that the HVID is greater and the mesopic pupil size is smaller in patients with keratoconus. To our knowledge, this is the first study that analyzes the mesopic pupil size and HVID in keratoconus subjects.

## Conflict of Interest

The authors declare no conflict of interest.

## Author Contributions

FÖ: manuscript writing/editing; TY: manuscript writing/editing; GG: protocol/project development, data analysis.

## Ethics Approval

The study was approved by Ethical Committee of Prof. Dr. Cemil Taşçıoğlu City Hospital and carried out in accordance with the Helsinki declaration of principles.

## Funding

The authors declare no financial support.

## References

- Baumeister M, Terzi E, Ekici Y, Kohnen T. Comparison of manual and automated methods to determine horizontal corneal diameter. *J Cataract Refract Surg* 2004;30:374–80.
- Rüfer F, Schröder A, Erb C. White-to-white corneal diameter: normal values in healthy humans obtained with the Orbscan II topography system. *Cornea* 2005;24:259–61.
- De Silva DJ, Khaw PT, Brookes JL. Long term outcome of primary congenital glaucoma. *J AAPOS* 2011;15:148–52.
- Allemann N, Chamon W, Tanaka HM, Mori ES, Campos M, Schor P, Baikoff G. Myopic angle-supported intraocular lenses: two-year follow-up. *Ophthalmology* 2000;107:1549–54.
- Rosen E, Gore C. Staar collamer posterior chamber phakic intraocular lens to correct myopia and hyperopia. *J Cataract Refract Surg* 1998;24:596–606.
- Paryani MJ, Kharbanda V, Kummelil MK, Wadia K, Darak AB. Pupil dynamics and corneal spherical aberrations in a set of Indian cataract patients and its implications for aberrometric customisation of intraocular lenses. *Indian J Ophthalmol* 2020;68:3012–5.
- Haw WW, Manche EE. Effect of preoperative pupil measurements on glare, halos, and visual function after photoastigmatic refractive keratectomy. *J Cataract Refract Surg* 2001;27:907–15.
- Cakmak HB, Cagil N, Simavli H, Raza S. Corneal white-to-white distance and mesopic pupil diameter. *Int J Ophthalmol* 2012;5:505–9.
- Galvis V, Sherwin T, Tello A, Merayo J, Barrera R, Acera A. Keratoconus: an inflammatory disorder? *Eye (Lond)* 2015;29:843–59.
- Rabinowitz YS. Keratoconus. *Surv Ophthalmol* 1998;42:297–319.
- Miháltz K, Kovács I, Kránitz K, Erdei G, Németh J, Nagy ZZ. Mechanism of aberration balance and the effect on retinal image quality in keratoconus: optical and visual characteristics of keratoconus. *J Cataract Refract Surg* 2011;37:914–22.
- Hashemia H, Khabazkhooba M, Emamianb MH, Shariatic M, Yektad A, Fotouhie A. White-to-white corneal diameter distribution in an adult population. *J Curr Ophthalmol* 2015;27:21–4.
- Hashemi H, Khabazkhoob M, Yazdani K, Mehravaran S, Mohammad K, Fotouhi A. White-to-white corneal diameter in the Tehran eye study. *Curr Eye Res* 2009;34:378–85.
- Wang L, Auffarth GU. White-to-white corneal diameter measurements using the eyemetrics program of the Orbscan topography system. *Dev Ophthalmol* 2002;34:141–6.
- Seitz B, Langenbacher A, Zagrada D, Budde W, Kus M. Corneal dimensions in patients with various types of corneal dystrophies and their impact on penetrating keratoplasty [Article in German]. *Klin Monbl Augenheilkd* 2000;217:152–8.
- Sanchis-Gimeno JA, Sanchez-Zuriaga D, Martinez-Soriano F. White-to-white corneal diameter, pupil diameter, central corneal thickness and thinnest corneal thickness values of emmetropic subjects. *Surg Radiol Anat* 2012;34:167–70.
- Lee DW, Kim JM, Choi CY, Shin D, Park KH, Cho JG. Age-related changes of ocular parameters in Korean subjects. *Clin Ophthalmol* 2010;4:725–30.
- Sulutvedt U, Zavagno D, Lubell J, Leknes S, de Rodez Benavent SA, Laeng B. Brightness perception changes related to pupil size. *Vision Res* 2021;178:41–7.
- Guler Alis M, Alis AJ. Compatibility of pupil size measured with Nidek ARK-1a table top autorefractometer and Plusoptix A12C photoscreene. *J Binocul Vis Ocul Motil* 2021;71:161–6.
- Mathot S, Fabius J, Heusden EV, Van der Stigchel S. Safe and sensible preprocessing and baseline correction of pupil-size data. *Behav Res Methods* 2018;50:94–106.
- Guillon M, Dumbleton K, Theodoratos P, Gobbe M, Wooley CB, Moody K. The effects of age, refractive status, and luminance on pupil size. *Optom Vis Sci* 2016;93:1093–100.
- Cakmak HB, Cagil N, Simavli H, Duzen B, Simsek S. Refractive error may influence mesopic pupil size. *Curr Eye Res* 2010;35:130–6.
- Netto MV, Ambrosio Jr R, Wilson SE. Pupil size in refractive surgery candidates. *J Refract Surg* 2004;20:337–42.
- Biçer GY, Zor KR, Küçük E. Do static and dynamic pupillary parameters differ according to childhood, adulthood, and old age? A quantitative study in healthy volunteers. *Indian J Ophthalmol* 2022;70:3575–8.
- Linke SJ, Baviera J, Munzer G, Fricke OH, Richard G, Katz T. Mesopic pupil size in a refractive surgery population (13,959 eyes). *Optom Vis Sci* 2012;89:1156–64.
- Tekin K, Sekeroglu MA, Kiziltoprak H, Doguiz S, Inanc M, Yilmazbas P. Static and dynamic pupillometry data of healthy individuals. *Clin Exp Optom* 2018;101:659–65.
- Birren J, Casperson R J. Age changes in pupil size. *J Gerontol* 1950;5:216–21.
- Kiel M, Grabitz SD, Hopf S, Koeck T, Wild PS, Schmidtman I, Lackner KJ, Munzel T, Manfred E, Beutel ME, Pfeiffer N, Alexander K, Schuster AK. Distribution of pupil size and associated

- factors: results from the population-based gutenberg health study. *J Ophthalmol* 2022;9:9520512.
29. Alarcón A, Rubiño M, Péeérez-Ocón F, Jiménez JR. Theoretical analysis of the effect of pupil size, initial myopic level, and optical zone on quality of vision after corneal refractive surgery. *J Refract Surg* 2012;28:901–6.
  30. Lee YS, Kim HJ, Lim DK, Kim MH, Lee KJ. Age-specific influences of refractive error and illuminance on pupil diameter. *Medicine (Baltimore)* 2022;101:e29859.
  31. Hondur G, Cagil N, Sarac O, Ozcan ME, Kosekahya P. Pupillary offset in keratoconus and its relationship with clinical and topographical features. *Curr Eye Res* 2017;42:708–12.
  32. Mihaltz K, Kranitz K, Kovacs I, Takács A, Németh J, Nagy ZZ. Shifting of the line of sight in keratoconus measured by a hartmann-shack sensor. *Ophthalmology* 2010;117:41–8.
  33. Schmitz S, Krummenauer F, Henn S, Dick HB. Comparison of three different technologies for pupil diameter measurement. *Graefes Arch Clin Exp Ophthalmol* 2003;241:472–7.
  34. Fernández-Velázquez F. Performance and predictability of a new large diameter contact lens design in keratoconic cornea. *Cont Lens Anterior Eye* 2019;42:289–94.
  35. Seitz B, Langenbucher A, Zagrada D, Budde W, Kus MM. Corneal dimensions in various types of corneal dystrophies and their effect on penetrating keratoplasty [Article in German]. *Klin Monbl Augenheilkd* 2000;217:152–8.
  36. Monsálvez-Romín D, González-Méijome JM, Esteve-Taboada JJ, García-Lázaro S, Cerviño A. Light distortion of soft multifocal contact lenses with different pupil size and shape. *Cont Lens Anterior Eye* 2020;43:130–6.

**ORCID ID:**

F. Özçelik 0000-0001-7153-2950;  
T. Yılmaz 0000-0002-4502-4423;  
G. Gümüş 0000-0003-4052-7280

deomed®

**Correspondence to:** Tolga Yılmaz, MD

Department of Ophthalmology, Beyoğlu Eye Training and Research Hospital, İstanbul, Türkiye  
Phone: +90 505 258 19 54  
e-mail: dr.tolgayilmaz@hotmail.com

*Conflict of interest statement:* No conflicts declared.

This is an open access article distributed under the terms of the Creative Commons Attribution-NonCommercial-NoDerivs 4.0 Unported (CC BY-NC-ND4.0) Licence (<http://creativecommons.org/licenses/by-nc-nd/4.0/>) which permits unrestricted noncommercial use, distribution, and reproduction in any medium, provided the original work is properly cited. *How to cite this article:* Özçelik F, Yılmaz T, Gümüş G. White to white cornea diameter and mesopic pupil size in patients with keratoconus. *Anatomy* 2022;16(3):159–164.

# Tarsal coalition in the Turkish population: an MRI study

Semra Duran , Esra Çıvgın 

Department of Radiology, Ankara City Hospital of Turkish Ministry of Health, Ankara, Türkiye

## Abstract

**Objectives:** Tarsal coalition describes a complete or partial union of two or more tarsal bones. We aimed to determine the anatomical features of tarsal coalition in patients undergoing ankle magnetic resonance imaging (MRI) and to report tarsal coalition prevalence in the Turkish population.

**Methods:** A total of 1075 ankle MRI were evaluated and patients with tarsal coalition were included to the study. Statistical analyses were performed to check whether there is a correlation between the presence of the tarsal coalition and age, gender and side (right/left) and to identify the talar beak sign accompanying the coalition and the presence of edema or cyst in the bones.

**Results:** We detected tarsal coalition in 18 patients (a total of 21 ankles) (1.68%). Out of these, seven were females (1.32%) and eleven were males (2.04%). The mean age was  $37.22 \pm 14.23$  years. Three (0.28%) patients had bilateral coalition. Eight patients (0.56%) had tarsal coalition on the right ankle and 13 patients (1.12%) had on the left. We detected osseous talocalcaneal coalition in 3 patients, non-osseous talocalcaneal coalition in 6 patients, non-osseous calcaneonavicular coalition in 10 patients and non-osseous cuboid navicular coalition in 2 patients. Talar beak was found in 11 (52.38%) patients, edema or cysts in the bones forming the coalition were found in 11 (52.38%) patients.

**Conclusion:** The prevalence of the tarsal coalition was determined to be 1.68 % in a Turkish population and was more common among men. Calcaneonavicular coalition followed by talocalcaneal coalition are the most common types.

**Keywords:** edema; magnetic resonance imaging; talar beak; tarsal coalition

Anatomy 2022;16(3):165–171 ©2022 Turkish Society of Anatomy and Clinical Anatomy (TSACA)

## Introduction

Tarsal coalition (TC) is defined as an abnormal union of two or more bones of the hindfoot or midfoot and is thought to be the result of the failure of segmentation of primitive mesenchyme. These unions can be osseous (synostosis), cartilaginous (synchondrosis), or fibrous (syn-desmosis).<sup>[1-4]</sup>

Although it is difficult to determine the prevalence of TC due to asymptomatic cases, previous studies have reported a prevalence of 1–13%.<sup>[3,5-7]</sup> The most common TCs are talocalcaneal and calcaneonavicular and the prevalence of bilateral occurrence of TC is 50–60%.<sup>[2,4,8]</sup>

TC can restrict normal subtalar motion (eversion, inversion, and anterior gliding) and cause pain, tenderness, peroneal tendon spasm, tarsal tunnel syndrome and flat foot deformity. TC can be asymptomatic and detected incidentally in these cases.<sup>[2,9]</sup>

Radiographs are used as the first-line imaging examination in diagnosis of TC. Computed tomography (CT) and magnetic resonance imaging (MRI) provide important information in understanding the anatomical features of the TC. MRI makes it possible to identify bone marrow edema which is common in the coalition region.<sup>[10]</sup>

We aim to determine the anatomical features of TC in patients undergoing ankle MRI and to report its prevalence in the Turkish population by examining a large series.

## Materials and Methods

We retrospectively evaluated 1075 ankle MRIs, performed between January and December 2021. The MRI examinations were performed for various reasons such as tendinopathy, pain, osteochondral lesion, ligament or tendon rupture). Patients younger than 18 years, or with a history of trauma and surgery, or with mass lesions, or

**Table 1**  
Sequences of MRI examination of the ankle joint.

Pulse sequence	TR/TE (ms)	Matrix	Field of view (cm)	Slice thickness (mm)
Sagittal T1-weighted FSE	720/10.69	320×256	17×17	3
Sagittal FS proton-density weighted FSE	2467/32.06	320×256	17×17	3
Coronal FS T2-weighted FSE	4479/89.73	320×256	18×18	3
Axial T1-weighted FSE	506/11.2	320×224	17×17	3
Axial FS proton-density weighted FSE	3131/42.85	320×256	17×17	3

cm: centimeter; FS: fat-suppressed; FSE: fast spin echo; mm: millimeter; ms: millisecond; TE: echo time, TR: repetition time.

with images that could not be evaluated due to operational artifacts or poor imaging quality were excluded from the study. Thus, a total of 1068 patients who met the criteria were included in the study. In the study group, 21 ankle MRI scans of 18 patients showed osseous/non-osseous TC.

The MRI images of patients were obtained with a 1.5 T MR scanner (Signa Explorer, GE Medical System, Milwaukee, WI, USA) equipped with an extremity coil. A standardized ankle MRI examination protocol was applied for each patient. The presence and characteristics of the TC were evaluated using all sequences in all three planes. The sequences included in the examination and their parameters are given in **Table 1**. The images

were analyzed on the hospital picture archiving and communications system.

The diagnostic criteria for TC in this study were as follows: the presence of a bone bridge, narrowing of the joint surface, irregular cortical bone surface and the presence of subchondral bone edema or cyst formation adjacent to the affected joint.

Anatomical types of TC were classified according to the united tarsal bone as talocalcaneal (**Figure 1**), calcaneonavicular (**Figure 2**), and cuboideonavicular (**Figure 3**). The superior projection of the distal part of the talus was defined as the talar beak (**Figure 2**). The presence of cyst or edema was noted in both bones in the coalition (**Figures 2 and 3**).

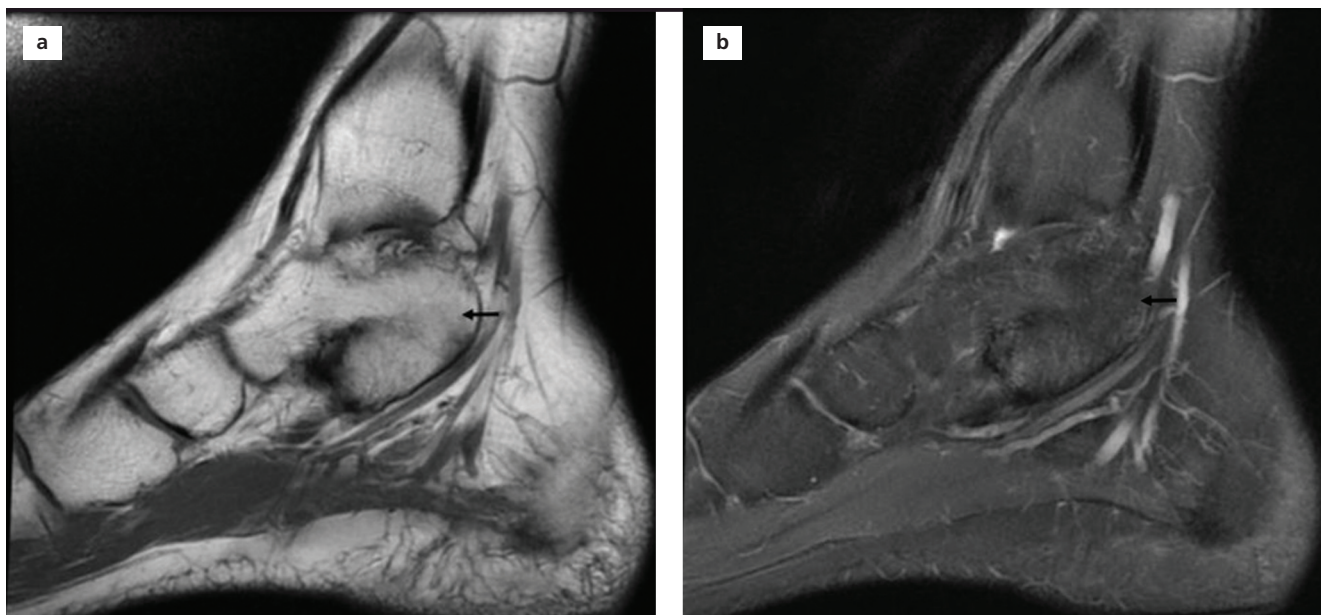


**Figure 1.** (a) Sagittal T1-weighted and (b) T2-weighted fat-suppressed images through the talocalcaneal joint show bone marrow signal (black arrow) continue across the fused articulation (osseous coalition) in the ankle MR images.

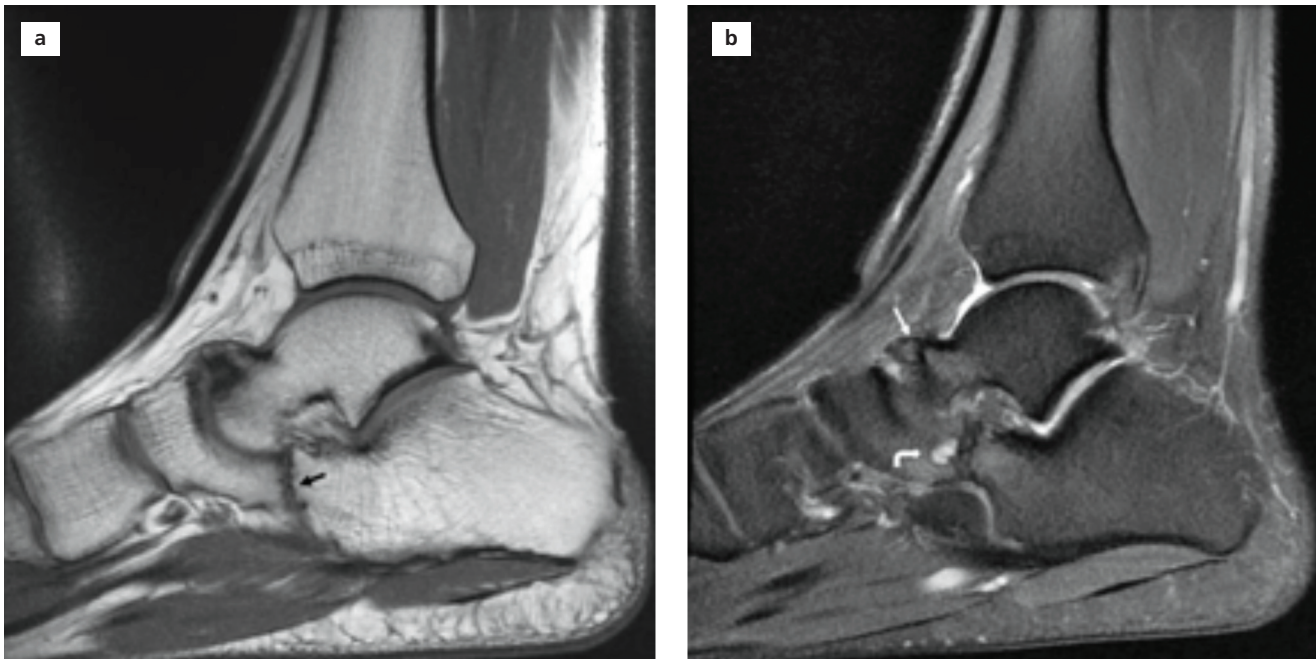


**Figure 2.** (a) Sagittal T1-weighted and (b) T2-weighted fat-suppressed images demonstrate the narrowing of the joint and irregularity of the bone margins in the calcaneonavicular joint. The sagittal T1-weighted image also shows the talar beak (white arrow) and accompanying medullary edema or cyst (curved white arrow).

Data was analyzed using IBM SPSS Statistics Standard Concurrent User v. 26 (IBM Corp., Armonk, NY, USA). Kolmogorov-Smirnov test was used for the

distribution and homogeneity analyses of the data. In addition to obtaining descriptive statistics, independent t-test analysis was applied to evaluate the mean differ-

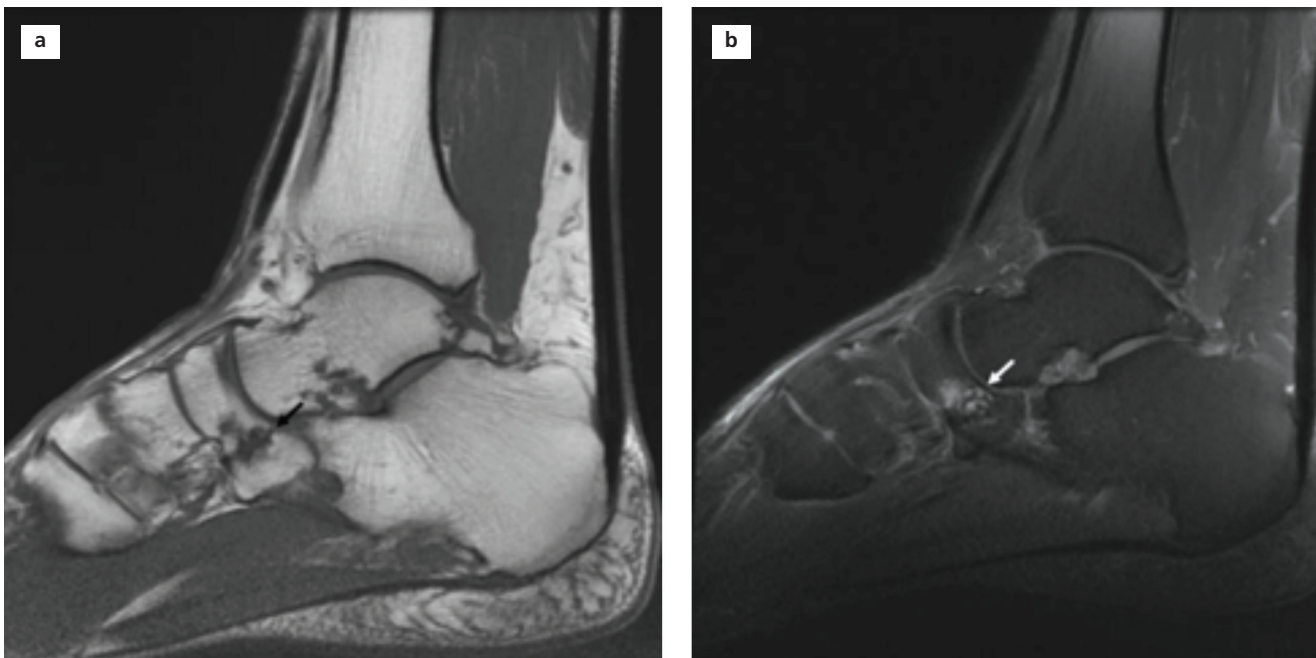


**Figure 3.** (a) Sagittal T1-weighted and (b) T2-weighted fat-suppressed images demonstrate the narrowing of the joint and irregularity of the bone margins in the cuboideonavicular joint (black arrow), and accompanying medullary edema/cyst (white arrow) on the bony surfaces.

ences between groups. Mann-Whitney U test was also conducted to differentiate inhomogeneous groups and Kruskal-Wallis test was used to compare three or more groups. A p-value of <0.05 was considered as statistically significant.

## Results

A total of 1075 patients were included to this study. Of the 1068 patients without TC, 529 were females and 539 were males; 511 of the patients were evaluated for right ankle and 557 for left ankle. Osseous, non-osseous TC was detected in 18 patients (21 ankles) (1.68%). The mean age of the patients with the TC was 37.22±14.23 years. There was no significant difference between the male and female patients in terms of the mean age ( $p>0.05$ ). **Table 2** presents the data on the mean age according to gender.

TC was detected in 7 of female patients (1.32%) and 11 of male patients (2.04%). There was a bilateral TC in three cases (0.28%); 2 males and 1 female. The TC was found in the right ankle in 8 patients (0.56%) and the left ankle in 13 (1.12%). **Table 3** shows the distribution of the osseous, non-osseous TC prevalence according to gender and side.

Osseous talocalcaneal coalition was detected in 3 ankles (14.2%), non-osseous talocalcaneal coalition in 6 ankles (28.5%), non-osseous calcaneonavicular coalition in 10 ankles (47.6%) of 8 patients, and non-osseous cuboidonavicular coalition in 2 ankles (9.5%). The distribution of these coalitions did not show correlation with age ( $p>0.05$ ). The distribution of coalition types by gender is given in **Figure 4**.

In patients with bilateral ankle MRI, talocalcaneal and calcaneonavicular coalition was detected in both ankles. Among the patients with bilateral ankle MRI,

**Table 2**  
Mean age according to gender.

Sex	n	Min-max	Mean±SD	p-value
Female	7	23–51	38.57±11.68	0.13
Male	11	18–58	36.36±16.44	

SD: standard deviation.

only one female patient had different coalition types in their right and left ankles (non-osseous talocalcaneal coalition on the left, osseous talocalcaneal coalition on the right), and two male patients had the same type of coalition (non-osseous calcaneonavicular) in each of the ankle MRIs. When the pathologies accompanying the TC were analyzed; talar beak was found in 11 (52.38%) patients, edema or cysts in the both bones forming the coalition were found in 11 (52.38%) patients. Patients who had edema or cysts in the coalition were over 40 years of age. In 3 patients, talar beak and cysts or edema on the bone faces adjacent to the talar coalition were found together.

There was no correlation between pathologies accompanying the TC and gender ( $p>0.05$ ). The histogram of the pathologies accompanying the TC according to age is given in **Figure 5**.

## Discussion

TC is defined as the absence of segmentation between two or more bones of the foot during embryological development due to failure of the joint cleft to develop.<sup>[1–6]</sup> Although the coalition may affect any tarsal joint, the calcaneonavicular joint is most commonly affected followed by the talocalcaneal joint; together these two coalitions account for 90% of all TC cases.<sup>[9]</sup>

**Table 3**  
Distribution of osseous/non-osseous tarsal coalition prevalence according to gender and side.

Patients without osseous/non-osseous tarsal coalition	1068			
Patients with osseous/non-osseous tarsal coalition	18	1.68%		
Bilateral/female	1	0.18%		
Bilateral/male	2	0.37%		
Right/male	4	0.74%	Right: 8	0.56%
Right/female	2	0.37%		
Left/male	7	1.29%	Left: 13	1.12%
Left/female	5	0.94%		

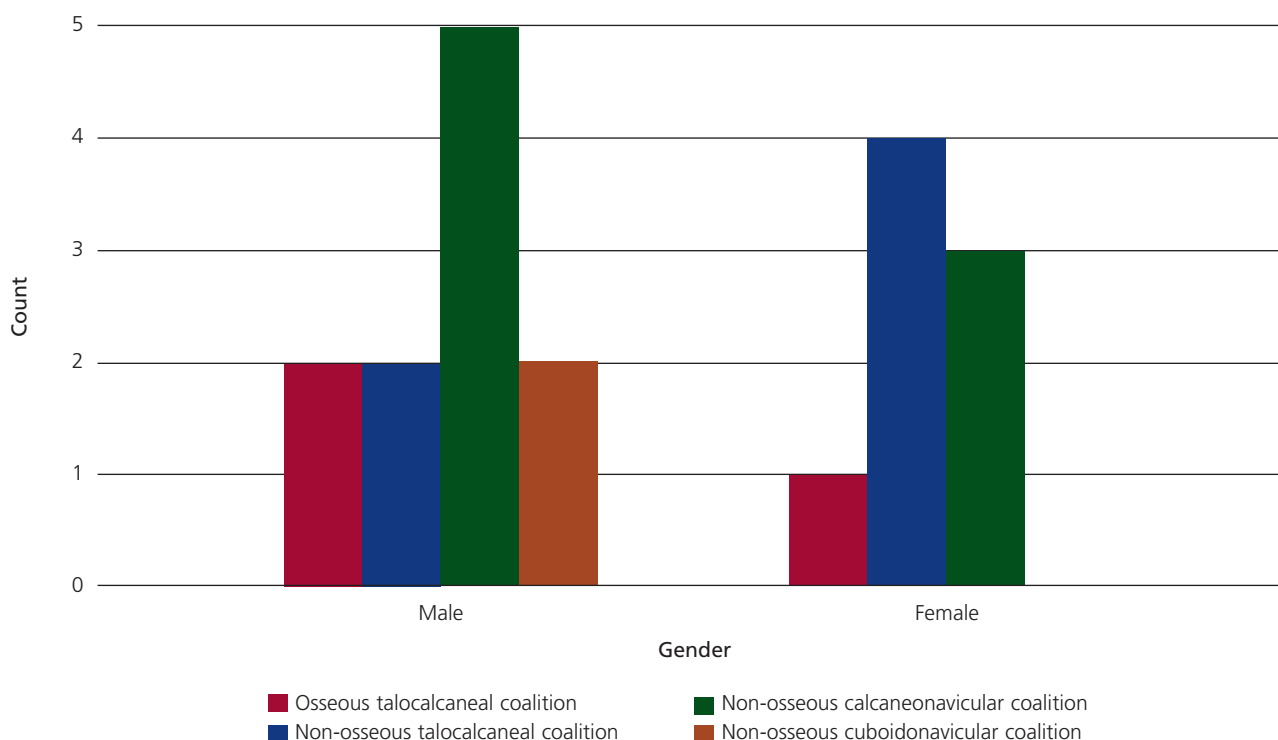


Figure 4. Distribution of coalition types by gender.

CT and MR imaging allow differentiation of osseous from non-osseous coalitions and reveal the extent of joint involvement as well as secondary degenerative changes. On MR images, bone marrow edema, abnormal articular orientation and joint space narrowing were frequently identified adjacent to the abnormal joint.<sup>[10]</sup>

Kim et al.<sup>[11]</sup> reported the prevalence of TC as 1% in their study including 733 patients, while Nalaboff and Schweitzer<sup>[6]</sup> reported the prevalence of TC as 11.5% in their MRI-based study including 574 patients. In our study, the prevalence was 1.68%.

Cilengir et al.<sup>[12]</sup> reported non-osseous TC in 57 (87.6%) of 65 patients with TC. Cheng et al.<sup>[13]</sup> reported the rate of non-osseous TC as 89% in their MRI-based study including 57 patients. In our study, the rate of non-osseous TC, which was 85.8%, was greater than the rate of osseous TC. Our findings were consistent with previous studies. This shows that the frequency of the osseous TC was lower than that of non-osseous TC.

Varner et al.<sup>[14]</sup> evaluated 32 ankles of the 27 patients with TC and reported 18 subtalar coalition, 14 calcaneonavicular coalition and 1 naviculocuneiform coalition. Nalaboff and Schweitzer<sup>[6]</sup> reported subtalar coalition in 18 (25.7%) patients and calcaneonavicular coalition

in 50 (71.4%) patients of 70 patients with TC. In our study, the most common TC was calcaneonavicular, followed by talocalcaneal coalition. Naviculocuboid coalition was the least common TC.

Some clinical studies have shown that TC is more common in males.<sup>[11,15,16]</sup> In our study, we found the incidence rate of TC as 2.4% in males, which is similar to

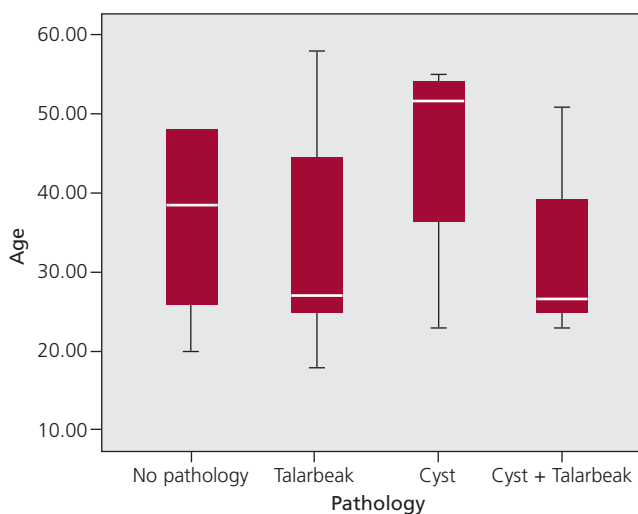


Figure 5. Histogram of pathologies detected with coalition by age.

the other studies. We also found that TC was more common in the left ankle in both genders.

Rühli et al.<sup>[17]</sup> found a bilateral TC in 2 of 7 calcaneonavicular TCs. Mendeszoon et al.<sup>[16]</sup> reported a bilateral incidence of 10% for talocalcaneal coalition and 21% for calcaneonavicular coalition. We found three patients (2 males, 1 female) with bilateral TC (0.28%). This low rate can be explained by the low number of bilateral examinations in our retrospective study. We found talocalcaneal and calcaneonavicular coalition in our all bilateral patients. In our only female patient, this talocalcaneal coalition was osseous in one ankle and non-osseous in the other.

The term “talar beak” refers to a flaring of the superior aspect of the talar head. This is an indirect sign of TC and is thought to occur as a result of impaired subtalar joint motion, causing the navicular bone to override the talus.<sup>[10]</sup> The talar beak sign may be seen in either calcaneonavicular or talocalcaneal coalition and is more common in talocalcaneal coalition.<sup>[2]</sup> The sensitivity and specificity of the talar beak sign for detecting talocalcaneal coalition are 48% and 91%, respectively.<sup>[8]</sup>

Nalaboff and Schweitzer<sup>[6]</sup> found the talar beak sign in 25 (50%) patients with calcaneonavicular coalition and 5 (27%) patients with subtalar coalition in their study of 70 patients with TC. Consistent with the aforementioned study, we found talar beak sign in 11 patients with TC, 5 with calcaneonavicular coalition and 6 with talocalcaneal coalition.

Lim et al.<sup>[4]</sup> found bone marrow edema in both bones in 37 (86%) of 43 ankles with MR imaging. We found medullary edema or cyst in both bones in 11 of 18 patients with TC. These patients were over 40 years of age. The non-osseous TC creates abnormal mechanical stress across the affected joint, causing bone marrow edema on the bony surfaces adjacent to the joint.<sup>[10]</sup>

Our study has some limitations. Our study was retrospective and consisted of symptomatic patients. The number of study population is small. Most of our patients' examinations were unilateral, which made it difficult to determine the bilateral prevalence. We did not access the clinical examination findings of the patients. Therefore, we could not evaluate the clinical impact of subchondral bone edema or cyst formation adjacent to the TC.

## Conclusion

The prevalence of the TC was found to be 1.68 % in a Turkish population and it was more common among

men. Calcaneonavicular coalition followed by talocalcaneal coalition are the most common types of TC.

## Conflict of Interest

The authors declare no conflict of interest regarding the methods and results in this study.

## Author Contributions

SD: project development, data collection and analysis, manuscript writing, editing; EÇ: data collection and analysis, manuscript writing.

## Ethics Approval

The study was approved by the University of Health Sciences Ankara City Hospital Clinical Research Ethics Committee (No: E2-22-2766) and carried out in accordance with the Helsinki declaration of principles.

## Funding

The authors declare no financial support.

## References

1. Zaw H, Calder JD. Tarsal coalitions. *Foot Ankle Clin* 2010;15:349–64.
2. Lawrence DA, Rolen MF, Haims AH, Zayour Z, Moukaddam HA. Tarsal coalitions: radiographic, CT, and MR imaging findings. *HSS J* 2014;10:153–66.
3. Soni JF, Valenza W, Matsunaga C. Tarsal coalition. *Curr Opin Pediatr* 2020;32:93–9.
4. Lim S, Lee HK, Bae S, Rim NJ, Cho J. A radiological classification system for talocalcaneal coalition based on a multi-planar imaging study using CT and MRI. *Insights Imaging* 2013;4:563–7.
5. Linklater J, Hayter CL, Vu D, Tse K. Anatomy of the subtalar joint and imaging of talo-calcaneal coalition. *Skeletal Radiol* 2009;38:437–49.
6. Nalaboff KM, Schweitzer ME. MRI of tarsal coalition: frequency, distribution, and innovative signs. *Bull NYU Hosp Jt Dis* 2008;66:14–21.
7. Stormont DM, Peterson HA. The relative incidence of tarsal coalition. *Clin Orthop Relat Res* 1983;(181):28–36.
8. Crim JR, Kjeldsberg KM. Radiographic diagnosis of tarsal coalition. *AJR Am J Roentgenol* 2004;182:323–8.
9. Park JJ, Seok HG, Woo IH, Park CH. Racial differences in prevalence and anatomical distribution of tarsal coalition. *Sci Rep* 2022; 12:21567.
10. Newman JS, Newberg AH. Congenital tarsal coalition: multimodality evaluation with emphasis on CT and MR imaging. *Radiographics* 2000;20:321–2.
11. Kim JH, Gwak HC, Lee CR, Kim YJ, Kim JG, Lee SJ, Lee JH, Park JH. Incidence of tarsal coalition: an institutional magnetic resonance imaging analysis. *Journal of Korean Foot and Ankle Society* 2016; 20:116–20.

12. Cilengir AH, Bayraktar ES, Dursun S, Ozdemir M, Altay S, Elmali F, Tosun O. A retrospective magnetic resonance imaging analysis of bone and soft tissue changes associated with the spectrum of tarsal coalitions. *Clin Anat* 2023;36:336–43.
13. Cheng KY, Fuangfa P, Shirazian H, Resnick D, Smitaman E. Osteochondritis dissecans of the talar dome in patients with tarsal coalition. *Skeletal Radiol* 2022;5:191–200.
14. Varner KE, Michelson JD. Tarsal coalition in adults. *Foot Ankle Int* 2000;21:669–72.
15. Elkus RA. Tarsal coalition in the young athlete. *Am J Sports Med* 1986;14:477–80.
16. Mendeszoon M, Mendeszoon E, Orabovic S, Valentine C. Tarsal coalitions: a review and assessment of the incidence in the Amish population. *The Foot Ankle Online Journal* 2013;6:1.
17. Rühli FJ, Solomon LB, Henneberg M. High prevalence of tarsal coalition and tarsal joint variants in a recent cadaver sample and its possible significance. *Clin Anat* 2003;16:411–5.

**ORCID ID:**

S. Duran 0000-0003-0863-2443;  
E. Çivgin 0000-0003-4790-3146

**Correspondence to:** Semra Duran, Assoc. Prof., MD

Department of Radiology, Ankara City Hospital of Turkish Ministry of Health,  
Ankara, Türkiye

Phone: +90 312 552 79 51

e-mail: semraduran91@gmail.com

*Conflict of interest statement:* No conflicts declared.

This is an open access article distributed under the terms of the Creative Commons Attribution-NonCommercial-NoDerivs 4.0 Unported (CC BY-NC-ND4.0) Licence (<http://creativecommons.org/licenses/by-nc-nd/4.0/>) which permits unrestricted noncommercial use, distribution, and reproduction in any medium, provided the original work is properly cited. *How to cite this article:* Duran S, Çivgin E. Tarsal coalition in the Turkish population: an MRI study. *Anatomy* 2022;16(3):165–171.

# Transposition of the great arteries: single center experiences

Başak Soran Türkcan<sup>1</sup> , Mustafa Yılmaz<sup>1</sup> , Yasemin Özdemir Şahan<sup>2</sup> , Ömer Ertekin<sup>3</sup> ,  
Ata Niyazi Ecevit<sup>1</sup> , Atakan Atalay<sup>1</sup> 

<sup>1</sup>Department of Paediatric Cardiovascular Surgery, Ankara Bilkent City Hospital, Ankara, Türkiye

<sup>2</sup>Department of Paediatric Cardiology, Ankara Bilkent City Hospital, Ankara, Türkiye

<sup>3</sup>Department of Neonatology, Ankara Bilkent City Hospital, Ankara, Türkiye

## Abstract

**Objectives:** Transposition of great arteries is the most common cyanotic congenital heart disease. It is characterized by ventriculoarterial discordance and atrioventricular concordance. The aim of the present study was to review the anatomical and embryological basis of this anomaly and to discuss the surgical outcomes of arterial switch operations.

**Methods:** The study included a total of 61 patients who underwent arterial switch operation. Demographic, anatomical, operative data, duration of stay in intensive care unit, need of postoperative extra corporeal membrane oxygenator, need of delayed sternal closure and mortality rate were retrieved from the institutional databases and medical records.

**Results:** The median age of the patients was 22.9±61.26 (1–455) days, and their weights ranged between 3391.97±686.6 (1900–5500) grams. Transposition of great arteries accompanied intact ventricular septum in 39 patients (63.9%) and ventricular septal defect in 22 patients (36.1%). Coronary arteries were abnormal in 11 patients (18%). Mortality was observed in 7 patients (11.5%) and was seen 5.71±2.98 (1–10) days after surgery. The incidence of coronary anomaly in patients with mortality was 28.6%. The most common coronary anomaly in patients with coronary anomaly with mortality is the anomaly in which the circumflex artery originates from the right coronary artery.

**Conclusion:** Arterial switch operations provide anatomical and complete correction in transposition of great arteries. It can be performed with appropriate timing, good preoperative, perioperative and postoperative management with low mortality. Coronary artery anomaly is not a contraindication for arterial switch operations, and with the detailed and careful evaluation of the appropriate coronary artery anatomy, transpositions with coronary anomalies are often uneventful.

**Keywords:** arterial switch operation; Jatene operation; Lecompte maneuver; transposition of great arteries

Anatomy 2022;16(3):172–178 ©2022 Turkish Society of Anatomy and Clinical Anatomy (TSACA)

## Introduction

Transposition of great arteries (TGA) is the most common cyanotic congenital heart disease. It constitutes 5% of all congenital heart diseases.<sup>[1]</sup> In this disease, the heart is characterized by ventriculoarterial discordance, atrioventricular concordance. The pulmonary artery (PA) arises from the left ventricle (LV), while the aorta arises from the right ventricle (RV).<sup>[2]</sup> If there is no other accompanying cardiac lesion, this disease is called TGA with intact ventricular septum (TGA-IVS). TGA is called as complex TGA in the presence of accompanying cardiac anomalies. These lesions are ventricular septal defect (VSD) (45%), left ventricular outflow tract

(LVOT) stenosis (25%), and aortic coarctation (5%). In general, there is no familial transmission in TGA. It has not been found to be associated with syndromes and chromosomal anomalies. It is seen two times more in males than in females.<sup>[3,4]</sup>

In TGA, the atria and ventricles have typical structural features and the conduction system is normally distributed. There is a fibrous continuity between the mitral and pulmonary valves. Coronary arteries usually arise from the aortic sinus, which faces the pulmonary trunk. Most commonly, the left anterior descending coronary artery (LAD) and circumflex artery (Cx) arise as a single root, while the right coronary artery (RCA)

arises as a separate root. In some patients, LAD, Cx and RCA emerge as a single root. There is also a variation in which LAD and Cx emerge as two separate ostiums on a single root. Apart from this, there is rarely a variation where the left main coronary artery (LMCA) or LAD is intramural between the pulmonary and aortic root.<sup>[5-12]</sup>

Embryological theories in the formation of TGA can be summarized as below:<sup>[5-7]</sup>

- Flat truncocoanal septation hypothesis, which blames abnormal septation of the aorta and PA,
- The hypothesis of an abnormal fibrous skeletal continuum in which the pulmonary-mitral fibrous continuum occurs instead of the normal aortic-mitral fibrous continuum.
- The hypothesis of abnormal embryonic hemodynamics due to obstructive and different flow patterns,
- Reverse truncal ridge hypothesis, which points to the reverse development of regions under the semilunar valves.

Due to this anomaly, the mixing is insufficient and this parallel circulation creates deep hypoxia. This results in hypoxia, acidosis, and death. In selected centers, short-term survival is above 95% with fast-acting preoperative management, timely surgery, and close postoperative monitoring.<sup>[2-4]</sup>

Arterial switch operation (ASO) was first described by Adib Jatene in 1976.<sup>[13]</sup> ASO is performed in the neonatal period and is the first-choice surgery in case of anatomical suitability. Atrial switch or two-stage ASO can be performed at later ages. Despite the medical and surgical advances in the diagnosis of TGA and low mortality rates, these patients should be followed up preoperatively, intraoperatively and postoperatively in a multidisciplinary manner, especially from the antenatal period. The aim of the present study was to review the anatomical and embryological basis of this anomaly and to discuss the surgical outcomes of arterial switch operations.

## Materials and Methods

This retrospective study was conducted at a paediatric heart center between February 2019-March 2022. The study included a total of 61 patients who underwent ASO.

Data including age, sex, type of TGA, surgical technique, presence of coronary anomaly, duration of cardiopulmonary bypass (CPB) and cross-clamp (CC) time, duration of stay in the pediatric cardiovascular surgery (CVS) intensive care unit (ICU), duration of stay in the neonatal ICU, need of postoperative extra corporeal

membrane oxygenator (ECMO) and duration of ECMO support, need of periton dialysis, need of continuous renal replacement therapy (CRRT), need of delayed sternal closure and duration of sternal closure and mortality rate were all retrieved from the institutional databases and medical records.

All TGA patients who underwent ASO by the same surgical team were included in the study. Aortobicaval cannulation was performed in all patients. The patients were cooled to 28°C and after the patients were taken to CPB, the patent ductus arteriosus (PDA) was ligated and divided after transfixation sutures. DelNido cardioplegia and topical cooling were used for myocardial protection after CC was placed, and antegrade cardioplegia was repeated every 60 minutes. Coronary arteries were moved to the neo-aorta by direct anastomosis or Trap-door technique. Which technique to use was decided after intraoperative evaluation of the aortic and pulmonary annulus. After translocation of the coronary arteries to the neo-aorta, the Lecompte maneuver was performed and the neo-aortic anastomosis was completed. Neopulmonary anastomosis was completed using fresh pericardium.

Interquartile range (IQR) was used to express continuous data, whereas frequency and percentages were used to represent categorical variables. A p-value of less than 0.05 was considered statistically significant for all statistical analyses, which were carried out using the SPSS for Windows version 25.0 program (SPSS Inc., Chicago, IL, USA).

## Results

The median age of the patients was 22.9±61.26 (1-455) days, and their weights ranged between 3391.97±686.6 (1900-5500) grams. 56 patients (91.8%) were in the neonatal period. The diagnosis was TGA-IVS in 39 patients (63.9%), and TGA with VSD (TGA-VSD) in 22 patients (36.1%). Diagnosis was made by transthoracic echocardiography (ECHO) in all cases. 22 patients (36.1%) had fetal ECHO during the antenatal period. Balloon atrial septostomy (BAS) was performed in the catheter laboratory in 42 patients (68.9%) with restrictive atrial septal defect (ASD). ASO was applied to all patients. Coronary artery anatomy was normal in 50 cases (82%). Coronary arteries were abnormal in 11 patients (18%). Cx was originating from the RCA in 4 cases (36.4%), and a single coronary root was present in 4 cases (36.4%). In 2 cases, LAD was dislocated from the RCA and Cx was dislocated from its normal position (18.2%) and in 1 patient, the coronary arteries were double looping (9.1%).

All patients were operated under CPB. Mean CPB time was  $135.44 \pm 29$  (78–247) minutes, CC time was  $87.95 \pm 18.8$  (52–136) minutes. Inotropic support was started in all patients after CPB. Depending on the hemodynamic status of the patients, the sternum was closed or left open, and they were followed up in the pediatric CVS ICU. Delayed sternal closure was performed to 40 patients. (65.6%) In these patients, the sternum was closed at the bedside in ICU on the appropriate day according to the hemodynamic status of the patient. Mean sternal closure time was  $3.58 \pm 3.22$  (1–16) days. Patients who continued to have hemodynamic instability and could not wean from CPB or needed CPB again after leaving were transferred to ICU under ECMO support. In patients who could leave ECMO according to hemodynamic status, weaning was performed at the bedside in ICU. The patients who needed ECMO were 7 (11.5%), 3 (4.9%) patients who could leave ECMO, mean time to leave ECMO was  $9 \pm 5$  (4–14) days. Peritoneal dialysis was performed in 7 patients (11.5%) and CRRT in 2 patients (3.3%).

Mortality was observed in 7 patients (11.5%). Mortality was seen  $5.71 \pm 2.98$  (1–10) days after surgery. The incidence of coronary anomaly in patients with mortality was 28.6%. The most common coronary anomaly in patients with coronary anomaly with mortality was the anomaly in which the Cx originates from the RCA.

The patients were followed up in the pediatric CVS ICU after ASO. The patients were taken to the neonatal ICU after the need for inotropes was over. The extubation and enteral feeding processes of the patients were performed in the neonatal ICU. The hospitalization period in the pediatric CVS ICU was  $7.92 \pm 8.73$  (1–62) days, and the hospitalization period in the neonatal ICU was  $24.62 \pm 20.8$  (0–90) days.

## Discussion

TGA was first described by Mathew Bailie in 1797 in the second edition of the book “The Morbid Anatomy of some of the Most important Parts of the Body”, but the term transposition was first used by Farre in 1814.<sup>[8]</sup> In this congenital cardiac malformation, there is atrioventricular concordance and ventriculoarterial discordance, that is, the morphological right atrium (RA) connects to the morphological RV, but this ventricle connects to the aorta instead of the PA, unlike the usual situation. Likewise, the morphological left atrium (LA) connects to the morphological LV, while the morphological LV connects to the PA.

TGA is the most common cyanotic congenital heart disease. It constitutes 5% of all congenital heart diseases.<sup>[1]</sup> TGA occurs in 20–30 of 100,000 live births.<sup>[9]</sup> It is seen two times more in male than in female.<sup>[3,4]</sup> This disease is accompanied by non-cardiac anomalies in 10% of cases.<sup>[10]</sup>

In 50% of cases, only ventriculoarterial discordance, atrioventricular concordance is found. This situation is called Simple TGA. In case of VSD, LVOT stenosis, arch anomalies or systemic venous return anomalies, it is called Complex TGA. VSD is relatively common, but its location and size are variable. There may be varying degrees of malalignment between the outlet and the trabecular septum. Anterior and right deviation of the outlet septum can cause pulmonary overriding and subaortic stenosis. Aortic hypoplasia, coarctation, or aortic interruption may be seen in these cases. If the outlet septum shows posterior and left malalignment, this results in subpulmonary stenosis.<sup>[11]</sup> LVOT stenosis occurs in approximately 25% of cases and is more common in VSD-TGA patients. In our series, the number of patients with TGA-IVS was 39 (63.9%), while the number of patients with TGA-VSD was 22 (36.1%). The incidence of coronary anomaly in transposition of the great arteries is not to be underestimated. While the incidence of coronary anomalies in our series was 18%, the most common coronary anomalies were Cx originating from RCA and coronary arteries originating as a single coronary root.

Contrary to what it should be, the systemic and pulmonary circulation in these patients progress in parallel, not in series. While oxygenated blood circulates between the left chambers of the lung and heart, systemic blood circulation is provided by another closed circulation starting from the right chambers of the heart and ending in the right chambers of the heart. In this case, life becomes possible only with a connection between these two circulations.<sup>[12]</sup>

Central cyanosis and deep hypoxia are seen due to parallel circulation in this pathology. The degree of hypoxia determines the amount of mixture between circulation. In cases where the ventricular septum is intact and the ASD is restrictive, hypoxia and cyanosis begin from the first hours of life. Hypoxia is exacerbated in the presence of accompanying LVOT stenosis or pulmonary stenosis. Conversely, if adequate mixing is achieved in the presence of a large VSD, cyanosis may be overlooked, and even heart failure due to increased ventricular load may occur.<sup>[13]</sup>

The exact etiology of this disease is unknown. Gestational diabetes, maternal exposure to rodenticides

and herbicides and maternal antiepileptic use are blamed in the etiology.<sup>[14]</sup> Although different mutations are prominent in this pathology, no clearly related gene has been detected. Although chest radiography and electrocardiography are helpful in diagnosis, they do not have specific findings. In TGA, the superior mediastinum is narrowed on chest radiography and there is a characteristic egg-shaped heart. Increased pulmonary vascularity with cardiomegaly can be seen in VSD-TGA. In the current era, TGA is diagnosed with transthoracic ECHO with ventriculoarterial discordance. Parasternal long axis and also the subcostal-parasternal apical chamber views of two-dimensional (2D) ECHO demonstrates PA originating from the LV coursing posteriorly and the aorta from RV in the same plane coursing anteriorly. Aorta is identified as the great vessel from which the coronary arteries are seen originating, PA is identified as the great vessel that bifurcates. Right anterior aorta and central position of pulmonary valve are seen. Important anatomical and presurgical details should be determined with ECHO including VSD, LVOT obstruction, morphology and the size of semilunar valves, the origins of coronary arteries and their branching.

Coronary anomalies are so common in TGA. According to Leiden convention and Yacoub and Radley-Smith classification, Type A (normal) coronary distribution is most common. Type B, single coronary ostium from a posterior facing sinus; type C, separate close origins of the left and right coronary arteries from a posterior facing sinuses (often with intramural course); type D, Cx from RCA; type E, Cx from right posterior sinus and LAD and RCA from the left posterior facing sinus are the other defined types. In our series the most common coronary anomalies are Cx arising from RCA and single coronary ostium with total 72.8%.

Prenatal diagnosis of TGA with fetal ECHO is increasing nowadays and leads counseling families of the diseases, delivery planning and to provide appropriate postpartum management. Fetal four-chamber view is normal but typical features include the aorta anterior to the PA and parallel outflow tracts at the outflow tract position. Restriction of ductus arteriosus and foramen ovale are two important point which may be predictive of severe hypoxemia after delivery.<sup>[15]</sup> In our series 37.7% of patients had antenatal diagnosis of TGA.

The main goal in this pathology is to provide an adequate mixture in the affected newborn. An adequate ASD or VSD can provide adequate mixing in the neonate and saves the patient time until corrective surgery. Patients who do not have a sufficiently large

ASD or VSD need different interventions before surgical correction. Intravenous infusion of prostaglandin E1 (PGE1) is necessary to maintain patency of the ductus arteriosus. In this way, pulmonary blood flow increases and pulmonary venous return and left atrial pressure increase. This creates a left-right shunt at the atrial level. Side effects of PGE1 are apnea, bradycardia, systemic hypotension, fluid-electrolyte imbalances, fever and flushing in the acute period. Its late side effects are dose-independent cortical hyperostosis.<sup>[16]</sup>

Although PGE1 increases mixing between circulations, it is often not sufficient and additional interference is needed. BAS also known as the Raskind procedure, has an important place in the presurgical follow-up of these patients. The purpose of this procedure is to increase interatrial mixing by widening the patent foramen ovale or restrictive ASD. This increases oxygen saturation. The Raskind procedure was applied in 42 of our patients. (63.8%) Thirty of these patients (%71.43) had nonrestrictive ASD and increased saturation. This saves time for surgery.

In addition to these interventions, medical support is often needed to stabilize the clinical situation. Mechanical ventilation and oxygen are required to resolve resistant hypoxia. However, oxygen supplementation accelerates ductal closure and reduces mixing. It triggers intercirculatory shunts by increasing alveolar tension in high-pressure ventilations. Sodium bicarbonate is important in the treatment of metabolic acidosis, and inotropic agents and diuretics can be added to the treatment when heart failure develops.

Accompanying lesions determine the surgical treatment of TGA. Many methods have been tried in the history of TGA treatment. In 1950, Blalock-Hanlon aimed to increase the mixing at the atrial level with atrial septectomy. Today, this procedure has been replaced by BAS. In our clinic BAS is the first choice in these patients with insufficient mixing.

Other surgeries performed in TGA pathology are atrial baffle surgeries described by Mustard and Senning.<sup>[17]</sup> This operation is basically physiological correction operations. Since the ventricle providing the systemic circulation is the RV, it is not an anatomical correction. In these operations, systemic and pulmonary venous return is directed to the associated ventricles via the atrial baffle. While fresh pericardium is used for baffle in Mustard operation, baffle is provided with right atrial flap in Senning operation. In this way, oxygenated blood enters the systemic circulation through the pul-

monary vein-RA-RV and aorta. Complications of these procedures are superior vena cava obstruction, baffle leak, atrial and ventricular arrhythmias, tricuspid valve insufficiency, RV failure.<sup>[17,18]</sup> Today, these operations have been replaced by ASO. In this study, we preferred to implement ECMO support with single stage ASO or two stage ASO in delayed patients.

ASO was accepted as the most appropriate treatment option in TGA patients after the first successful repair by Jatene et al.<sup>[13]</sup> In IVS-TGA patients, surgery should be performed within the first 2 weeks. Because in these patients, the pulmonary pressure returns to normal within 2–3 weeks, and accordingly, the LV pressure decreases in cases that exceed two weeks. Two-stage arterial switch surgery is performed in patients who have undergone the neonatal period for various reasons. In cases longer than 3 weeks, if the IVS is deviated to the left on ECHO, the ratio of left ventricular systolic pressure to right ventricular systemic pressure is below 70%, and the LV posterior wall thickness is less than 4 mm, arterial switch surgery should be performed with a two-stage approach.<sup>[19]</sup> In the first stage, banding and systemic-pulmonary arterial shunt are applied to the PA.

In ECHO after this operation, the IVS is curved to the right and the LV has a spherical structure, synergistic contraction with the IVS, the LV and RV systolic pressures are close to each other (left ventricular systolic pressure / right ventricular systolic pressure > 70%), and In case of detection of posterior wall thickness, LV volume and muscle mass which is appropriate to the patient's age, arterial switch surgery can be performed by proceeding to the second stage.<sup>[20,21]</sup>

The incidence of coronary anomaly in TGA patients is between 30–45%. In our series, this rate was found to be 18%. Coronary translocation is the most critical part of Jatene surgery. A possible malposition results in myocardial ischemia due to coronary perfusion deterioration. This may cause death due to myocardial ischemia. In our series, the incidence of coronary anomaly in patients with mortality was 28.6%. The most common coronary anomaly in patients with coronary anomaly with mortality was the anomaly in which the Cx originates from the RCA.

While preparing the coronary arteries, the coronary arteries should be freed by very careful dissection. In some cases, thin conal branches may be sacrificed during this preparation. The sinuses in the PA to which the coronary arteries will be transferred can be prepared by removing the piece or using the linear incision technique

(trap-door). In some cases, coronary artery transfer after neo-aortic anastomosis reduces distortion. We did not use this method in any of our patients.

The most common reason for reoperation in arterial switch surgery is neo-pulmonary artery stenosis. The risk factors for PA stenosis are age, previous pulmonary banding operation, the patch material and shape used in the reconstruction, and the surgical technique applied. Neo-PA stenosis is not associated with complex cardiac and coronary anomalies. It is directly related to the surgical technique and patch material used.<sup>[22]</sup>

Treatment alternatives in complex transpositions depend on the type and severity of pulmonary stenosis, and the size and location of the VSD. In patients with severe pulmonary stenosis and small VSD, cyanosis is serious from the neonatal period and palliative operations are preferred instead of corrective operations. (BAS and/or systemic-pulmonary shunt operations). More balanced combinations can be expected for corrective operations. The classical corrective procedure applied in these patients is the Rastelli Procedure, which directs the left ventricular flow to the aorta through an intraventricular tunnel and ensures the continuity of the right ventricular outflow tract with a valved conduit. To prevent tunnel-related subaortic stenosis, the VSD should be wide and associated with both major vessels. The most important late complication in this procedure is stenosis developing in the conduit and the need for conduit replacement.<sup>[23]</sup>

To avoid repetitive operations for conduit replacement, the REV procedure for the right ventricular outflow tract without the use of a conduit was described by Lecompte.<sup>[24]</sup> In this procedure, an intraventricular tunnel is created to divert left ventricular flow to the aorta after infundibular resection to widen the VSD. Afterwards, the Lecompte maneuver is performed and the PA is directly connected to the RV by widening it with a patch.<sup>[23]</sup>

The logic of the Nikadih procedure is to eliminate the shortcomings of the Rastelli procedure. The Rastelli procedure has disadvantages such as requiring septal resection during the expansion of the VSD for the intraventricular tunnel, risk of developing subaortic stenosis or stenosis in the tunnel due to tunnel malposition, and reduction of the RV cavity. In the aortic translocation type repair, that is, the Nikadih procedure, a path free of stenosis is created between the LV and the neo-aorta, reducing the need for septal resection and wide right ventriculotomy required in the Rastelli operation. Although this technique seems effective, limited experi-

ence in the literature limits its use. Long-term complications of this technique include neo-aortic regurgitation, coronary obstructions, and pulmonary regurgitation.<sup>[23]</sup>

The life expectancy of newborns with transposition is mostly less than 1 year and the mortality rate in the first year is 89.3%.<sup>[25]</sup> These rates have been reversed with new surgical methods and developments in intensive care. Survival over a 15-year period is around 90%. In addition, reintervention rates in a 10-year period are 6% and event-free survival is 88%.<sup>[24,25]</sup>

## Conclusion

In conclusion, ASO, which provides anatomical and complete correction in TGA, can be performed with appropriate timing, good preoperative, per operative and postoperative management with low mortality and morbidity. When appropriate left ventricular functions are examined in detail in the light of the literature, ASO surgery can be performed even outside the neonatal period, and full correction is successfully performed with the help of close postoperative follow-up and left ventricular support devices when necessary. Coronary artery anomaly is not a contraindication for ASO, and with the detailed and careful evaluation of the appropriate coronary artery anatomy, transpositions with coronary anomalies are often uneventful.

## Conflict of Interest

The authors declare no conflict of interest.

## Author Contributions

All authors contributed equally to protocol/project development, data collection, data analysis, manuscript writing/editing.

## Ethics Approval

The study was carried out in compliance with the Declaration of Helsinki's guiding principles and the protocol was accepted by the ethics committee of the Institution (No: E2-23-3743).

## Funding

The authors declare no financial support.

## References

- Marek J, Tomek V, Skovránek J, Povysilová V, Samánek M. Prenatal ultrasound screening of congenital heart disease in an unselected national population: a 21-year experience. *Heart* 2011;97:124–30.
- Fricke TA, d'Udekem Y, Richardson M, Thuys C, Dronavalli M, Ramsay JM, Wheaton G, Grigg LE, Brizard CP, Konstantinov IE. Outcomes of the arterial switch operation for transposition of the great arteries: 25 years of experience. *Ann Thorac Surg* 2012;94:139–45.
- Kempny A, Wustmann K, Borgia F, Dimopoulos K, Uebing A, Li W, Chen SS, Piorowski A, Radley-Smith R, Yacoub MH, Gatzoulis MA, Shore DF, Swan L, Diller GP. Outcome in adult patients after arterial switch operation for transposition of the great arteries. *Int J Cardiol* 2013;167:2588–93.
- Oda S, Nakano T, Sugiura J, Fusazaki N, Ishikawa S, Kado H. Twenty-eight years' experience of arterial switch operation for transposition of the great arteries in a single institution. *Eur J Cardiothorac Surg* 2012;42:674–9.
- Shaner RF. Anomalies of the heart bulb. *J Pediatr* 1962;61:233–41.
- Grant RP. The morphogenesis of transposition of the great vessels. *Circulation* 1962;26:819–40.
- Grant RP. The embryology of ventricular flow pathways in man. *Circulation* 1962;25:756–79.
- Martins P, Castela E. Transposition of the great arteries. *Orphanet J Rare Dis* 2008;3:27.
- Samánek M, Slavík Z, Zborilová B, Hrobonová V, Vorísková M, Skovránek J. Prevalence, treatment, and outcome of heart disease in live-born children: a prospective analysis of 91,823 live-born children. *Pediatr Cardiol* 1989;10:205–11.
- Güçer S, Ince T, Kale G, Akçören Z, Ozkutlu S, Talim B, Çağlar M. Noncardiac malformations in congenital heart disease: a retrospective analysis of 305 pediatric autopsies. *Turk J Pediatr* 2005;47:159–66.
- Ho SY, Baker EJ, Rigby ML, Anderson RH. Color atlas of congenital heart disease - morphologic and clinical correlations. London: Mosby-Year Book; 1995. 192 p.
- Ashworth M, Al Adnani M, Sebire NJ. Neonatal death due to transposition in association with premature closure of the oval foramen. *Cardiol Young* 2006;16:586–9.
- Jatene AD, Fontes VF, Paulista PP, Souza LC, Neger F, Galantier M, Sousa JE. Anatomic correction of transposition of the great vessels. *J Thorac Cardiovasc Surg* 1976;72:364–70.
- Loffredo CA, Silbergeld EK, Ferencz C, Zhang J. Association of transposition of the great arteries in infants with maternal exposures to herbicides and rodenticides. *Am J Epidemiol* 2001;153:529–36.
- Qureshi AM, Justino H, Heinle JS. Transposition of the great arteries. In: Shaddy RE, Penny DJ, Feltes TF, Cetta F, Mital S, editors. *Moss and Adams' heart disease in infants, children and adolescents, including fetus and young adult*. 10th ed. Philadelphia (PA): Wolters Kluwer; 2022. p. 3336–57.
- Tálosi G, Katona M, Rác K, Kertész E, Onozó B, Túri S. Prostaglandin E1 treatment in patent ductus arteriosus dependent congenital heart defects. *J Perinat Med* 2004;32:368–74.
- Hörer J, Herrmann F, Schreiber C, Cleuziou J, Prodan Z, Vogt M, Holper K, Lange R. How well are patients doing up to 30 years after a mustard operation? *Thorac Cardiovasc Surg* 2007;55:359–64.
- Hörer J, Karl E, Theodoratou G, Schreiber C, Cleuziou J, Prodan Z, Vogt M, Lange R. Incidence and results of reoperations following the Senning operation: 27 years of follow-up in 314 patients at a single center. *Eur J Cardiothorac Surg* 2008;33:1061–7.
- Mavroudis C, Backer CL. Transposition of the great arteries. In: Mavroudis C, Backer CL, editors. *Pediatric cardiac surgery*. 4th ed. Oxford, UK: Wiley-Blackwell; 2013. p. 492–529.

20. Yacoub MH, Radley-Smith R, Maclaurin R. Two-stage operation for anatomical correction of transposition of the great arteries with intact interventricular septum. *Lancet* 1977;1:1275–8.
21. Kınoğlu B, Sarıoğlu T, Çalık MK, Sarıoğlu A, Tekin S, Turan T, Olga R. Two stage arterial switch for transposition of the great arteries. *Turkish Journal of Thoracic and Cardiovascular Surgery* 1997;5:11–18.
22. Kalko Y, Hökenek F, Sever K, Söyler İ, Tireli E, Dayıoğlu E, Onursal E, Dindar A. The early results of arterial switch operations for transposition of the great arteries. *Turkish Journal of Thoracic and Cardiovascular Surgery* 2001;9:35–8.
23. VanMierop LH, Alley RD, Kausel HW, Stranahan A. Pathogenesis of transposition complexes. I. Embryology of the ventricles and great arteries. *Am J Cardiol* 1963;12:216–25.
24. Lecompte Y. Réparation à l'Etage ventriculaire - the REV procedure: technique and clinical results. *Cardiol Young* 1991;1:63–70.
25. Warnes CA. Transposition of the great arteries. *Circulation* 2006;114:2699–709.

**ORCID ID:**

B. Soran Türkcan 0000-0002-0694-5211; M. Yılmaz 0000-0002-3212-2673; Y. Özdemir Şahan 0000-0003-4219-9532; Ö. Ertekin 0000-0002-7846-7634; A. N. Ecevit 0000-0002-8820-9305; A. Atalay 0000-0002-7700-5964



**Correspondence to:** Başak Soran Türkcan, MD

Department of Paediatric Cardiovascular Surgery,  
Ankara Bilkent City Hospital, Ankara, Türkiye  
Phone: +90 532 477 66 27  
e-mail: basaksoran@gmail.com

*Conflict of interest statement:* No conflicts declared.

This is an open access article distributed under the terms of the Creative Commons Attribution-NonCommercial-NoDerivs 4.0 Unported (CC BY-NC-ND4.0) Licence (<http://creativecommons.org/licenses/by-nc-nd/4.0/>) which permits unrestricted noncommercial use, distribution, and reproduction in any medium, provided the original work is properly cited. *How to cite this article:* Soran Türkcan B, Yılmaz M, Özdemir Şahan Y, Ertekin Ö, Ecevit AN, Atalay A. Transposition of the great arteries: single center experiences. *Anatomy* 2022;16(3):172–178.

# Can high resolution 3D resin printed models be used in anatomy education? A randomized controlled trial

Ramazan Kurul<sup>1</sup> , Murat Dıramalı<sup>2</sup> , Dilruba Özdemir<sup>1</sup> , Kevser Ezgi Erdoğan<sup>1</sup> 

<sup>1</sup>Department of Physiotherapy and Rehabilitation, Faculty of Health Sciences, Bolu Abant İzzet Baysal University, Bolu, Türkiye

<sup>2</sup>Department of Anatomy, Faculty of Medicine, Bolu Abant İzzet Baysal University, Bolu, Türkiye

## Abstract

**Objectives:** Resin printing is a rapidly growing technology with a diverse range of applications. This study aims to examine the usability of 3D resin printed models in anatomy education.

**Methods:** The study included 84 students who were randomly assigned to either a 3D resin print group (n=42) or a plastic model group (n=42) based on their sex, lateralization, anatomy quiz scores, and Purdue spatial visualization test rotations scores. After attending a lecture, each participant examined an original sacrum and either a 3D printed or a plastic model, depending on their group. The participants were then asked to compare the models to the original using a visual analog scale (VAS) questionnaire, which consisted of four questions about the model's weight, anatomical accuracy, level of detail, and texture quality. The participants' ability to identify the models was evaluated using a 3-point Likert scale.

**Results:** The results showed that the 3D printed model had significantly higher ratings than the plastic model in terms of weight, level of detail, and texture quality ( $p < 0.05$ ). There was no significant difference in accuracy scores ( $p > 0.05$ ) or the participants' ability to identify the models ( $p > 0.05$ ).

**Conclusion:** 3D resin printed models are superior to plastic models in some aspects. These results suggest that 3D resin printed model can be used as in the conventional anatomy training approach.

**Keywords:** 3D print, education, resin, spatial ability

Anatomy 2022;16(3):179–184 ©2022 Turkish Society of Anatomy and Clinical Anatomy (TSACA)

## Introduction

Traditional anatomy education primarily relies on presentation materials, atlases, models, digital resources, and wet and dry plastinated cadavers.<sup>[1,2]</sup> The correct placement of anatomical structures is crucial for the success of health professionals in their practice.<sup>[3]</sup> Three-dimensional direct manipulation of the human body by touch is of great importance in anatomy education, and cadaver dissection is still considered the most appropriate source to achieve this goal.<sup>[4,5]</sup> However, there are many obstacles to use cadavers in anatomy education, including social, ethnic, religious, cultural, and donor laws and the high cost of cadaver acquisition and management for worldwide anatomy education.<sup>[6,7]</sup> Students need to take the anatomical structures, rotate, and examine them from every angle, such as the contribution of direct manipulation.<sup>[8]</sup> It is known that direct manipula-

tion makes great contributions to students' practical knowledge.<sup>[9]</sup>

In addition to traditional methods (dissection and plastination), a modern three-dimensional (3D) printing system technique has recently been added to the anatomy curriculum.<sup>[8,10,11]</sup> This new tool looks promising and could supplement and replace more traditional methods of anatomy education. Studies evaluating the impact of different pedagogies in anatomical education highlight the potential role of new methods (such as the use of 3D printed material) in anatomical education. 3D-printed examples can be a valuable, helpful tool, especially in contexts where human dissection is hampered by lack of facilities, human material, and problematic cultural and/or religious backgrounds.<sup>[10,12]</sup>

In the last decade, 3D printing has become more accessible and affordable, with systems and materials that can be

used at home. 3D printing is a technology that reduces production to individual dimensions without the need for supply systems based on a computer-generated model.<sup>[13]</sup> In the computer controlled 3D printing process, the physical material is created layer by layer until it is virtually identical to the designed one.<sup>[14]</sup> Compared with other tissue engineering methods and rapid tissue prototyping methods, 3D printing has several advantages, including high precision, fast production, low cost and good integration.<sup>[15]</sup> 3D modeling can help medical professionals or students better understand complex structures.<sup>[16]</sup> The most common materials used in 3D printers are durable nylon, aluminum, gypsum, textile raw materials, polylactic acid, and resin.<sup>[17]</sup> Among these materials, photosensitive resin provides the opportunity to produce higher quality, more complex structures that are closer to reality and smoother without showing its own raw material texture.<sup>[18]</sup>

This study aimed to examine the usability of tissues printed with a 3D resin printer in anatomy education to increase direct manipulation in applied training.

## Materials and Methods

The study involved a total of 84 participants, all 2nd-year medical students. This prospective, double-blinded, and parallel-group study was performed in line with the Helsinki Declaration with permission from the ethical committee of Bolu Abant İzzet Baysal University. The inclusion criteria were to enroll in the anatomy course in both periods and participate in the cadaveric and model

practical lectures. Exclusion criteria were if the candidate had upper extremity traumatic injury in the last three months, a sensory deficit in either of the hands or scar tissue on their fingertips.

Participants were randomly assigned into two, 3D print (n=42) and plastic model (n=42) groups, with stratified randomization based on Purdue spatial visualization test. Rotation (PSVT-R) scores, laterality scores, sex, and age of the participants were recorded. Sample size calculation was performed with G\*Power software based on previous research, which yielded an estimated effect size of 0.701 and it was found that 33 participants were required for each group to achieve 80% power with a  $p < 0.05$  significance level.<sup>[19]</sup>

For 3D printing, the department's Elegoo Saturn 8k 3D resin printer (Elegoo Inc, HK, China) and Elegoo 8K grey resin were used, with a 2.5-second exposure time and 0.05mm slice layer height. The printable sacrum model was based on a human sacrum, and the interior wall was hollowed and sliced for printing using Chitubox basic software (Chitubox Inc, Guangdong, China). The hollow part of the model was filled with fast-cure resin until the model weight matched the original sacrum (Figure 1). After printing, the model was washed with 95% isopropyl alcohol and cured for 30 minutes under direct ultraviolet light.

Both groups received a 30-minute theoretical lecture on the anatomy and clinical implications of the sacrum. After the lecture, participants were instructed to examine

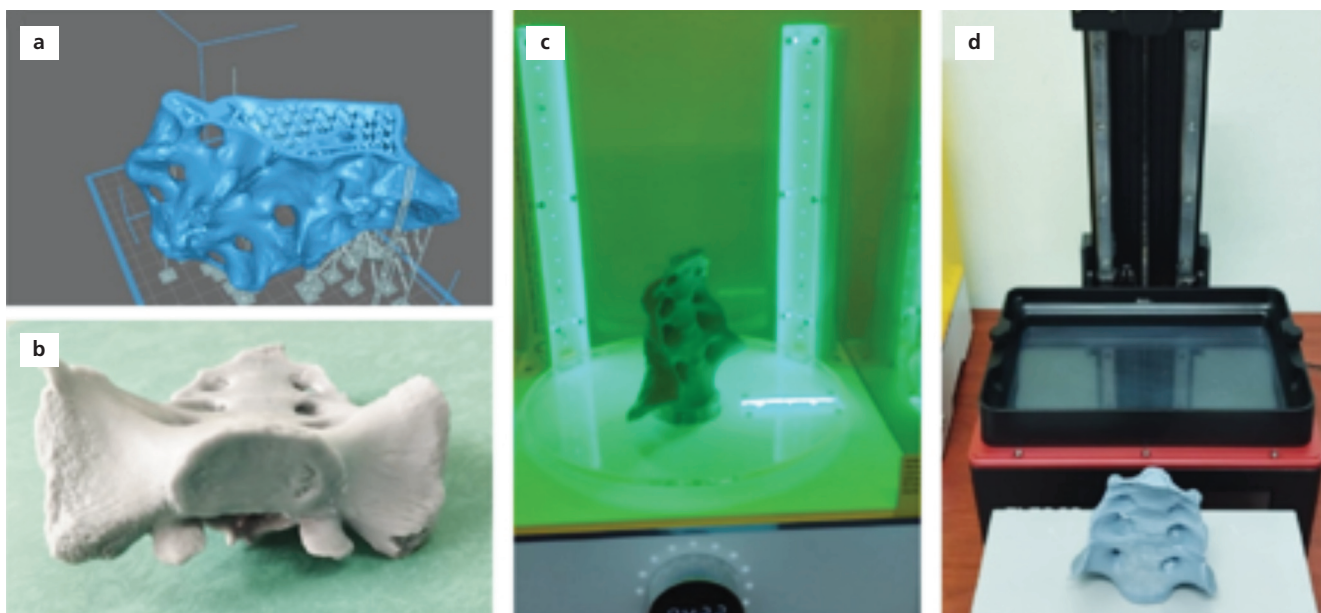


**Figure 1.** (a) Preparation of the model in the slicing program for printing; (b) Detailed bone texture of the printed model; (c) Curing process of the model with rotating ultraviolet light device; (d) 3D printer and completed model of the sacrum.

and identify structures on the original sacrum for 10 minutes with direct manipulation. Then, they received either a 3D or plastic model of the sacrum according to their group allocations and were instructed to examine and compare the models to the original.

The outcome assessments included a 10-question multiple-choice quiz to assess participants' post-exposure knowledge of anatomical structures after the practical lecture. Participants were also asked to compare the models to the original with a Visual Analog Scale (VAS) questionnaire consisting of 4 questions about the model's weight, anatomical accuracy, level of detail, and texture quality. After completing assessments, blinded participants were asked to identify both models as 3D printed and plastic models.

Purdue spatial visualization test-Rotation was used to assess three-dimensional perception of participants in this study. The test was developed by Guay in 1977 and revised by Yoon in 2011 and consists of 30 items. The participants were asked to solve each multiple-choice question (MCQ) rotation according to the given rotations. Low scores indicate lower spatial perception capabilities. Subjects completed the task in approximately 15 min.<sup>[20]</sup>

The hand laterality task was used to assess participants' mental motor imaginary capabilities, which is required for imaging three-dimensional objects. The test consists of 4 images of both hands and six difficulty levels. Levels consist of a 60-degree rotation for each set of images. A total

score of 48 indicates perfect laterality. Subjects completed the task in approximately 10 min.<sup>[21]</sup>

The printed model's weight, anatomical accuracy, level of detail, and texture were assessed with VAS. Participants were instructed that 0 indicates no similarity to 10 indicates identical to the original model and asked to mark on a 10 cm straight line.

After completing previous assessments, participants received both 3D printed and plastic models and were asked to identify each model on a 3-point Likert scale as 0-cannot decide, 1-plastic, 2-3D printed.

The chi-square test was used to compare the distribution of sex and the participants' discernment capabilities of models. The Shapiro-Wilk test was used to test for the normal distribution of continuous variables. Normal distribution was observed for age, quiz, PSVR-T, and laterality scores. The independent t-test was used to analyze the differences between the groups. A p-value of less than 0.05 was considered statistically significant. The chi-square test was used to analyze sex distribution between groups. All statistical analyses were performed using the SPSS statistical package for Windows, version 24 (IBM Inc., Armonk, NY, USA).

## Results

Eighty-four participants who met the inclusion criteria were included in this study (Figure 2). In the 3D print

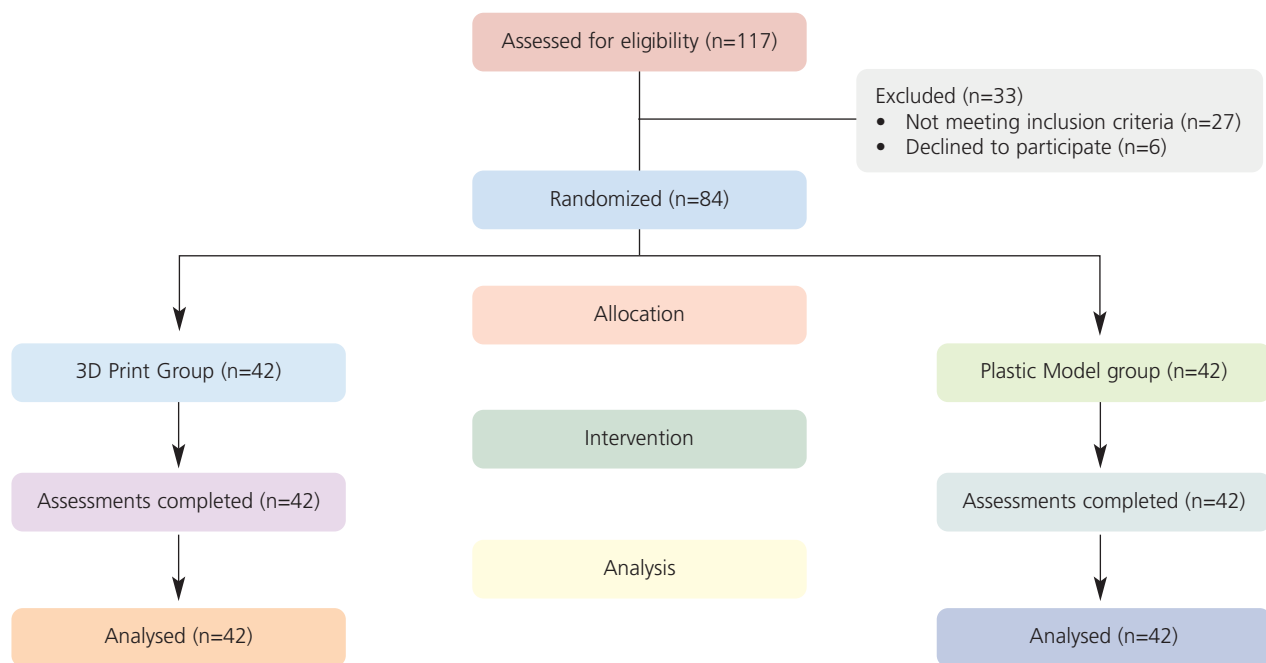


Figure 2. Flowchart of the study.

**Table 1**  
Baseline characteristics of the participants.

		3D Print (n=42)		Plastic model (n=42)			
		X±SD		X±SD		t	p-value
Age (years)		19.90±1.33		19.38±01.41		1.743	0.085
Lateralization		34.61±7.69		35.04±10.15		-0.218	0.828
PSVT:R		24.28±3.95		23.26±3.65		1.232	0.221
		n	%	n	%	χ <sup>2</sup>	p-value
Sex	Female	38	90.5	37	88.1	0.124	0.724
	Male	4	9.5	5	11.9		

PSVT:R: purdue spatial visualization test rotations; t: independent samples t-test, p<0.05; χ<sup>2</sup>: Chi-square test.

group, the mean age was 19.90±1.33 years, the lateralization score was 34.61±7.69 points, and the PSVT-R score was 24.28±3.95 points. In the plastic model group, the mean age was 19.90±1.33 years, the lateralization score was 35.04±10.15 points, and the PSVRT score was 23.26±3.65 points. There were 4 (9.5%) males and 38 (90.5%) females in the 3D print group and 5 (11.9%) men and 37 (88.1%) women in the plastic model group. There was no difference between the groups in terms of age, lateralization scores, sex, and PSVRT scores (p<0.05) (**Table 1**). Participants' model assessment VAS scores and quiz scores showed a normal distribution (p>0.05).

Independent sample t-test results showed that there was no difference between the quiz scores of 3D print (6.28±2.03) and plastic model groups (6.76±2.22) (p=0.310) (**Table 2**). 3D Printed model's weight, level of detail, and texture quality VAS scores showed significantly higher scores than the plastic model (p<0.001). However, there was no significant difference between the groups regarding anatomical accuracy scores (p=0.142) (**Table 2**).

## Discussion

In this study it was found that, 3D resin-printed models are superior to plastic models and resin-printed models can replicate details and textures better than plastic models. This outcome shows a high potential for creating accurate anatomical models for anatomy education with 3d resin printing.

Anatomy education requires mental imaging and spatial skills.<sup>[22]</sup> Sex-based allocation was necessary due to reported differences in the spatial abilities of male and female participants.<sup>[23]</sup> Studies investigating the efficiency of 3D-printed models showed an increase in favor of 3D-printed groups' written tests and quiz scores. In this study, a pre-test quiz was used to assess participants' anatomic knowledge after the lecture. This ensured that the initial anatomy knowledge of the groups was similar and prevented both the heterogenous distribution of reluctant/enthusiastic participants and sex distribution.

3D printing is a cheaper option compared to both cadaveric and plastic model-based education.<sup>[10]</sup> Kim et.

**Table 2**  
Independent t-test result of mean differences between groups.

	3D Print (n=42)		Plastic model (n=42)			
	X±SD		X±SD		t	p-value
Quiz	6.28±2.03		6.76±2.22		-1.022	0.310
Weight	8.28±1.87		5.60±2.16		6.049	<0.001
Anatomical accuracy	7.85±2.21		7.50±3.07		1.483	0.142
Level of detail	8.14±1.49		5.51±1.53		7.948	<0.001
Texture quality	8.71±1.24		4.08±2.33		11.359	<0.001

t: independent samples t-test, p<0.05.

al.<sup>[6]</sup> reported that next-generation printers with higher precision capabilities increased the printed models' level of detail and accuracy. Fasel et al.<sup>[24]</sup> verified the accuracy of models and showed that scans could be adapted to 3D-printed models. In order to achieve a real-life texture, studies tried various methods, such as covering printed tissue with a silicon-based coating.<sup>[25]</sup> The main concern of 3D-printed models is their accuracy and resemblance to the original tissue.<sup>[6]</sup> A 3D upper extremity model study pointed to the same limitations and implied that with technological advancements a printed model's texture could become identical to the original.<sup>[26]</sup> In this study, we found that the resin printed model's texture closely resembled the original one. In addition, the resin model's fine slice height resulted in a smooth transition which was a main concern for previous studies which used a PLA printer that produces rough textures. Moreover, the level of detail of the 3D printed models was found to be superior compared to the plastic model which uses a mould to mass produce models.

Young et al.<sup>[27]</sup> reported that increased cognitive load might impact the effectiveness of educational material. The complexity of the pelvis region is higher and increases the cognitive load on students that examine models. Another study focusing on 3D printed organs showed that the pelvis is a more complex region than the heart and recommends higher resolution prints for complex areas.<sup>[6]</sup> Studies investigating 3D prints on anatomy education report its benefits, however these studies also remark on the low detail level of 3D printers.<sup>[6,28,29]</sup> Printed and plastic models' resemblance to the original is vital. Level of detail is a crucial parameter when comparing plastic and printed models since the moulding procedure prevents the production of fine details due to the high risk of tearing during mould release.

Studies investigating the effectiveness of 3D printed models on anatomy education report promising results. A study comparing cadaveric and 3D printed model's post-test results showed that the 3D print group scores higher marks.<sup>[6]</sup> A randomized controlled study comparing cadaveric, 3D printed and atlas found similar results in favor of the 3D printed model group.<sup>[28]</sup> Another study using color coded 3D printed models also reports high scores in favor of the printed model group.<sup>[26]</sup> Studies investigating the effect of 3D printed models based on students learning reported that 3D printing does not cause disadvantages for students' learning activities and has a positive effect on junior students who do not want to make contact with cadaveric materials and avoid direct manipulation.<sup>[30-32]</sup> Similar to the previous studies, we found that the resin printed model scores higher marks and can be used in anatomy education. Post-test scores

were not collected from participants due to the design limitation of the study. Although previous studies showed that 3D models do not cause a disadvantage in anatomy learning, it was unclear whether resin models are free from the same problems.

3D printing is a cheap, accurate, feasible, and innovative way of providing anatomy teaching materials. The findings of this study show that resin printed models compared to plastic models, are more realistic and similar to originals. 3D printing is a relatively new area for anatomy education and this study showed that resin printing is a better solution compared to plastic models. The use of 3D prints can enhance anatomy education by providing a flexible tool. As students become more proficient in understanding normal anatomy, they can gradually be introduced to models that include pathological conditions. However, printing time is a downside of resin printing which can take 4-6 hours to print a single model. The cost of printing varies depending on the model's size, the resin's cost, and the inner area's hollowing. As a result, almost all bones, except cranial bones, can be printed using a small amount of resin. In this study, the cost of the sacrum was 4.7 USD, including the support for the models. This is cheaper than commercial sacrum models, typically costing 29 to 75 USD per model.

### Conflict of Interest

The authors have declared that they have no conflict of interest.

### Author Contributions

All authors contributed equally to protocol/project development, data collection, data analysis, manuscript writing/editing.

### Ethics Approval

The study was approved by Ethical Committee of Bolu Abant Izzet Baysal University (Clinical Researches Ethics Committee NBo: 2022/322-526) and performed in accordance with the Helsinki declaration of principles.

### Funding

This study was funded by The Scientific and Technological Research Council of Turkey (ID:2209-A 1919B012205918) and BAIBU Scientific Research Projects (ID: 2023-BDP-6.12.61-0003).

### References

1. McBride JM, Drake RL. National survey on anatomical sciences in medical education. *Anat Sci Educ* 2018;11:7-14.
2. Estai M, Bunt S. Best teaching practices in anatomy education: a critical review. *Ann Anat* 2016;208:151-7.

3. Sugand K, Abrahams P, Khurana A. The anatomy of anatomy: a review for its modernization. *Anat Sci Educ* 2010;3:83–93.
4. Winkelmann A. Anatomical dissection as a teaching method in medical school: a review of the evidence. *Med Educ* 2007;41:15–22.
5. Kerby J, Shukur ZN, Shalhoub J. The relationships between learning outcomes and methods of teaching anatomy as perceived by medical students. *Clin Anat* 2011;24:489–97.
6. Lim KHA, Loo ZY, Goldie SJ, Adams JW, McMenamin PG. Use of 3D printed models in medical education: a randomized control trial comparing 3D prints versus cadaveric materials for learning external cardiac anatomy. *Anat Sci Educ* 2016;9:213–21.
7. Robison RA, Liu CY, Apuzzo ML. Man, mind, and machine: the past and future of virtual reality simulation in neurologic surgery. *World Neurosurg* 2011;76:419–30.
8. Azer SA, Azer S. 3D anatomy models and impact on learning: a review of the quality of the literature. *Health Professions Education* 2016;2:80–98.
9. Peeler J, Bergen H, Bulow A. Musculoskeletal anatomy education: evaluating the influence of different teaching and learning activities on medical students perception and academic performance. *Ann Anat* 2018;219:44–50.
10. McMenamin PG, Quayle MR, McHenry CR, Adams JW. The production of anatomical teaching resources using three-dimensional (3D) printing technology. *Anat Sci Educ* 2014;7:479–86.
11. Vaccarezza M. Best evidence of anatomy education? Insights from the most recent literature. *Anat Sci Educ* 2018;11:215–6.
12. Bergman EM, Prince KJ, Drukker J, van der Vleuten CP, Scherpbier AJ. How much anatomy is enough? *Anat Sci Educ* 2008;1:184–8.
13. Silver A. 3D printing in the lab. *Nature* 2019;565:123–4.
14. Ye Z, Dun A, Jiang H, Nie C, Zhao S, Wang T, Zhai J. The role of 3D printed models in the teaching of human anatomy: a systematic review and meta-analysis. *BMC Med Educ* 2020;20:1–9.
15. Jones DB, Sung R, Weinberg C, Korelitz T, Andrews R. Three-dimensional modeling may improve surgical education and clinical practice. *Surg Innov* 2016;23:189–95.
16. Lauridsen H, Hansen K, Nørgård MØ, Wang T, Pedersen M. From tissue to silicon to plastic: three-dimensional printing in comparative anatomy and physiology. *R Soc Open Sci* 2016;3:150643.
17. Sharma S, Goel SA. 3D printing and its future in medical world. *Journal of Medical Research and Innovation* 2019;3:e000141.
18. Arefin AM, Khatri NR, Kulkarni N, Egan PF. Polymer 3D printing review: materials, process, and design strategies for medical applications. *Polymers (Basel)* 2021;13:1499.
19. Salazar D, Thompson M, Rosen A, Zuniga J. Using 3D printing to improve student education of complex anatomy: a systematic review and meta-analysis. *Med Sci Educ* 2022;32:1209–18.
20. Maeda Y, Yoon SY. A meta-analysis on gender differences in mental rotation ability measured by the Purdue spatial visualization tests: visualization of rotations (PSVT:R). *Educational Psychology Review* 2013;25:69–94.
21. Voyer D. On the reliability and validity of noninvasive laterality measures. *Brain Cogn* 1998;36:209–36.
22. Guillot A, Champely S, Batier C, Thiriet P, Collet C. Relationship between spatial abilities, mental rotation and functional anatomy learning. *Adv Health Sci Educ Theory Pract* 2007;12:491–507.
23. Terlecki MS, Newcombe NS, Little M. Durable and generalized effects of spatial experience on mental rotation: gender differences in growth patterns. *Applied Cognitive Psychology* 2008;22:996–1013.
24. Fasel JH, Aguiar D, Kiss-Bodolay D, Montet X, Kalangos A, Stimec BV, Ratib O. Adapting anatomy teaching to surgical trends: a combination of classical dissection, medical imaging, and 3D-printing technologies. *Surg Radiol Anat* 2016;38:361–7.
25. O'Reilly MK, Reese S, Herlihy T, Geoghegan T, Cantwell CP, Feeney RN, Jones JFX. Fabrication and assessment of 3 D printed anatomical models of the lower limb for anatomical teaching and femoral vessel access training in medicine. *Anat Sci Educ* 2016;9:71–9.
26. Mogali SR, Yeong WY, Tan HKJ, Tan GJS, Abrahams PH, Zary N, Low-Beer N, Ferenczi MA. Evaluation by medical students of the educational value of multi-material and multi-colored three-dimensional printed models of the upper limb for anatomical education. *Anat Sci Educ* 2018;11:54–64.
27. Young J, Van Merriënboer J, During S, Ten Cate O. Cognitive load theory: implications for medical education: AMEE guide no.86. *Med Teach* 2014;36:371–84.
28. Chen S, Pan Z, Wu Y, Gu Z, Li M, Liang Z, Zhu H, Yao Y, Shui W, Shen Z, Zhao J, Pan H. The role of three-dimensional printed models of skull in anatomy education: a randomized controlled trial. *Sci Rep* 2017;7:575.
29. Smith CF, Tollemache N, Covill D, Johnston M. Take away body parts! An investigation into the use of 3D-printed anatomical models in undergraduate anatomy education. *Anat Sci Educ* 2018;11:44–53.
30. Garas M, Vaccarezza M, Newland G, McVay-Doornbusch K, Hasani J. 3D-Printed specimens as a valuable tool in anatomy education: a pilot study. *Ann Anat* 2018;219:57–64.
31. Boeckers A, Brinkmann A, Jerg-Bretzke L, Lamp C, Traue HC, Boeckers TM. How can we deal with mental distress in the dissection room?—An evaluation of the need for psychological support. *Ann Anat* 2010;192:366–72.
32. Singh K, Gaur U, Hall K, Mascoll K, Cohall D, Majumder MAA. Teaching anatomy and dissection in an era of social distancing and remote learning. *Advances in Human Biology* 2020;10:90.

**ORCID ID:**

R. Kurul 0000-0001-8605-8286;  
 M. Diramali 0000-0001-5824-6159;  
 D. Özdemir 0009-0008-3657-9452;  
 K. E. Erdoğan 0009-0008-1543-6364

**Correspondence to:** Ramazan Kurul, PhD

Department of Physiotherapy and Rehabilitation, Faculty of Health Sciences,  
 Bolu Abant İzzet Baysal University, Bolu, Türkiye  
 Phone: +90 543 641 47 31  
 e-mail: ramazankurul2@hotmail.com

*Conflict of interest statement:* No conflicts declared.

This is an open access article distributed under the terms of the Creative Commons Attribution-NonCommercial-NoDerivs 4.0 Unported (CC BY-NC-ND4.0) Licence (<http://creativecommons.org/licenses/by-nc-nd/4.0/>) which permits unrestricted noncommercial use, distribution, and reproduction in any medium, provided the original work is properly cited. *How to cite this article:* Kurul R, Diramali M, Özdemir D, Erdoğan KE. Can high resolution 3D resin printed models be used in anatomy education? A randomized controlled trial. *Anatomy* 2022;16(3):179–184.

# Is the iliocapsularis muscle ubiquitous and consistent?

Daniel W. Copeland , Allison L. Pickron , Jocilyn R. Girouard , Philip A. Fabrizio 

Department of Physical Therapy, Philadelphia College of Osteopathic Medicine Georgia, Suwanee, GA, USA

## Abstract

The iliocapsularis muscle has been defined as originating from anterior superior iliac spine and iliac fossa and inserting into the lesser trochanter. Dissection of twenty-nine cadaveric hips yielded five iliocapsularis muscles, with two novel variations. Prevalence of iliocapsularis was found to be 17.2%. Iliocapsularis is important during dynamic hip stabilization and its role in preventing impingement of the anterior hip capsule. Therefore, understanding the current variations and prevalence may improve our understanding of the role of this muscle and its impact in the efficacy of surgical procedures in the area. The decreased prevalence of iliocapsularis muscles in the current study, the two variants, and the clinical significance is discussed.

**Keywords:** hip; iliocapsularis; ilioprochantericus

Anatomy 2022;16(3):185–188 ©2022 Turkish Society of Anatomy and Clinical Anatomy (TSACA)

## Introduction

The iliocapsularis muscle, also known as the ilioprochantericus, when present, has been reported to act as a hip flexor, located deep to rectus femoris and iliacus positioned over the anterior medial hip capsule. The iliocapsularis muscle has been described as having a proximal attachment from inferior to anterior superior iliac spine (ASIS) and anteromedial hip capsule with a common distal attachment accompanying the iliopsoas at the lesser trochanter.<sup>[1–3]</sup> Prevalence of this muscle has been reported in humans to range from 71–100%. Plante et al.<sup>[4]</sup> dissected 14 hips, 10 of which an iliocapsularis muscle was found present deep to the iliacus. Elvan et al.<sup>[5]</sup> discovered that 92% of 21 fetuses dissected contained an iliocapsularis muscle, and further considered this a common muscle. The iliacus and iliocapsularis muscles were described as having a distinct fascial layer separating the two muscles, as seen in 34 out of 39 hips, while in contrast, the other 5 hips did not show a clear fascial separation between the two muscles.<sup>[2,5]</sup>

The understanding of iliocapsularis muscle as an individual muscle has been challenged by D'Costa (2008) and Sato (2016). Sato et al.<sup>[6]</sup> showed that iliocapsularis muscle may actually be a deep slip of the iliacus if there was not a layer of investing fascia to distinctly separate

the muscle from the iliacus. The innervation of iliocapsularis muscle has been demonstrated in macaques as coming from a branch of the femoral nerve entering from the upper surface of this muscle after piercing the iliacus.<sup>[7]</sup> Similarly, in human fetuses, the innervation to iliocapsularis muscle was also described as a thin nerve branch from the femoral nerve, piercing through iliacus and superficially innervating iliocapsularis muscle.<sup>[5]</sup>

The iliocapsularis muscle has been shown to be present in embryological development by Elvan et al.<sup>[5]</sup> beginning as early as 26 weeks' gestation lateral to the iliopsoas and deep to the rectus femoris. The most common proximal attachments of the muscle were observed just below the common tendon attachment for rectus femoris or on the anteromedial part of the hip joint capsule. Innervation of the iliocapsularis muscle was found to be from a small branch of the femoral nerve.

The conflicting information and ambiguity regarding the iliocapsularis muscle created a drive for further exploration in order to understand the iliocapsularis muscle's function and possible implications in hip pathology. The aim of this study was to gather clinically significant information on the variations of the iliocapsularis muscle. Knowledge of hip anatomic variations was crucial to understanding hip pathology, determining

differential diagnoses, and to more accurately develop a plan of care in symptomatic hips.

## Case Report

During routine dissection of 29 hips of human adult cadavers in the anatomy laboratory, five iliocapsularis muscles were found. Three of the iliocapsularis muscles matched previous descriptions in the literature, with only one displaying innervation provided by a primary branch of the femoral nerve that passed through the belly of the iliacus, and the other two of the muscles were variations of iliocapsularis muscle.<sup>[1]</sup> Each variant iliocapsularis muscle was found to lie in a fascial compartment that was separate and distinct from the iliacus. In the present study, all of the iliocapsularis muscles had the commonality of being positioned directly beneath the iliopsoas immediately anterior to the femoral-acetabular

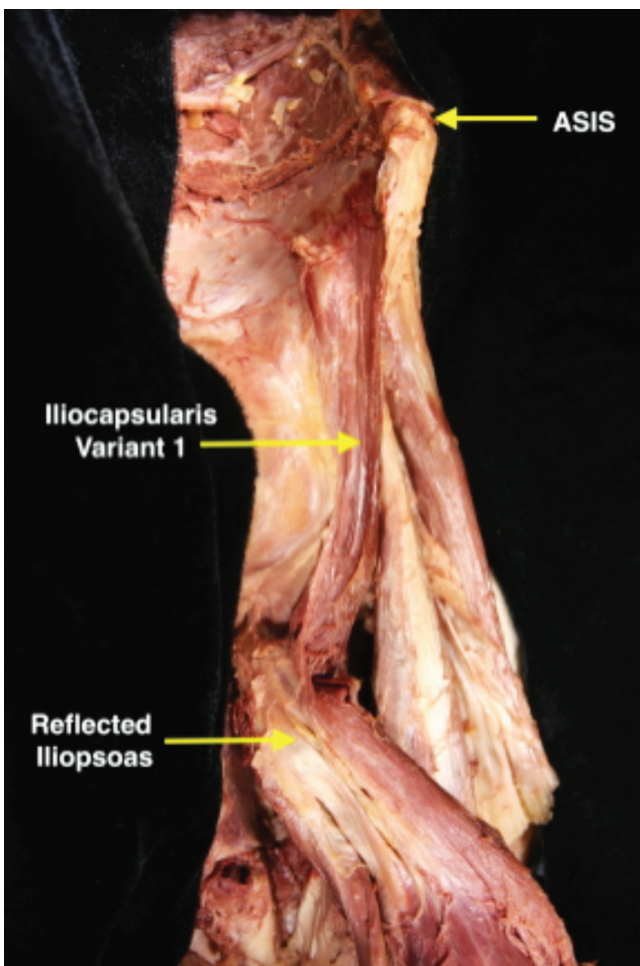


**Figure 1.** Photograph of anterior aspect of the left hip and thigh demonstrating unique twist of iliocapsularis muscle belly, as discussed in case 1.

joint. However, the two variations exhibited differences in their attachments as well as differences in their position along the hip joint. Although there was great ambiguity regarding the prevalence, function, and clinical significance of the iliocapsularis muscle; the authors are not aware of any human variations that match the variant iliocapsularis muscles described in the current cases.

## Case 1

The iliocapsularis muscle in case one was identified in its own fascial compartment of the left hip, deep to the iliacus muscle. The proximal attachment arose from the ilium between the ASIS and anterior inferior iliac spine (AIIS). The muscle belly blended into the iliacus muscle, and the distal attachment inserted into the lesser trochanter along with the iliopsoas tendon. In this case, the muscle displayed a unique twist that resulted in a ribbon-like appearance of the muscle belly as it traversed toward its distal attachment. Along its course, deep fibers from the iliocapsularis muscle blended with the anterior hip capsule (**Figure 1**).

## Case 2

The iliocapsularis muscle in case two was also located in its own fascial compartment of the right hip, deep to the iliacus muscle. The proximal attachment arose from a point on the iliac fossa just medial to ASIS. The muscle fibers blended with the anterior aspect of the hip capsule. After crossing the joint capsule, the belly of the iliocapsularis muscle bifurcated into medial and lateral bands. The lateral band blended into the vastus intermedius muscle while the medial band joined the common iliopsoas tendon inserting into the lesser tubercle (**Figure 2**).

## Discussion

The varying descriptions of the iliocapsularis muscle in humans, and questionable function may contribute to the general ambiguity of this muscle. One purpose of this study was to determine if this muscle is indeed consistent in humans. To determine prevalence, this would require a working definition of what classifies the iliocapsularis as a muscle. As a guideline, the authors have defined iliocapsularis muscle as completely separated from iliopsoas by a fascial layer, had an origin on the iliac fossa or medial to AIIS, inserts into the lesser trochanter and intertrochanteric line, and was seen to be innervated by a first order nerve off of the femoral nerve.<sup>[8]</sup> Unlike previous claims that this muscle was constant in all humans,<sup>[1]</sup> the prevalence of iliocapsularis muscle in this study was found to be 17.2%, concluding that this muscle was not constant in all humans. With only five ilio-

capsularis muscles present in this study, and two of them being variations from what is described as typical, the authors speculate that the actual prevalence of iliocapsularis muscle was much lower than previously reported. Elvan et. al. described five iliocapsularis muscles that did not have a clear fascial layer separating the iliocapsularis muscle from the iliacus.<sup>[5]</sup> Taking into account the work of Sato and the definition of the iliocapsularis muscle, then Elvan's 92% prevalence rate would be decreased to 87% in human fetuses.<sup>[5,6]</sup>

The innervation of the iliocapsularis muscle has previously been described in human fetuses and macaques,<sup>[5,7]</sup> but rarely, if ever, in adult cadavers. Of the five muscles found during this study, one presents as a typically defined iliocapsularis muscle with innervation by a branch of the femoral nerve after piercing through the iliacus. This innervation course was similar to what is

described in macaques by Satoh and in human fetuses by Elvan.<sup>[5,7]</sup> The research was not clear if the innervation provides a motor component to iliocapsularis muscle or was purely sensory. Regardless, proposed functions of the iliocapsularis muscle would lend to the assumption that there was an important motor component to the innervation to the iliocapsularis muscle.

Limitations in the current study were that cadavers were used, and in vivo function of this muscle could not be completed. For this purpose, future research will include diagnostic ultrasound imaging and EMG to confirm the hypothesized studies. Another limitation of this study in addressing prevalence was the lack of identifying innervation. We only discovered innervation in one out of five iliocapsularis muscles in this present study, however, more careful dissection techniques should be implemented in further studies to clearly define iliocapsularis muscle as a distinct and separate muscle with intact innervation.

Functions of the iliocapsularis muscle were largely unknown.<sup>[9]</sup> The authors discussed how the anatomy of the muscle might influence the function. The iliocapsularis muscle's direct attachment to the anterior hip capsule, as described in this report as well as previous reports, implied that the muscle plays a role in pulling the capsule away from the hip joint during hip flexion. This would aid in preventing anterior synovial impingement during hip flexion exceeding 90 degrees.<sup>[3,10]</sup> In the absence of iliocapsularis muscle, increased incidence of synovial hip impingement was likely, and must be considered during the differential diagnosis of hip pathology. Iliocapsularis muscle has also been postulated to aid in hip stability.<sup>[1,2,10]</sup> The iliocapsularis muscle is commonly presented as hypertrophied in dysplastic hips, leading to assumptions that it actively contributed to anterior hip stabilization versus passive form closure that has been seen in a non-pathologic hip joint.<sup>[1]</sup>

### Acknowledgments

The authors wish to thank Mr. Jeffrey Seiple and Mr. Ronald Wilde for their assistance. The authors also thank the individuals who have donated their bodies and tissues for the advancement of education and research.

### Conflict of Interest

The authors declare that they have no conflicts of interest.

### Author Contributions

DWC: dissections, manuscript writing; ALP: dissections, project development, manuscript writing; JRG: dissec-

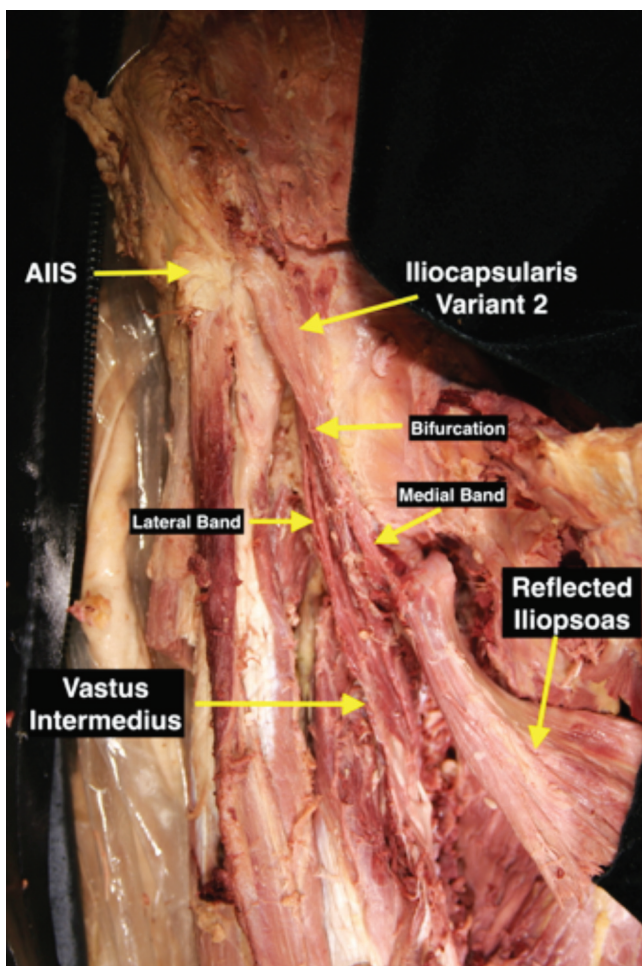


**Figure 2.** Photograph of anterior aspect of the right hip and thigh demonstrating variant bifurcation with medial and lateral bands, as discussed in case 2.

tions, project development, manuscript writing; PAF: manuscript writing/editing.

### Ethics Approval

Compliant with all institutional guidelines per the PCOM IRB, Code of Federal Regulations (CFR)-45 CFR Part 46 as well as with the Declaration of Helsinki, the Belmont Report and the Nuremberg Code.

### Funding

This research did not receive any specific grant from funding agencies in the public, commercial, or not-for-profit sectors.

### References

1. Babst D, Steppacher SD, Ganz R, Siebenrock KA, Tannast M. The iliocapsularis muscle: an important stabilizer in the dysplastic hip. *Clin Orthop Relat Res* 2011;469:1728–34.
2. Walters BL, Cooper JH, Rodriguez JA. New findings in hip capsular anatomy: dimensions of capsular thickness and pericapsular contributions. *Arthroscopy* 2014;30:1235–45.
3. Lawrenson P, Grimaldi A, Crossley K, Hodges P, Vicenzino B, Semciw AI. Iliocapsularis: technical application of fine-wire electromyography, and direction specific action during maximum voluntary isometric contractions. *Gait Posture* 2017;54:300–3.
4. Plante D, Janelle N, Angers-Goulet M, Corbeil P, Takech MA, Belzile EL. Anatomical variants of the rectus femoris motor innervation. *J Hip Preserv Surg* 2019;6:170–6.
5. Elvan O, Aktekin M, Şengezer E, Kurtoğlu Olgunus Z, Bayramoğlu A. Iliocapsularis muscle in human fetuses. *Surg Radiol Anat* 2019;41:1497–503.
6. Sato T, Sato N, Sato K. Review of the iliocapsularis muscle and its clinical relevance. *Anatomy & Physiology: Current Research* 2016;6:237.
7. Satoh J. The m. ilirotrochantericus (m. iliocapsulotrochantericus) in macaques. *Okajimas Folia Anat Jpn* 1965;40:323–37.
8. Segal RL, Wolf SL, DeCamp MJ, Chopp MT, English AW. Anatomical partitioning of three multiarticular human muscles. *Acta Anat (Basel)* 1991;142:261–6.
9. Ward WT, Fleisch ID, Ganz R. Anatomy of the iliocapsularis muscle. Relevance to surgery of the ghip. *Clin Orthop Relat Res* 2000;(374):278–85.
10. Pourcho AM, Sellon JL, Lachman N, Krych AJ, Smith J. Sonographic appearance of the iliocapsularis muscle of the hip. *PM R* 2015;7:94–6.

#### ORCID ID:

D. W. Copeland 0000-0003-0208-137X;  
A. L. Pickron 0000-0001-8027-8595;  
J. R. Girouard 0000-0002-8034-5708;  
P. A. Fabrizio 0000-0001-8833-8484



#### Correspondence to:

Daniel Copeland, PhD  
Department of Physical Therapy, Philadelphia College of Osteopathic Medicine  
Georgia, 625 Old Peachtree Road NW, Suwanee, GA, 30024, USA  
Phone: +1 9125857616  
e-mail: dc9071@pcom.edu

*Conflict of interest statement:* No conflicts declared.

This is an open access article distributed under the terms of the Creative Commons Attribution-NonCommercial-NoDerivs 4.0 Unported (CC BY-NC-ND4.0) Licence (<http://creativecommons.org/licenses/by-nc-nd/4.0/>) which permits unrestricted noncommercial use, distribution, and reproduction in any medium, provided the original work is properly cited. *How to cite this article:* Copeland DW, Pickron AL, Girouard JR, Fabrizio PA. Is the iliocapsularis muscle ubiquitous and consistent? *Anatomy* 2022;16(3):185–188.

# Occipital spur: an incidental finding on a diagnostic cone-beam computed tomography – a case report

Shakeel Ahmed Valai Kasim<sup>1</sup> , Mehboob Mohammed Mustafa Shariff<sup>2</sup> , Sonu Danish<sup>3</sup> ,  
Naveed Ahmed Valai Kasim<sup>4</sup> 

<sup>1</sup>Department of Orthodontics and Dentofacial Orthopaedics, Ragas Dental College and Hospital, The Tamil Nadu Dr. M.G. R. Medical University, Uthandi, Tamil Nadu, India

<sup>2</sup>SRM Dental College, Bharathi Salai, Ramapuram, Chennai, Tamil Nadu, India

<sup>3</sup>Private Practitioner, Chennai, Tamil Nadu, India

<sup>4</sup>Private Practitioner, NK Dental Clinic Orthodontic Center, Chennai, Tamil Nadu, India

## Abstract

Exaggerated bony outgrowth of the external occipital protuberance is called occipital spur. The current report presents a case of a 20-year-old male patient seeking orthodontic treatment. The patient was referred for a cone-beam computed tomography scan to determine the position of impacted maxillary canines. An incidental finding on the scan was the existence of a focal spine-like hyperostosis in the occipital protuberance, and confirmed to be an occipital spur (Type III spine form). Clinical examination showed a palpable bone swelling without any tenderness, infection or discharge. He was referred to an orthopaedic surgeon should any symptoms get aggravated in the future. This case supports the essential role of cone-beam computed tomography to detect, analyse and identify the lesion as an occipital spur. This is the first such case report of its kind, which measures the size of occipital spur using cone-beam computed tomography and 3D imaging software. Usually asymptomatic, awareness of this uncommon presentation can expedite emergency medical care in the event of pain, or trauma leading to fracture or avulsion of the spur fragment. In such an event, the readily available CBCT data will be indispensable to surgeons for planning surgery with precise linear and volumetric measurements. Knowledge of these bony spurs is of untold value to anatomists, who will benefit greatly from being able to study the variants *in vivo*, in addition to studies on dry skulls or preserved cadavers. It is also of interest to clinicians and radiologists for diagnostic purposes, and sports physicians.

**Keywords:** Cone-beam computed tomography (CBCT); external occipital protuberance; inion hook; occipital spur

Anatomy 2022;16(3):189–192 ©2022 Turkish Society of Anatomy and Clinical Anatomy (TSACA)

## Introduction

External occipital protuberance (EOP) is a normal anatomical structure located on the posterior surface of the occipital bone, and the highest point of this structure is called inion. It is the insertion site of the ligamentum nuchae and trapezius muscle. Prominence of EOP has been used in the determination of sex in forensic investigations, and it is often more prominent in males than females. Based on its shape, Broca et al. classified EOP into six anatomical types using radiographs of dry skulls, which was later simplified by Gülekon and Turgut<sup>[1]</sup> into three subtypes: Type I, smooth; Type II, crest form; Type III, spine form.

While the EOP is widely reported in anthropological literature, there is a dearth of information regarding it within medical publications. Recently, this anatomical structure has been mired in controversy. The term entheses describes the site of insertion of a tendon, ligament, fascia or articular capsule into bone. An enthesophyte is a bony projection arising at an entheses. Exaggerated bony outgrowth of the external occipital protuberance is called Occipital spur or Inion hook. They are seen rarely in radiographic findings in young adults, as these bony adaptations are assumed to develop slowly over time.<sup>[2]</sup> However, in recent years, the presence of an enlarged external occipital protuberance

(EEOP) has been observed frequently in radiographs of relatively young patients.<sup>[3]</sup>

There are studies being conducted to investigate whether EEOP is linked to excessive use of smartphones and associated posture-related health issues in young adults. This article presents an incidental finding of this exaggerated anomaly in an orthodontic patient using cone-beam computed tomography.

### Case Report

A 20-year-old male patient reported with the chief complaint of malalignment and irregularity of his upper anterior teeth. On clinical and oral examination, he had an anterior crossbite, bilateral class III molar relationship, constricted maxillary arch and class III skeletal pattern. Interestingly, the patient was unaware of the absence of the maxillary canines from the dental arch. Patient's medical history showed no systemic diseases. Routine records were taken to assist in diagnosis and treatment planning, which included intra-oral and extra-oral photographs, plaster study models, cephalometric and panoramic radiographs.

The patient was referred for a cone-beam computed tomography (CBCT) scan to determine the position of the impacted maxillary canines and evaluate possible root resorption of the adjacent teeth. The scan was carried out on a CBCT (CS 9000 3D Imaging system Kodak, Rochester, NY, USA) and data processing was done using 3D imaging software version 11.95 (Dolphin imaging and management solutions, Chatsworth, CA, USA). The resultant images identified the exact position of the impacted canines in the maxilla and confirmed that there was no root resorption of the maxillary lateral incisors or the maxillary first bicuspids (**Figure 1**).

An incidental finding on the CBCT was the existence of a focal spine-like hyperostosis which was seen in the occipital protuberance extending in a craniocaudal direction (**Figure 2**). The measurements of the spur done on the CBCT at the level of EOP showed the spur width at the base was 13.2 mm and 3.5 mm at the apex (**Figure 3**). The length of the spur was 17.4 mm, measured at the base of EOP to the apex of the spur. The distance of the spur from the base of the skull was 6.5 mm (**Figure 2**). This incidental CBCT finding was confirmed to be an occipital spur (Type III spine form).

Clinical examination showed a palpable bone swelling without any tenderness, infection or discharge. Though asymptomatic, the patient gave a history of mild discomfort while sleeping on a hard pillow.



**Figure 1.** Three-dimensional reconstruction in coronal view shows the exact position of the impacted canines in the maxilla.

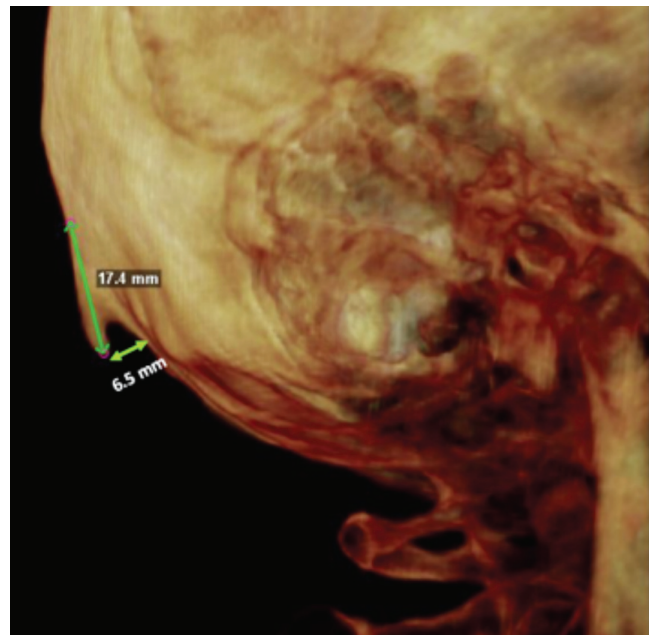


**Figure 2.** Three-dimensional reconstruction in lateral view shows a focal spine-like hyperostosis in the occipital protuberance extending in a craniocaudal direction. The length of the spur is 17.4 mm, measured at the base of external occipital protuberance to the apex of the spur. The distance of the spur from the base of the skull is 6.5 mm.

He was managed conservatively and advised to use a soft pillow. He was referred for an opinion from an orthopaedic surgeon should any symptoms get aggravated in future. He is currently undergoing orthodontic treatment for malalignment of teeth and class III skeletal malocclusion.

## Discussion

The diagnostic value of CBCT has risen in regular orthodontic practice, with benefits which cannot be achieved with conventional 2D radiographs. Based on these advantages, CBCT has been utilized in orthodontics, and several pathological findings and abnormalities in the oral and maxillofacial region have been incidentally reported on CBCT scans.<sup>[4,5]</sup>

In the present case report of a 20-year-old male patient seeking orthodontic treatment for malalignment of teeth, the occipital spur was an incidental finding in the CBCT. It was missed in the diagnostic cephalometric records, since the suboccipital area is routinely cropped out of the field of view in conventional lateral cephalograms. Hence, incidental findings detected in CBCT images can contribute significantly to the identification of subclinical pathologic abnormalities. It is of major importance that the ALARA principle (radiation dose “as low as reasonably achievable”) is respected. In such cases, however, the benefits outweigh the expected risk from radiation.

Previous studies have quantified occipital spurs conventionally using either dry skulls,<sup>[6]</sup> two-dimensional radiographs,<sup>[7]</sup> ultrasonography<sup>[8]</sup> or CT studies.<sup>[9]</sup> The disadvantage of studies on dry skulls is that the dimensional

changes due to the effects of prolonged cadaver preservation have not been researched extensively. Two-dimensional radiographs cannot ensure the same degree of accuracy that are obtained through three-dimensional reconstruction in CBCT.<sup>[10]</sup> Helical CT studies have a much higher risk from radiation compared with CBCT,<sup>[11]</sup> which has the specific advantage of choosing the field of view according to convenience and requirement.

In this case report, the patient primarily sought treatment for malocclusion and had no history of pain, with only mild discomfort while using a hard pillow in spite of the increased size of the occipital spur. In the normal course of events, the possibility of detecting and identifying the lesion would have been low, putting the patient at risk of injury from trauma to the occipital spur. The incidental discovery of the occipital spur in the CBCT and its immediate identification by the clinician enabled the patient to be apprised of the condition. The patient was advised to take necessary caution in case of accidents or trauma to the back of the head, and referred to an orthopaedic surgeon should his symptoms get aggravated in future. Though occipital spurs are usually asymptomatic, awareness of this uncommon presentation can expedite emergency medical care and management in a cost-effective manner in the event of any pain or trauma leading to fracture or avulsion of the spur fragment.<sup>[12]</sup> In such a scenario, the readily available CBCT data will prove to be indispensable to the surgeon for planning and executing surgery. This is the first such report of its kind, which measures the size of occipital spur using cone-beam computed tomography and 3D imaging software. This imag-



**Figure 3.** Three-dimensional reconstruction in posteroanterior view shows the width of the spur at the base is 13.2 mm and 3.5 mm at the apex, measured at the level of external occipital protuberance.

ing modality is more sensitive than conventional radiography for precise linear and volumetric measurements, and the depiction of changes in bone spur. Knowledge of these bony spurs is of untold value to clinicians and radiologists for diagnostic purposes. Anatomists and anthropologists will benefit greatly from being able to study the variants in vivo, in addition to studies on dry skulls or preserved cadavers. Also, sports physicians cognizant of such an anomaly will be better able to provide adequate protection to the athletes in their care.

### Conflict of Interest

The authors declare no conflict of interest.

### Author Contributions

SAVK: protocol/project development, data analysis; MMMS: protocol/project development, data analysis; SD: data analysis, manuscript writing/editing; NAVK: protocol/project development, data analysis.

### Ethics Approval

This case report has been prepared in accordance with the Helsinki Declaration and does not require any kind of approval of the Ethical committee. However, informed consent obtained from the patient for the report to be published.

### Funding

There has been no financial support for this work that could have influenced its outcome.

### References

- Gülekon IN, Turgut HB. The external occipital protuberance: can it be used as a criterion in the determination of sex? *J Forensic Sci* 2003;48:513–6.
- Matsumoto M, Okada E, Ichihara D, Watanabe K, Chiba K, Toyama Y, Fujiwara H, Momoshima S, Nishiwaki Y, Hashimoto T, Takahata T. Age-related changes of thoracic and cervical intervertebral discs in asymptomatic subjects. *Spine (Phila Pa 1976)* 2010;35:1359–64.
- Shahar D, Sayers MGL. A morphological adaptation? The prevalence of enlarged external occipital protuberance in young adults. *J Anat* 2016;229:286–91.
- Rogers SA, Drage N, Durning P. Incidental findings arising with cone-beam computed tomography imaging of the orthodontic patient. *Angle Orthod* 2011;81:350–5.
- Cha JY, Mah J, Sinclair P. Incidental findings in the maxillofacial area with 3-dimensional cone-beam imaging. *Am J Orthod Dentofacial Orthop* 2007;132:7–14.
- Srivastava M, Asghar A, Srivastava NN, Gupta N, Jain A, Verma J. An anatomic morphological study of occipital spurs in human skulls. *J Craniofac Surg* 2018;29:217–9.
- Varghese E, Samson RS, Kumbargere SN, Pothan M. Occipital spur: understanding a normal yet symptomatic variant from orthodontic diagnostic lateral cephalogram. *BMJ Case Rep* 2017; bcr2017220506.
- Gómez Zubiatur A, Alfageme F, López-Negrete E, Roustan G. Type 3 external occipital protuberance (spine type): ultrasonographic diagnosis of an uncommon cause of subcutaneous scalp pseudotumor in adolescents. *Actas Dermosifiliogr (Engl Ed)* 2019;110:774–5.
- Jacques T, Jaouen A, Kuchcinski G, Badr S, Demondion X, Cotten A. Enlarged external occipital protuberance in young French individuals' head CT: stability in prevalence, size and type between 2011 and 2019. *Sci Rep* 2020;10:6518.
- Jung PK, Lee GC, Moon CH. Comparison of cone-beam computed tomography cephalometric measurements using a midsagittal projection and conventional two-dimensional cephalometric measurements. *Korean J Orthod* 2015;45:282–8.
- Li G. Patient radiation dose and protection from cone-beam computed tomography. *Imaging Sci Dent* 2013;43:63–9.
- Sattur M, Korson C, Henderson F Jr, Kalthorn S. Presentation and management of traumatic occipital spur fracture. *Am J Emerg Med* 2019;37:1005.e1-1005.e2.

#### ORCID ID:

S. A. Valai Kasim 0000-0001-8642-4776;  
M. M. Mustafa Shariff 0000-0003-2759-5860;  
S. Danish 0000-0002-0715-4016;  
N. A. Valai Kasim 0000-0003-0502-926X



**Correspondence to:** Shakeel Ahmed Valai Kasim, MDS, MOrth RCPS, Prof. Department of Orthodontics and Dentofacial Orthopaedics, Ragas Dental College and Hospital, Tamil Nadu Dr. M.G. R. Medical University, Uthandi, India  
Phone: +91 9840862274  
e-mail: drshakeelahmed\_vk@yahoo.com

*Conflict of interest statement:* No conflicts declared.

This is an open access article distributed under the terms of the Creative Commons Attribution-NonCommercial-NoDerivs 4.0 Unported (CC BY-NC-ND4.0) Licence (<http://creativecommons.org/licenses/by-nc-nd/4.0/>) which permits unrestricted noncommercial use, distribution, and reproduction in any medium, provided the original work is properly cited. *How to cite this article:* Valai Kasim SA, Mustafa Shariff MM, Danish S, Valai Kasim NA. Occipital spur: an incidental finding on a diagnostic cone-beam computed tomography – a case report. *Anatomy* 2022;16(3):189–192.

## Index

http://dergipark.org.tr/en/pub/anatomy  
Anatomy 2022;16(3):193–195 ©2022 Turkish Society of Anatomy and Clinical Anatomy (TSACA)

## Author Index to Volume 16, 2022

(The bold typed references are the ones in which the person is the first author.)

<b>A</b>		Eren S	33
Adıgüzel E	114	Ersoy S	<b>152</b>
Akay E	69	Ertekin Ö	172
Akünel Türel C	152		
Alphan A	114	<b>F</b>	
Altunay ZM	<b>114</b>	Fabrizio PA	185
Apan A	19	Filgueira L	19
Apaydın N	<b>133</b>	Frišhons J	<b>108</b>
Atalay A			
	76, 172	<b>G</b>	
<b>B</b>		Geneci F	<b>1, 7, 62</b>
Balaban M	7, <b>13</b> , 26, 33	Girouard JR	185
Bayraktar D	56	Gökhan MB	124
Bezdickova M	108	Gümüş G	159
Buckley HR			
	93	<b>H</b>	
<b>C-Ç</b>		Halcrow SE	93
Candar E	<b>46</b>	Hatipoğlu ŞC	7
Canlı A	<b>69</b>	Hızlı Ö	<b>88</b>
Cheruiyot I	127		
Copeland DW	<b>185</b>	<b>İ</b>	
Çelik HH	62	İdilman İS	13
Çetin Ö	152		
Çıvgın E	165	<b>J</b>	
Çilengir AH		Jelev L	41
	<b>26</b>		
<b>D</b>		<b>K</b>	
Danish S	189	Kahiloğulları G	51
De La Paz JS	<b>93</b>	Kayabaşı S	88
Demirçubuk İ	46	Kına H	<b>139</b>
Demirtaş İ	139	Kipkorir V	<b>127</b>
Demiryürek D	<b>131</b>	Kislov MA	108
Dıramalı M	179	Krastev N	<b>41</b>
Duran S	<b>124, 165</b>	Kurul R	<b>179</b>
Dzetskolicová V		Kuş KÇ	139
	108		
<b>E</b>		<b>M</b>	
Ecevit AN	172	Malas MA	56
Erdoğan K	<b>56</b>	Malinova L	41
Erdoğan KE	179		

## 194 Author Index

Misiani M	127	Soysal H 1	
Moralı Güler T	51	Surhan Çınar A	19
Munguti J	127	Şahin A	81
Mustafa Shariff MM	189	Şengül G	46
<b>N</b>			
Ndung'u W	127	Tivcheva Y	41
Nyaanga F	127	Torun Bİ	1, 7, 19, 33
<b>O-Ö</b>			
Ocak H	62	Tubbs RS	19
Ocak M	1, 62	<b>U-Ü</b>	
Ochieng D	127	Uz A	19
Olabu B	127	Uzunlar H	56
Özcan C	81	Ünal ÖF	51
Özçelik F	146, 159	<b>V</b>	
Özdemir D	179	Valai Kasim NA	189
Özdemir Şahan Y	172	Valai Kasim SA	189
Özer Kaya D	56	Vatansever A	69
Özkan D	88	<b>W</b>	
<b>P</b>			
Pickron AL	185	Woodley SJ	93
<b>S-Ş</b>			
Sigit İkiz S	13	<b>Y</b>	
Soran Türkcan B	76, 172	Yılmaz M	76, 172
		Yılmaz T	146, 159

## Acknowledgment

<http://dergipark.org.tr/en/pub/anatomy>  
Anatomy 2022;16(3):195 ©2022 Turkish Society of Anatomy and Clinical Anatomy (TSACA)

### Acknowledgment of Reviewers for Volume 16, 2022

The Editorial Staff of Anatomy expresses their appreciation to the following reviewers who have evaluated the manuscripts for Volume 16, 2022.

---

Salih Murat Akkın	İlkay İdilman
Ömer Nuri Aksoy	S. Tuna Karahan
Mustafa Aldur	Simel Kendir
Aybegüm Balcı	Necdet Kocabıyık
Çağatay Barut	Zeliha Kurtoğlu Olgunus
Süha Beton	Ali Seyed Mirjalili
Burak Bilecenoğlu	Yasemin Özdemir Şahin
Murat Bozkurt	Esra Özkavukçu
Gülen Burakgazi	Freidrich Paulsen
Arda Büyüksungur	Necati Salman
Ayhan Cömert	Serap Şahinoğlu
Nurdan Çay	Mustafa Şırlak
Servet Çelik	İlkan Tatar
Emine Dağistan	Bilge İpek Torun
Mirela Eric	Özgür Tosun
Quentin Fogg	Selçuk Tunalı
Ceren Güneç Beşer	Eray Tüccar
Mehmet Ali Güner	Emel Ulupınar
Yahya Efe Güner	Aysun Uz
İlke Ali Gürses	Mehmet Yılmaz

---



---

# Table of Contents

---

Volume 16 / Issue 3 / December 2022

(Continued from back cover)

## Teaching Anatomy

- Can high resolution 3D resin printed models be used in anatomy education?  
A randomized controlled trial** 179  
Ramazan Kurul, Murat Dıramalı, Dilruba Özdemir, Kevser Ezgi Erdoğan

## Case Reports

- Is the iliocapsularis muscle ubiquitous and consistent?** 185  
Daniel W. Copeland, Allison L. Pickron, Jocilyn R. Girouard, Philip A. Fabrizio
- Occipital spur: an incidental finding on a diagnostic cone-beam computed tomography –  
a case report** 189  
Shakeel Ahmed Valai Kasim, Mehboob Mohammed Mustafa Shariff, Sonu Danish,  
Naveed Ahmed Valai Kasim

## Index

- Author Index to Volume 16, 2022** 193

## Acknowledgment

- Acknowledgment of Reviewers for Volume 16, 2022** 195

### On the Front Cover:

Medially to the pterygoid triangle, the Vidian nerve was found in all cadavers and the Vidian artery in one cadaver. **N.V2:** maxillary nerve; **PN:** palatine nerve; **PPG:** pterygopalatine ganglion; **SPA:** sphenopalatine artery; **VA:** vidian artery; **VN:** vidian nerve. From Kına H, Kuş KÇ, Demirtaş I. Clinical implications of the anatomical relationships of the pterygopalatine fossa and Vidian canal: an endonasal endoscopic cadaveric study. *Anatomy* 2022;16(3):139–145.

---

## Table of Contents

---

Volume 16 / Issue 3 / December 2022

### Original Articles

- Clinical implications of the anatomical relationships of the pterygopalatine fossa and Vidian canal: an endonasal endoscopic cadaveric study** 139  
Hakan Kına, Koral Çağlar Kuş, İsmet Demirtaş
- The influence of brightness, age and refractive errors on pupil size** 146  
Tolga Yılmaz, Ferah Özçelik
- Investigation of the relationship between inflammatory markers and grade of disease in patients with acute ischemic stroke with partial anterior circulation infarct** 152  
Sadettin Ersoy, Canan Akünal Türel, Ömer Çetin
- White to white cornea diameter and mesopic pupil size in patients with keratoconus** 159  
Ferah Özçelik, Tolga Yılmaz, Güneş Gümüş
- Tarsal coalition in the Turkish population: an MRI study** 165  
Semra Duran, Esra Çıvgın
- Transposition of the great arteries: single center experiences** 172  
Başak Soran Türkcan, Mustafa Yılmaz, Yasemin Özdemir Şahan, Ömer Ertekin, Ata Niyazi Ecevit, Atakan Atalay

*(Contents continued on inside back cover)*